Republic of Iraq
Ministry of Higher Education
and Scientific Research
University of Babylon
College of Engineering
Civil Engineering Department

BEHAVIOR OF TWO-WAY CONCRETE SLAB REINFORCED BY PERFORATED STEEL PLATE USING SELF-COMPACTING CONCRETE

A Dissertation

Submitted to the College of Engineering of the University of Babylon in Partial Fulfillment of the Requirements for the Degree of Doctor of Philosophy in Engineering/ Civil Engineering/ Structures

By

Ali Adnan Abid Jawad

Supervised by

Prof. Dr. Nameer A. Alwash

2022 A.D

بِسْمِ اللَّـهِ الرَّحْمنِ الرَّحِيمِ

وَ الْبَيْتِ الْمَعْمُورِ وَ السَّقْفِ الْمَرْفُوعِ

صَدَقَ اللهُ العَلِيُّ العَظِيم

من سورة الطور

الآيــة :- (٤) و (٥)

To . . .

the greatest support from God to my soul. . . my

parents

the second part of me . . . my wife

the best gift that I ever received . . . my children

more precious than myself. . . my brothers and sisters

my relatives and friends

all students

I put this humble effort between their hands

Ali Adnan Al-Zahid

Certificate

I certify that the preparation of this dissertation titled "**Behavior of Two-Way Concrete Slab Reinforced by Perforated Steel Plate Using Self-Compacting Concrete**", is prepared by "**Ali Adnan Al Zahid**", under my supervision at the Department of Civil Engineering in the University of Babylon in partial fulfilment of the requirements for the Degree of Doctor of Philosophy in Civil Engineering (Structural Engineering).

Signature:

Name: Prof. Dr. Nameer A. Alwash

Date: / / 2022

EXAMINING COMMITTEE CERTIFICATION

We certify as an Examining Committee that have read this dissertation entitled ***"Behavior of Two-Way Concrete Slab Reinforced by Perforated Steel Plate Using Self-Compacting Concrete"***, which is submitted by ***"Ali Adnan Abid"*** and examined the student in its content and what related to it, and found it meets the standard of a dissertation for the degree of Doctor of Philosophy in Civil Engineering (Structure Engineering).

Signature:
Name: ***Prof. Dr. Nameer A. Alwash Hassan***
(Member and Supervisor)
Date: / / 2022

Signature:
Name: ***Assist. Prof. Dr. Rafea F.***
(Member)
Date: / / 2022

Signature:
Name: ***Assist. Prof. Dr. Yousif A. Mansoor***
(Member)
Date: / / 2022

Signature:
Name: ***Prof. Dr. Wissam D. Salman***
(Member)
Date: / / 2022

Signature:
Name: ***Prof. Dr. Faris J. Altalqany***
(Member)
Date: / / 2022

Signature:
Name: ***Prof. Dr. Haitham H. Muteb***
(Chairman)
Date: / / 2022

Approved by the Head of the Civil Engineering Department

Signature:
Name: ***Prof. Dr. Thair J. Mizhir***
(The Head of the Civil Engineering Department)
Date: / / 2022

Approved by the Dean of the College of Engineering

Signature:
Name: ***Prof. Dr. Hatem H. Obeid***
(The Dean of the College of Engineering)
Date: / / 2022

ACKNOWLEDGEMENTS

IN THE NAME OF ALLAH, THE MERCIFUL THE COMPASSIONATE

There can be no completed thanks to the Creator unless you express gratitude to the creature. So, firstly and lastly, I am thankful to God, who enabled me to achieve this research, and then I would like to express my thanks and appreciation to my supervisor, Prof. Dr. Nameer A. Alwash, for his suggestions, encouragement, guidance, and many kinds of support during all the stages of research.

As well, I would like to thank Al Nawafith company for their support and facilities.

Furthermore, I'd like to express my gratitude to all of my family members who assisted and supported me, especially my parents, my wife, my two brothers, “Dr. Muaid Adnan” and “archaeologist Hasaneen Adnan”, my two sisters and their husbands, my two sons “A Reciter of the Holy Qur'an Ali Al Akber” and “infant Muhammed”, my only sweet daughter, Fatima, the son of the brother "Med. Lab. Technologist Ahmed Muaid" and the son of the sister "Agricultural Engineer Haider Mustafa", my relatives and friends.

Thanks, from my deep heart.

ABSTRACT

The experimental and analytical parts of this dissertation aim to establish a new technique concerning reinforcing two-way concrete slabs by using perforated steel plates rather than traditional bar reinforcement, employing a special type of concrete known as self-compacting concrete.

The experimental program consists of casting and testing twenty scaled slabs with overall dimensions equal to (1050×1050×60) mm into two groups. Ten of these slabs were tested under concentrated load while the remainder were tested under uniform load. Each group has one specimen reinforced by traditional bar reinforcement, whereas the rest nine specimens reinforced by perforated steel plate. Taking into consideration that the amount of steel is structurally equivalent in all specimens.

The studied variables were the effects of changing the shape, size and number of openings, confirming that the amount of steel is the same. The shapes are circular, octagonal and square, while each shape had three sizes: small openings with 144 openings (12×12), medium openings with 64 openings (8×8) and large openings with 16 openings (4×4). The effect of changing the thickness of the plate was investigated numerically by using the nonlinear finite element method, program Ansys18.1.

The results proved that using this style of reinforcement is very effective in two-way concrete slabs where the slabs reinforced by perforated steel plate reflects ultimate load higher than slabs reinforced by classical reinforcement in both types of loading, concentrated and uniform.

In the case of concentrated load, the average ultimate load of the models reinforced by perforated steel plate is greater than the ultimate load of model reinforced by deformed bar reinforcement by about 67.5%, while this increase is equal to 12.8% in case of uniform load.

According to the adopted openings' size, the medium size (Opening Aspect Ratio, OAR, = 8.17×10-3)[1] under concentrated and uniform load shows ultimate load capacity more than small and large openings; it was about 7.6% and 18.4% (in the case of concentrated load) and it was about 20.3% and 21.5% (in the case of uniform load), respectively.

Furthermore, the square openings exhibit better ultimate load than circular and octagonal shapes, so, upon the current experimental program, the specimens reinforced by perforated steel plate with medium-sized square openings are the optimal considered choice.

The numerical analysis by finite element method using Ansys 18.1 program proved that the adjustment of plate thickness from 1 mm to 1.5 mm and 2 mm, with same volume of steel, has no effect on the behavior of slabs reinforced using the proposed technique in both concentrated and uniform load.

[1] Opening aspect ratio represents the ratio of area of one opening to area of a perforated plate.

Contents **Page**

List of Tables

List of Figures

Notation

Symbol	Descriptions
τ	Shear stress (Pa)
τ_o	Yield stress (Pa)
γ	Shear rate
μ_p	Plastic viscosity
E_c	Modulus of elasticity of concrete, (GPa)
$f`_c$	Concrete compressive strength, (MPa)
b	Width of rectangular cross section, (mm)
d	Distance from extreme compression fiber to centroid of tension reinforcement, (mm) (effective depth)
$f_{y_{tr}}$	Yield strength of traditional steel bar, (MPa)
fy_{psp}	Yield strength of steel plate, (MPa)
T_{50}	Measurement of the unconfined flow rate, (sec)
ε_o	Strain corresponding to *fc'*
ν	Poisson's ratio
ρ	The ratio of main reinforcement

Abbreviations

Abbreviation	Description
Ansys	Finite element package
ACI	American Concrete Institute
ASTM	American Society for Testing and Materials
cm	Centimeter
et al.	And others
FA	Fly ash
FEM	Finite element method

IQS	Iraqi Quality Standardization
m	Meter
max.	Maximum
MDF	Medium Density Fiber (wood)
min.	Minute (s)
mm	Millimeter
MPa	Mega Pascal (MN/m^2)
No.	Number (issue)
OAR	Opening aspect ratio (the ratio of area of one opening to area of perforated plate)
SCC	Self-compacting concrete
SCFRC	Self-compacting fiber reinforced concrete
SF	Silica fume
SP	Superplasticizer, (L)
VSI	Visual stability index
W/C	Water to cement ratio

CHAPTER ONE
INTRODUCTION

1.1 General

Conventional slabs (one-way or two-way), flat slabs, hollow core slabs, post or pretension slabs, and other types of slabs use the structural concept that benefits from the concrete compressive strength in the compression zone and provides steel in the tension zone to benefit from steel tensile strength. For more than a century since the first trial of using reinforced concrete, till now, the steel which is used in concrete slabs is bar reinforcement (traditional reinforcement).

The main steps that are needed to produce the steel reinforcement mat are cutting the steel bars according to the required length depending on slab dimensions, then spreading them, taking into consideration the alignment and direction of the bars (vertically and horizontally). After that, it should provide the required distance between bars (spacing of bars) according to the pre-step (design of slabs) with providing adequate overlapping. Finely contact the bars between them (making the bars as a one unit reinforcing mat). Each previous point needs to check it. The mistakes that always happen during the implementation of reinforcing slabs obligate the researchers to find an optimal solution with minimum effort.

This study will introduce new steel modeling instead of bar reinforcement in two-way concrete slabs. The technique consists the use of perforated steel plate instead of classical reinforcement for providing steel in the tension zone with a suitable special type of concrete. From all the types of concrete, the self-compacting concrete is the best for using in this case because it has important

characteristics, filling ability, passing ability and stability. These properties will be important keys to success the concept.

According to the present study, the time, cost and specification will be upgraded to another level. The reinforcing by perforated plate needs fewer workers, may be no need for skilled workers, as well as less effort and time for situ engineer and supervisor engineers.

1.2 Slabs Behavior System

Slab is the structural member that provides a horizontal plane surface. It has structural functions like support loads and serviceability advantages like sound and heat insulating. Moreover, it is protecting the residents, materials and equipment from environmental effect since the slabs became as a ceiling to the beneath floor.

1.2.1 One-way slabs

A one-way slab is a slab which has a longer span to shorter span ratio equal to or higher than two, see equation (1.1), or supported only on two opposite sides. It carries the loads in the short direction only.

$$\frac{longer\ span}{shorter\ span} \geq 2 \qquad \text{.....} \quad (1.1)$$

The main reinforcement is provided in shorter span and secondary reinforcement in a longer span as shown in figure (1.1). It will bend only in one direction, taking approximately a half cylindrical shape [1].

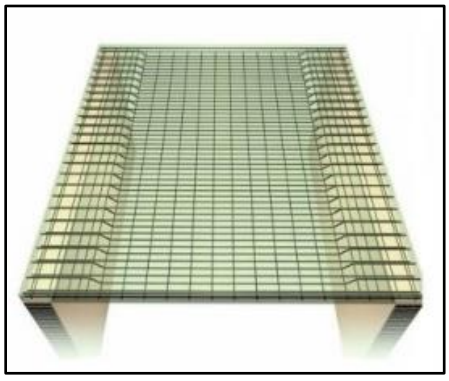

Figure (1.1): One-way slab

1.2.2 Two-way slabs

A two-way slab is a slab which has a longer span to shorter span ratio less than two, see equation (1.2). It carries the loads in both short and long directions.

$$\frac{longer\ span}{shorter\ span} < 2 \quad \ldots\ldots\ldots\ldots\ldots\ldots\ldots\ldots\ldots\ldots\ldots\ldots\ldots\ldots\ldots\ldots\ldots\ldots\ldots\ldots\ldots\ldots \quad (1.2)$$

The primary reinforcement is supplied in both directions, as seen in Figure (1.2). It will bend in two directions, taking approximately a dish shape [1].

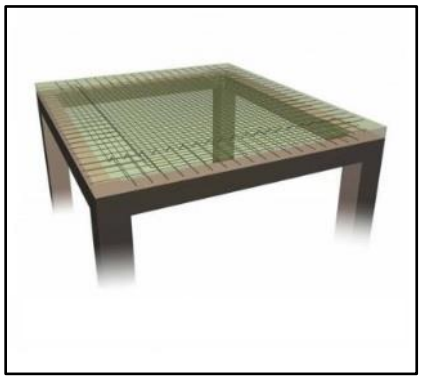

Figure (1.2): Two-way slab

1.3 Self Compacting Concrete

Self-compacting concrete can be defined as a special type of concrete that has two significant versus properties: highly flowable and non-segregating, these properties serve important requirements such as spreading and filling the formwork, in addition to encapsulating the reinforcement without the need for mechanical consolidation [3].

To understand the flow of fresh SCC, it should understand the modifying Bingham rheology model. Rheology is summarily defined as the science of deformation and flow; Concrete rheology is evaluated by using the relate variations between shear stress and shear rate. For standard concrete, the initial shear stress more than (τ_o) is needed for flow and spread in the formwork while the effect of adding water or finest grain is clarified in Figure (1.3) below. In

SCC, there are some techniques to minimize the required initial shear stress less than (τ_o) [2].

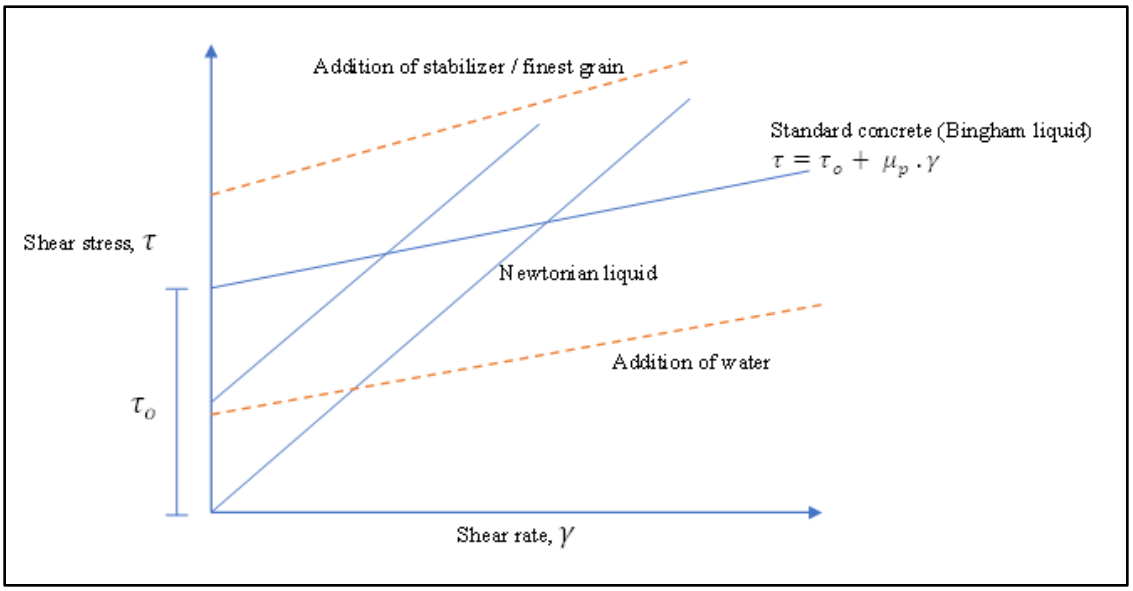

Figure (1.3): Modified Bingham rheology model

Note:

τ : shear stress (Pa)
τ_o : yield stress (Pa)
γ : shear rate
μ_p : plastic viscosity (Pa. S)

The processers that are needed to achieve self-compacting concrete are [2]:

1- Limit coarse aggregate to about 50% of solid volume and limit fine aggregate to about 40% of mortar volume.
2- Low water - powder ratio.
3- Using superplasticizer.

Figure (1.4) shows the flow chart which clarifies the methods that are needed to achieve self-compacting concrete:

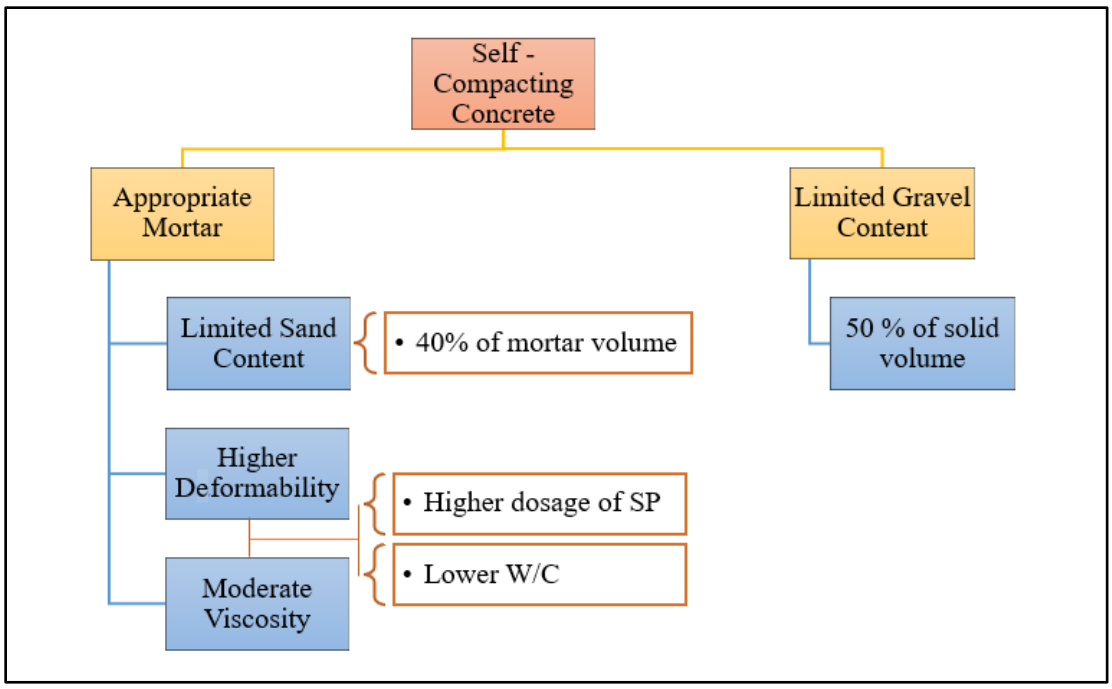

Figure (1.4) Methods for achieving self-compacting concrete [2]

The selection of materials should be satisfied the excess paste theory. "Excess Paste Theory" was explained the mechanism governing the workability of concrete. This theory states that enough paste should be provided to surround the surface area of the coarse aggregates, this will attain the workability, and minimize the friction among the mix ingredients to give better flow ability. Without the paste layer, high friction will be generated and concrete mix would need for vibration. That means the aggregates moving would be impossible without external stress. Not only excess paste should be provided but also this paste should have a suitable consistency.

1.3.1 Selection of Materials

The main materials that are needed to achieve this type of concrete are [3]:

1- **Cement:** All cement types can be used for the production of SCC. There are no special requirements, but it should be in an acceptable range in both physical and chemical testing.

2- **Supplementary powders as a cementitious material:** The most common famous materials that are used to produce the SCC explained in A and B items. The chosen one of these is sufficient to achieve self-compacting concrete.

A- Silica fume: It is a small and rounded particles that is used to reduce friction between larger cement particles, effectively lubricating the paste matrix and increasing the stability of SCC mixtures.

B- Fly ash: The majority of fly ash particles are spherical with a smooth surface and might serve as ball bearings within the SCC mix. As a result, fly ash may improve the slump flow which would subsequently enhance workability.

3- **Aggregate selection:** It includes coarse and fine aggregate.

A- Coarse aggregate: It is important to choose a rounded coarse aggregate as much as possible to increase the filling ability. As compared with a crushed aggregate, for the same water content and same size of aggregate, the rounded type shows better filling ability.

B- Fine aggregate: the fine aggregate component should be will – graded.

4- **Admixtures**

A- Superplasticiser / High range water reducing admixtures: It has a significant dual role by controlling the viscosity of the mix and increasing the fluidity.

B- Viscosity modifying admixtures: beneficial materials for adjusting the viscosity and improving the stability of SCC.

1.3.2 Advantages of Using Self-Compacting Concrete

The use of self-compacting concrete has a several significant advantages, such as:

1- There is no need for vibration to achieve adequate consolidation, this will lead to:

a- Savings on equipment supplying, as well as on equipment operation and maintenance.

b- Reduce the pollution of the job site through reducing noise especially in parts that need heavy vibration in urban areas.

c- Reduce the crew of cast workers.

2- Screeding operations need less effort since this type of concrete has self-leveling characteristics, so:

a- Create a smooth surface free of honeycombing and unpreferable signs.

b- A good underlay surface will be prepared for the final flooring materials, such as carpeting or tiles, with the least effort.

3- Less point of casting and that mean:

a- Reducing the pump lines during the casting (either reducing the frequent movements of the pumps or reducing the number of pumps).

b- Higher rate of casing and shorter construction duration.

1.3.3 Application and Uses of Self-Compacting Concrete

There are several huge structural constructions used self-consolidating concrete for different purpose like [3]:

1- Pedestrian Overpass, Seminole Country, Orlando, Fla.: It has an anchor block structure as part of pedestrian overpass, this made the use of a vibrator impossible so the self-consolidating concrete was the best solution for this case as shown in Figure (1.5).

Figure (1.5): Pedestrian Overpass, Seminole Country, Orlando, Fla:

2- National Museum of the American Indian, Washington, D.C.: because of the overcrowded reinforcement and the complicated shapes of the structure they used self-consolidating concrete, see Figure (1.6).

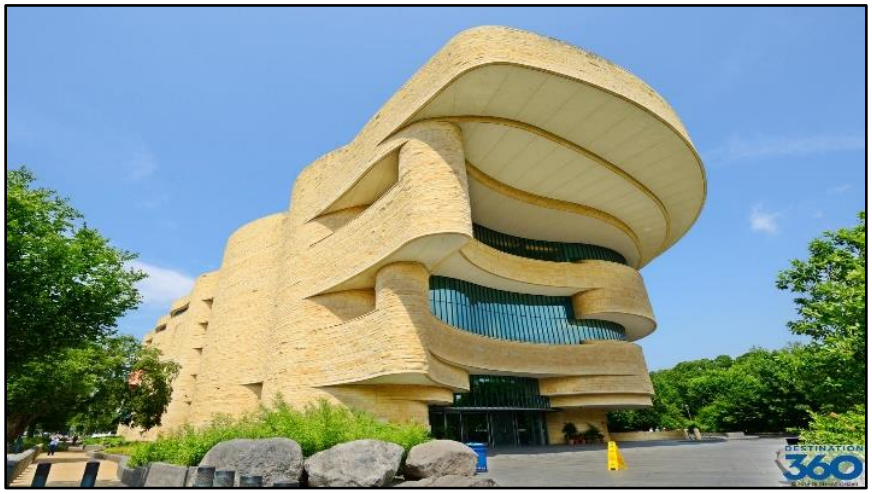

Figure (1.6): National Museum of the American Indian, Washington, D.C.

3- Double – Tee Production, Nitterhouse Concrete Prodcts Inc., Chambersburg, Pa. as depicted in Figure (1.7): here other reasons for using self-consolidating concrete, cost saving, improved appearance of the concrete and reduction in noise levels led to use self-compaction concrete.

Figure (1.7): Double – Tee Production, Nitterhouse Concrete Prodcts Inc., Chambersburg, Pa.

4- Rosenthal Center for Contemporary Arts, Cincinnati, Ohio that shown in Figure (1.8): the challenge was design of some components provided very little access and other parts considered as a dead area for reaching suitable vibrator inside there.

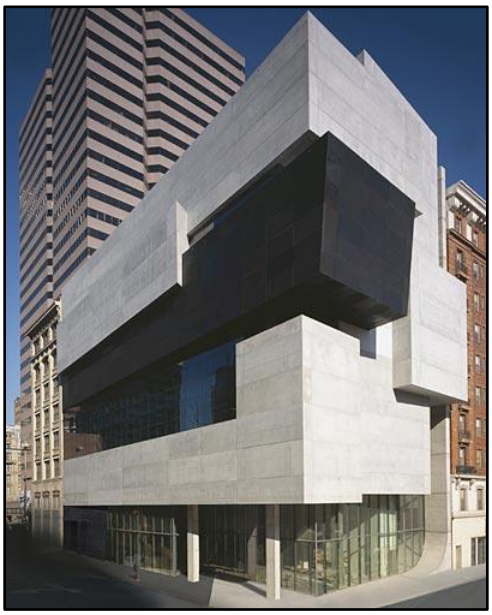

Figure (1.8): Rosenthal Center for Contemporary Arts, Cincinnati, Ohio

5- As illustrated in Figure (1.9), the reaction wall in the structural laboratory at the University of Sherborooke, Quebec, Canada: the wall measures 9.3 m wide, 7 m high and 4 m thick. The using of self-consolidating concrete enabled the placing of the concrete from two points along the wall. High

quality was secured and reduce the noise in laboratory with facilitated construction activities in a working environment.

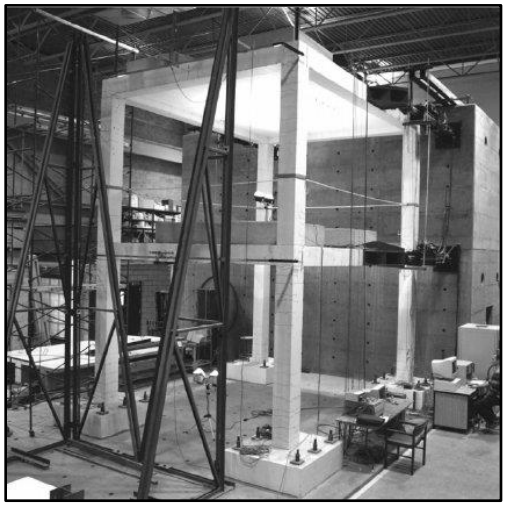

Figure (1.9): Reaction Wall in Structural Laboratory, University of Sherborooke, Quebec, Canada

1.4 Perforated Steel Plate

Plates are plane units with a small thickness in comparison to their planar dimensions [4]. Perforated plate is the same previous definition but it has opening inside as shown in Figure (1.10).

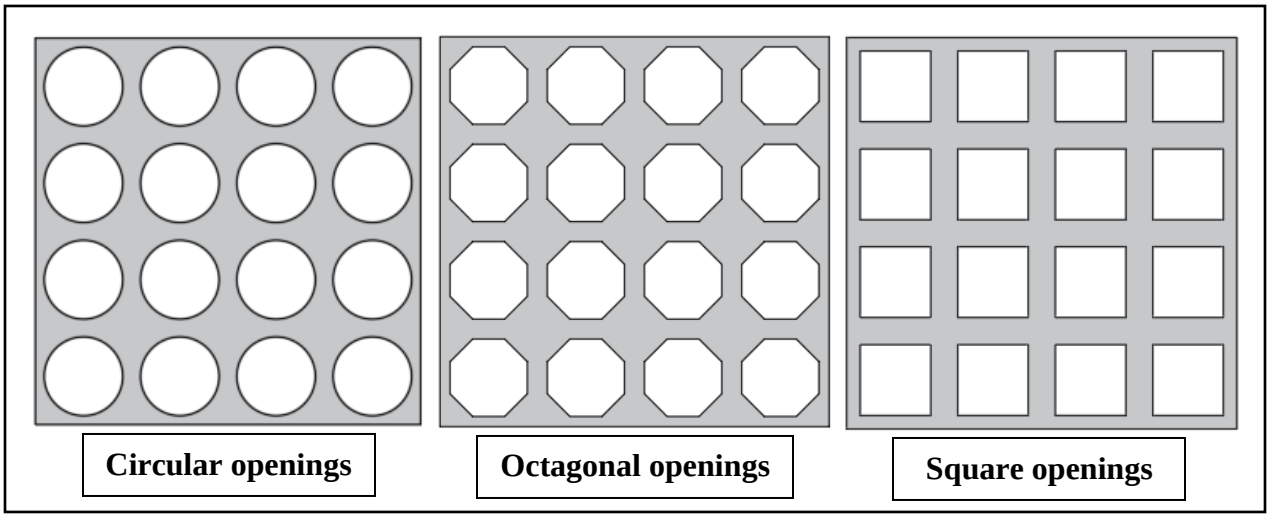

Figure (1.10): Different shapes of openings in perforated steel plate

The present study suggests that the perforated steel plate will be used as a reinforcing technique instead of traditional bar reinforcements in two-way concrete slabs, according to that, there are some characteristics that should be provided in the openings as:

1- The same shape and size to evaluate the influence of shape openings separately without the interaction effects of different shapes in one specimen.
2- Distributed symmetrically in both directions. It is necessary to get regular behavior and an obvious understanding of the suggested method.
3- Have smooth edges as shown in Figure (1.11) to prevent the point of stress concentration, it will be a starting point for failure.

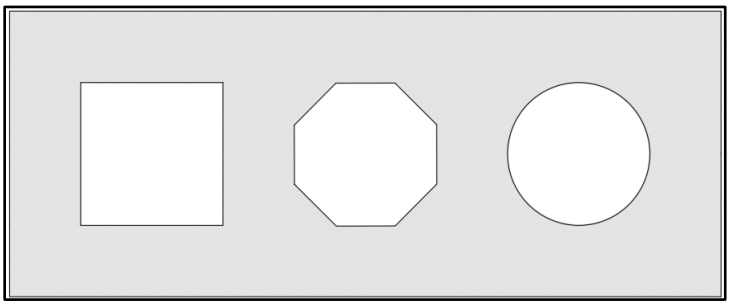

Figure (1.11): Characteristics of openings edges

1.5 The Philosophy of Reinforcing System

The main philosophy of reinforcing the two-way slabs is providing large number of individual elements (bar reinforcements) and then connect them to make these elements work as a one unit (the net of reinforcement), so this study will provide one unit (perforated plate) instead of bars reinforcement as shown in Figure (1.12). According to that, the study will introduce a new technique used for reinforcing two-way concrete slabs.

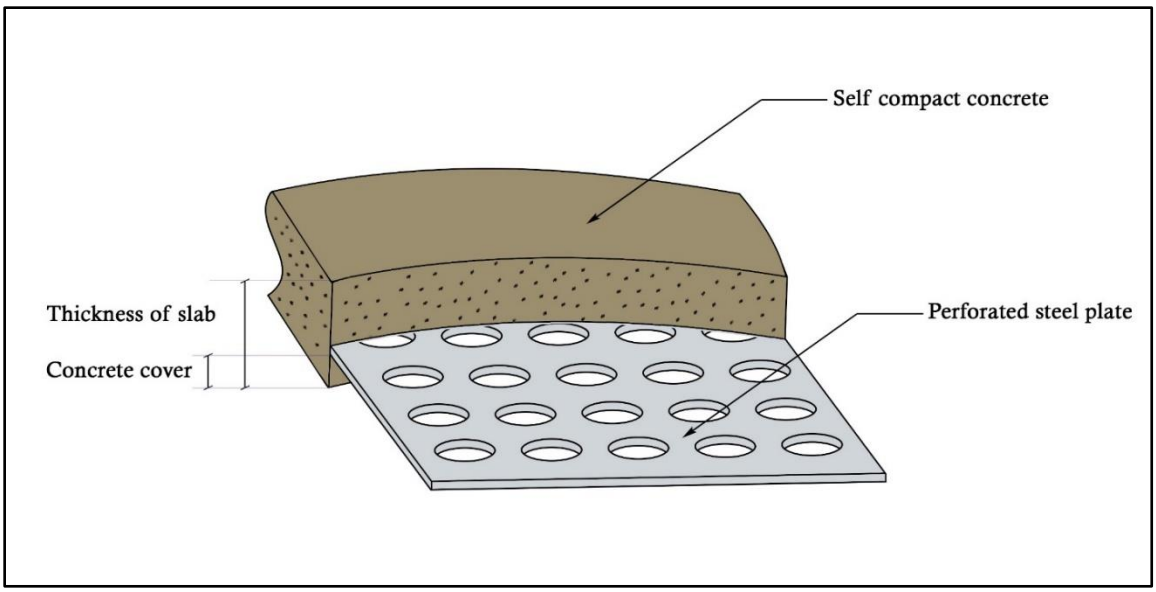

Figure (1.12): Slab reinforced by perforated steel plate

1.6 Advantages of Proposed Reinforcing System

The reinforcing system according to the present concept will achieve many advantages as it is listed below:

1- Reduce the time of implementation.
2- Reduce the number of workers especially skilled workers.
3- Reduce the effort and the time of checking reinforcement by engineers.
4- Reduce the cost of implementation.
5- Provide a precise distance between the openings (spacing).
6- Important application in Sustainable Engineering (if the plate was available on site or if it was a byproduct of some metal processing).

1.7 Advantage of Using the Suggested Reinforcing System with Self-Compacting Concrete

The advantages of using perforated steel plate with self-compacting concrete are:

1- Accelerate construction.
2- Eliminate for many equipment considered very important in casting.

3- Decrease the number of workers.
4- Decrease employee injuries.
5- Reduce the cost of casting.
6- Improving in specifications.
7- A promising concept for green building (The pollution and waste reduction measures, and the enabling of re-use and recycling, are one of the most important things that a "green" building does).

Previous points can be summarized in scheme (1.13) below:

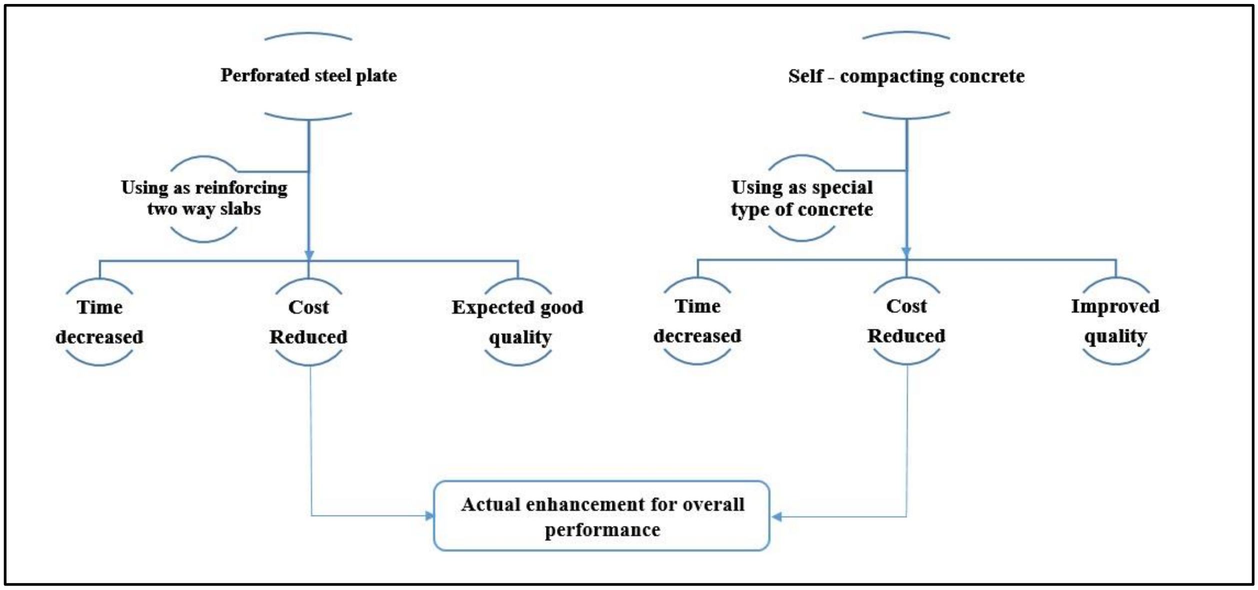

Figure (1.13): Advantage of using the suggested reinforcing system with self-compacting concrete

* The price of one cubic meter from self – compacting concrete more expensive but the overall cost of casting will be less [5].

1.8 Principles of Computing the Amount of Steel

The main principle that the structural engineer depends on for computing the quantity of steel is the ratio between the amount of steel to the amount of concrete, where is called as Latin letter Rho (ρ):

$$\rho = \frac{Area\ of\ steel\ (As)}{Area\ of\ concrete\ (bd)} \quad \ldots\ldots (1.3)$$

But in the previous equation, there is a hidden value that represents one unit length from each steel reinforcement and concrete cross section, so that can be mathematically interpreted as:

$$\rho = \frac{As*1}{bd*1} \quad \text{..... (1.4)}$$

Or can be rewrite above equation as

$$\rho = \frac{Volume\ of\ steel}{volume\ of\ concrete} \quad \text{..... (1.5)}$$

According to the previous equation, the amount of steel in slabs reinforced by perforated steel plate will be considered.

1.9 Equivalent Amount of Perforated Steel Plate

Because of the difference between the yield strength of steel reinforcements and the yield strength of perforated steel plate, an equivalent amount of perforated steel plate will be adopted.

Generally, in case of $f_{y_{psp}} = f_{y_{tr}}$

$$\rho_{psp} = \rho_{tr} \quad \text{..... (1.6)}$$

Note that the subscription:

psp = perforated steel plate

tr = traditional bar reinforcement

But in fact, the yield strength of bar reinforcements and steel plate never have the same value so

(ρ_{tr})= Equivalent ρ_{psp} ..... (1.7)

The base point that should be satisfied is

$$As_{psp} * fy_{psp} = As_{tr}\ fy_{tr} \quad \text{..... (1.8)}$$

Substitute equation (1.8) in equation (1.6) and equation (1.4)

$$\frac{As*fy_{psp}*1}{bd*1} = \frac{As\ fy_{tr}*1}{bd*1}$$

$$\frac{Volume\ of\ PSP*\ fy_{psp}}{volume\ of\ concrete} = \frac{Volume\ of\ tr*\ fy_{tr}}{volume\ of\ concrete} \quad \text{..... (1.9)}$$

$$Volume\ of\ PSP * fy_{psp} = Volume\ of\ tr * fy_{tr} \quad \ldots\ldots\ldots\ldots\ldots\ldots\ldots \quad (1.10)$$

1.10 Aim of the Study and Scope of the Work

The present work aims to evaluate the new suggested reinforcing system and present a finite elements modeling. The evaluation will be done through a comparison between slabs reinforced by normal reinforcement and slabs reinforced by perforated steel plate with the same equivalent amount of steel and it is including:

1- Comparison between load deflection curves.
2- The ultimate strength of the slabs with corresponding deflection.
3- Comparison between deflection at service load with allowable values in ACI-Code.
4- The number, type of cracks and crack pattern.
5- Maximum crack width at different stages of load.

The work includes studying the behavior of two-way slabs reinforced by perforated steel plate under concentrated and uniform load.

The parametric study for various cases that have been undertaken into the consideration are: -

1- Investigate the effect of changing the shape of opening, the study will adopt the comparison between square, octal and circle shapes with same amount of steel.
2- Study the effect of changing the opening size for the same amount of steel.
3- Type of load will be concentrated and uniform.

All previous parameters will be experimentally investigated while the effect of changing the thickness will be investigated numerically by the finite element method.

1.11 Dissertation Layout

The dissertation is presented in six chapters, the following points will illustrate briefly the content of each chapter: -

- Chapter one presents an introduction about the basic concepts that are related to the current study. It includes general information about the importance of the current study, the slabs systems, a brief description of self-compacting concrete, basic information about perforated steel plate, The philosophy and advantages of the suggested reinforcing system, in addition to the main objectives and the outlines of the dissertation.
- Chapter two includes the literature review of some research related to strengthening two-way slabs by steel plate, using self-compacting concrete in two-way slabs and some concepts concerning the use of perforated steel plate in two-way slabs as a rib to increase the stiffness of the slabs.
- Chapter three describes the developing stages of achieving the experimental program which includes the details of all the ingredients and materials that are used to prepare and cast all specimens with their suitable laboratory tests. Furthermore, the style of preparing the perforated steel plates is specified. Description of models and test setup with an explanation of the loading style are presented too.
- Chapter four regards the experimental results, this chapter clarifies the results of the experimental tests, ultimate load and corresponding deflections, load deflection curves, cracks investigations include the width and pattern of cracks with computerized modeling clarifying the growth of

cracks from initial visible crack till failure. Moreover, all the results are graphically represented with their appropriate discussions.

- Chapter five comprises the use of Ansys 18.1 to make a numerical analysis depending on finite elements methods. The comparison between experimental results with results of the presented model is also included. Moreover, a parametric study discussed other parameters concerning the suggested reinforcing system.
- Chapter six includes the obtained conclusions and recommended suggestions for future work.

CHAPTER TWO
LITERATURE REVIEW

2.1 General

A real search has been done about using perforated steel plate instead of using traditional bar reinforcement in two-way concrete slabs with using self-compacting concrete but there are no researches were found. However, the plates are used as a strengthening system for concrete slabs. Other researches study the use of self-compacting concrete in concrete slabs. Steel plate strips with suitable holes are used in some research to increase the shear resistance of the slabs. Therefore, this chapter is subdivided into three main categories to give an overview concerning the concepts that are relative to the current study.

2.2 Steel Plates as a Strengthening Technique in Concrete Slabs

Strengthening or repairing of the structural members is usually required. Slabs is one of these members. Many techniques that are available for strengthening slabs but the simple method, fast of application and minimum increases in self – weight and size is the using the steel plates. For the aforementioned reasons, it has become an attractive method for researchers in recent years.

In previous studies, there were two main techniques which were used for strengthening two-way concrete slabs with steel plates: either the plate was bonded to the slab by using a suitable epoxy or using steel bolts.

Zhang et. al. (2001)[6] studied the behavior of two way reinforced concrete slabs which they strengthened by externally bonded with steel plate under a concentrated load subjected at the center of the slab. The experimental program included casting and curing five two-way RC square slabs that had the same

dimensions. Each one had a dimension (1800×1800×70) mm, and the properties of reinforcement, steel plate, and concrete are clarified in the Table (2.1).

Table (2.1): Properties of materials [6]

Materials (1)	Details (2)	Elastic modulus (N/mm2) (3)	Compressive strength (N/mm2) (4)	Yield stress (N/mm2) (5)	Ultimate tensile stress (N/mm2) (6)
Concrete	---	---	26.4	---	---
Rebar (identical for bottom and top reinforcement with top reinforcement limited to an area of 500 mm × 500 mm at each corner	Mild steel ϕ = 6.5, at 150 mm centers, in both directions, average concrete cover for the two directions = 16.5 mm	---	---	340	431
Steel plate	Mild steel	---	---	335	417
Adhesive	Et epoxy resin	5.960	94	---	11

The surface of the steel plate was roughened by a suitable grinder, washed with acetone and cleaned before it was bonded to the concrete slab. A uniform layer of epoxy resin was used to bond the plates to the slabs with a thickness of four millimeters. Three different sizes of plates were used for strengthening as shown in Figure (2.1) below:

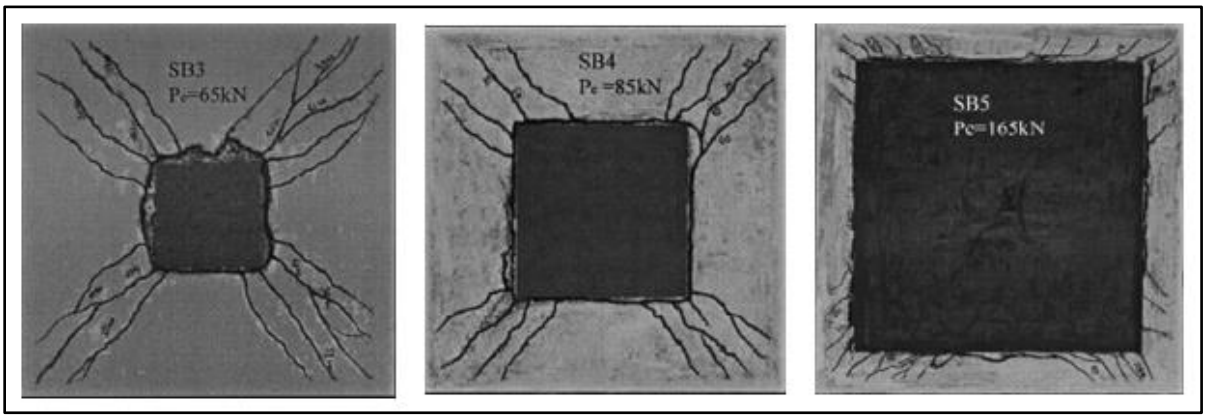

Figure (2.1): Strengthened slabs by steel plate [6]

The testing of slabs was conducted under the condition of simple supports, and the applying load was a central concentrated load over an area of 150×150

mm. The supporting had a distance of 50 mm from the edge of the slabs, so the effective span was 1700 mm. The load was gradually increased with an increment of 0.3 kN till the failure. The results of load deflection curves are summarized in Figure (2.2).

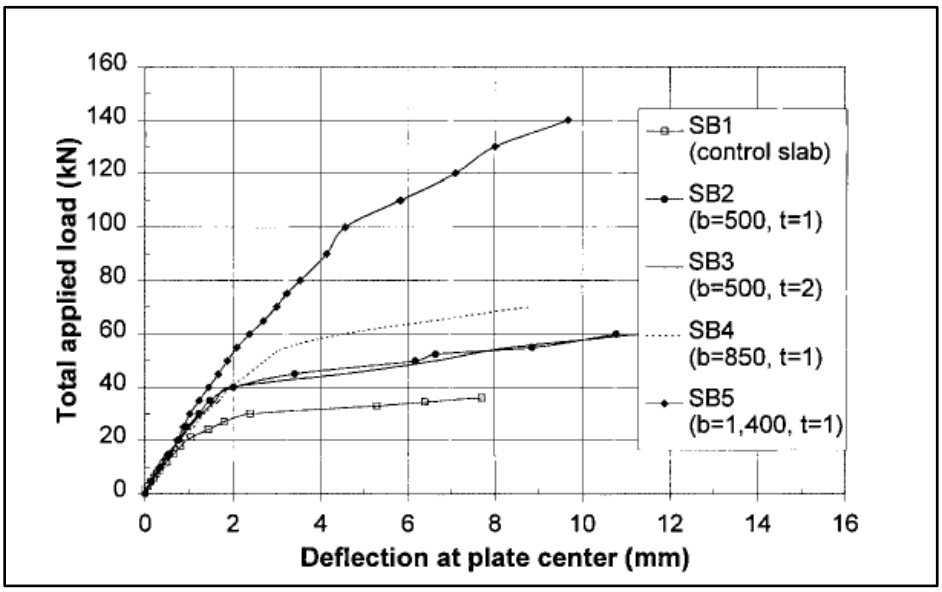

Figure (2.2): experimental load deflection curves [6]

The study found that this technique for strengthening had enhanced and increased cracking and ultimate load. Although the failure mode is mostly ductile for strengthened slabs. There was no debond failure that took place for all specimens. According to previous points, this technique is considered suitable for strengthening slabs.

Ebead and Marzouk (2002)[7] claimed to introduce an innovative strengthening technique for two-way slabs. In fact, the overall idea was previously mentioned by Zhang et. al. (2001)[6] but the method of anchoring the plates is different. Here, steel bolts were utilized to make the slabs and the plate work as a one unit. This method led to enhance the performance of two-way concrete slabs against flexural and shear stresses. The researchers used an epoxy resin in the holes of steel bolts. The experimental program consists of tests of five

square specimens with a side length and thickness equal to 1900 mm and 150 mm respectively. The corners of the specimens were free to lift.

Square cross-section columns were located at the middle of slabs specimens with dimensions of 250×250 mm, by which an axial load was subjected. The identity of the control slab is C, while the strengthened slabs were A1 to A4, all of them were simply supported along their edges.

The compressive strength of concrete mix was deigned to get 35 MPa at 28 days. Type of bar reinforcement was Grade 400 while the plates which were used for strengthening A 36. The thickness of steel strengthening plates were six millimeters. The steel bolts which were employed for fixing the plate had diameters 19 mm, type A 325. Epoxy adhesive was used to fill the holes of bolts before fixed them to enhance the bond strength.

Four different arrangements of steel bolts were evaluated, Figure (2.3) shows these patterns of arrangements.

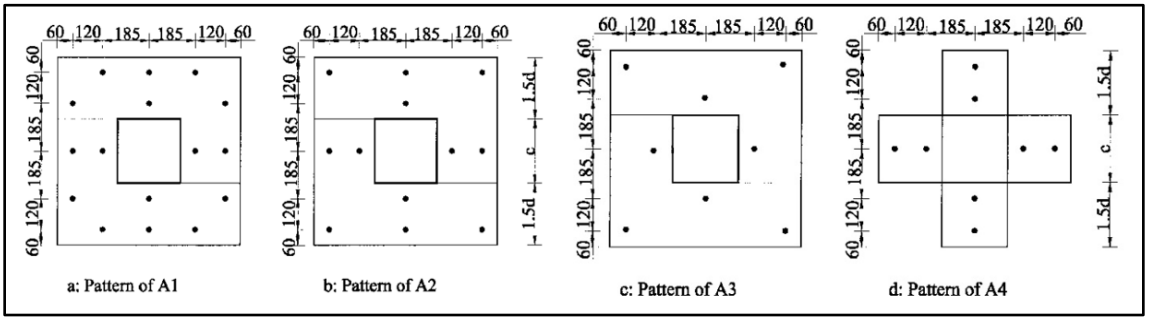

Figure (2.3): Arrangement's pattern of steel bolts [7]

This technique showed increases in both stiffness and energy absorption. Moreover, a slight improvement was achieved in ductility. The number of bolts was effective on ultimate load, it was increased by 56.5, 57.7 and 64.5 percent when number of bolts was 8, 12, and 16 sequentially, as a comparing with reference slab C (control slab). Load deflection curves are shown in Figure (2.4):

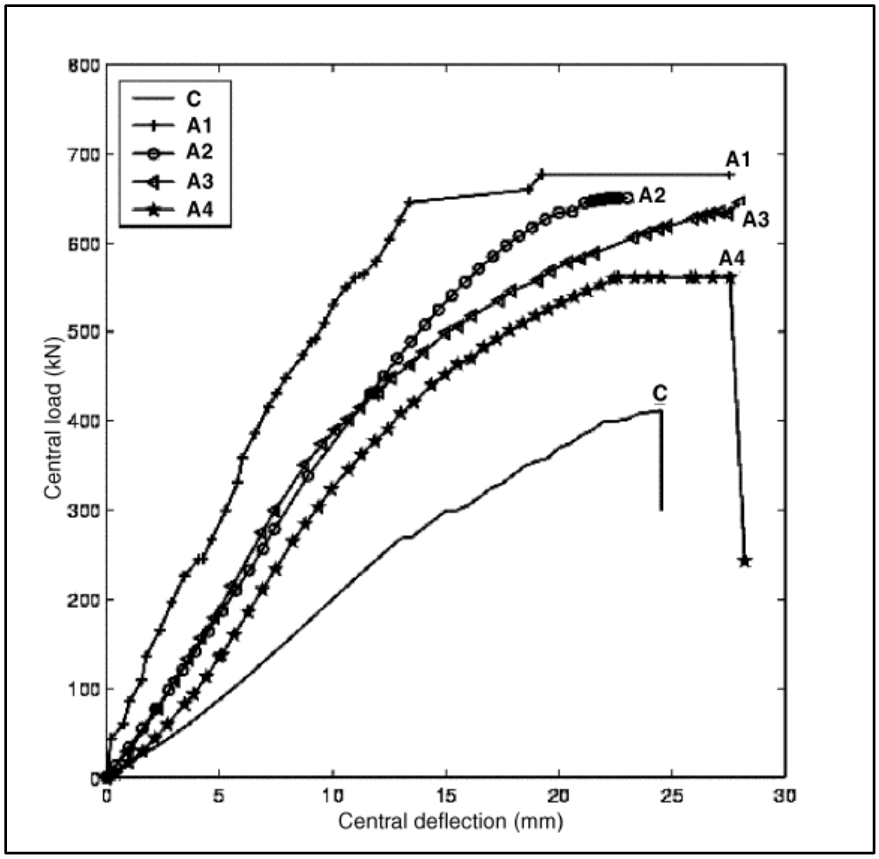

Figure (2.4): Load deflection curves for C, A1, A2, A3 and A4 specimens [7]

The most important conclusions were:

1- The recommended dimensions of the strengthening plate are equal to the dimension of the column plus four times the slab thickness, while the thickness was six millimeters.

2- The average ultimate load was increased about 53% over the control slabs.

3- The researchers suggested that the minimum number of fixing bolts were eight to make the strengthening steel plate and slab work as a one unit.

4- The average ductility was increased about 29% higher than the control slab.

5- The energy absorption of the strengthened slabs was approximately 100% higher than that of the control slab.

Rasheed and Al-Azawi (2013) [8] looked for the effect of the thickness, dimensions, and location of steel plates which they used for strengthening the reinforced one-way concrete slabs. Five specimens were experimentally tested with dimensions (60 ×600×1500) mm while the plates have different details as shown in Table (2.2) below. Each slab was reinforced with four longitudinal steel bars with a diameter of 6 mm at a spacing of 150 mm:

Table (2.2): Details of test specimens and strengthening plats [8]

Specimens type	Symbols	Slab dimensions (mm)	Steel plate dimensions (mm)
Slabs	S1 (control)	60×600×1500	No plate
	S2	60×600×1500	(1.5×100×600)
	S3	60×600×1500	(1.5×100×1200)
	S4	60×600×1500	(1.0×100×600)
	S5	60×600×1500	(1.0×100×1200)

One dial gage was put in the center of the slabs to measure the deflection when they were loaded. For all specimens, the load was applied at the one-third point as it illustrated in Figure (2.5).

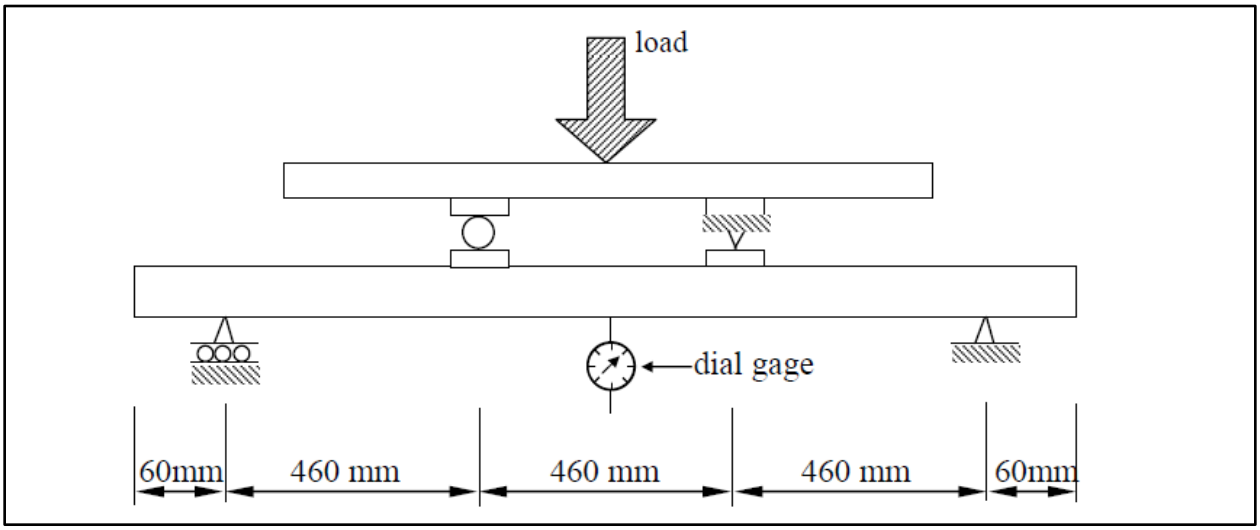

Figure (2.5): Sketching of the flexural test [8]

The researchers found that the overall behavior of slabs was improved. About 59.6% to 161.29 % for the cracking load while the ultimate load increased about 1.85% to 135 %. Also, they were observed in tests that the influence of the steel plate dimensions used in strengthening was significantly greater than the thickness of the plate. Summary of the experimental results were briefed in Table (2.3).

Table (2.3): Experimental results of test [8]

Slab specimen	$\rho = \frac{V.plate}{V.beam}$	Initial crack load (kN)	Debonding load (kN)	Experimental ultimate load (kN)	$\frac{\text{Ult. Load for Si}}{\text{Ult. Load for S1}}$
S1	-----	6.2	-------	16.2	1.0
S2	0.005	9.9	**	18.1	1.11
S3	0.01	26.9	37.9	38.1	2.35
S4	0.002	9.9	**	16.5	1.01
S5	0.004	16.2	29.1	29.1	1.79

** no debonding was observed.

Metwally (2014)[9] depended on previously available experimental results by Laith S. R. and Th. K. Al-Azawi (2013) to introduce a nonlinear finite element model for analysis of reinforced concrete slabs which were strengthened by steel plates. ABAQUS program was successful in making a good simulation close to the real behavior of strengthened slabs. The verification of this models showed in Figure (2.6).

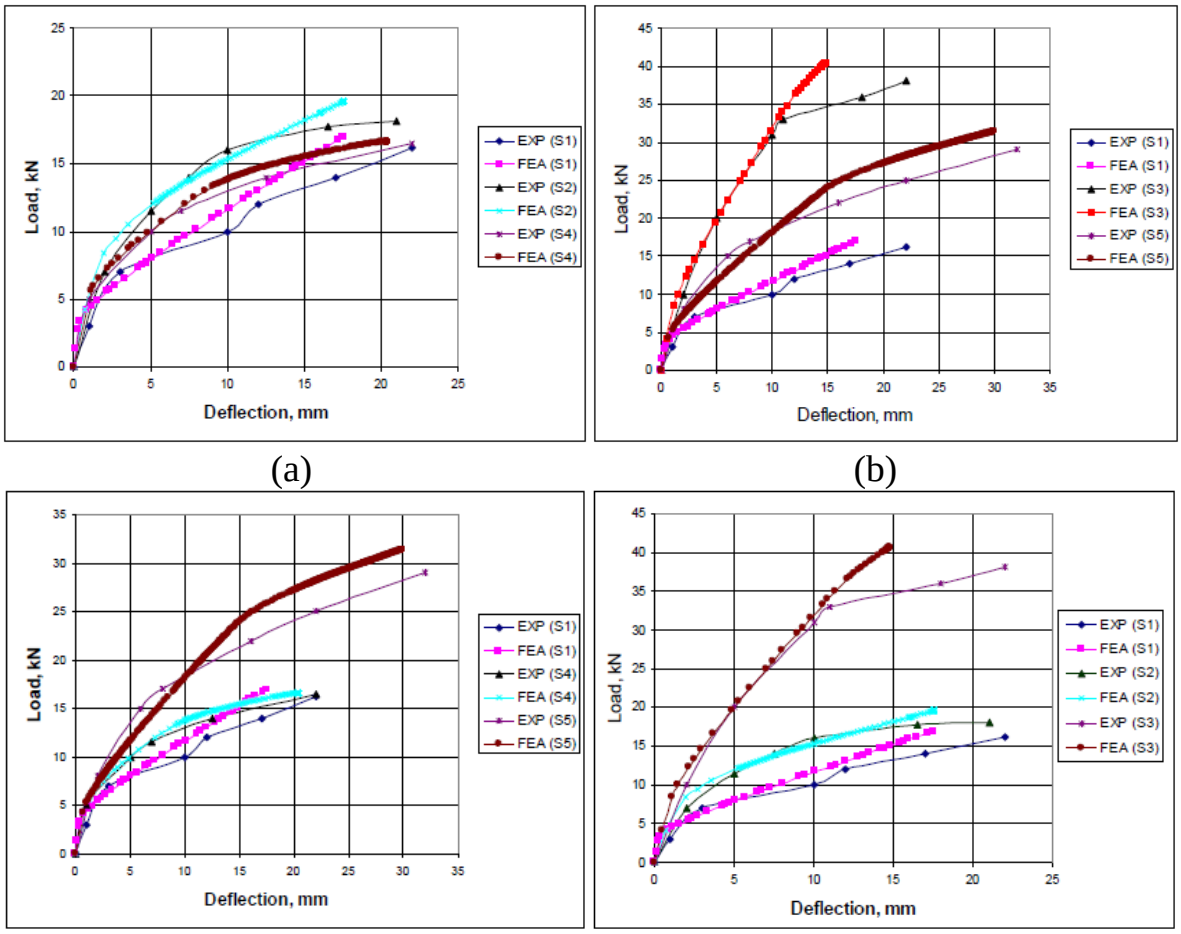

(a) plate thickness = 1.5 mm, (b) plate thickness = 1 mm, (c) plate length = 600 mm, (d) plate length = 1200 mm (see Table 2.2)

Figure (2.6): Load-deflection curves of strengthened slabs with steel plates (experimentally and finite elements model) [9]

Furthermore, parametric studies were done to evaluate the effect of steel plate thickness and epoxy layer strength on the performance of plated slabs. The influence of plate thickness was examined up to 7 mm; this study found that thickness contributed to increased stiffness and ultimate load up to 5 mm, after which the effect was ignored due to epoxy strength. Another parametric study found that using aluminum plates instead of steel plates for strengthening RC slabs resulted in a significant increase in both strength and stiffness when compared to un-plated slabs, as well as less stiffness, strength, and consequently high ductility when compared to those strengthened with steel plates.

The researcher demonstrated that the nonlinear finite element approach based on ABAQUS 3D models is a potent and reasonably efficient instrument that can successfully simulate the close to true behavior of reinforced concrete slabs.

Elbakry and Allam [10] presented in 2015 a practical concept used to increase the capacity of punching shear. An external steel plate with a shear anchor is used as a strengthening technique in two-way concrete slabs. The experimental program included casting five reinforced concrete slabs with dimensions of 1200×1200×100 mm. Simply supported under four edges, the span was 1000 mm. The load was subjected over an area of 100×100 mm up to failure. To demonstrate the effect of this technique on punching shear, the specimen had been controlled to fail in this mode of failure. The mesh reinforcing was *13ϕ 10* as it is clarified in Figure (2.5).

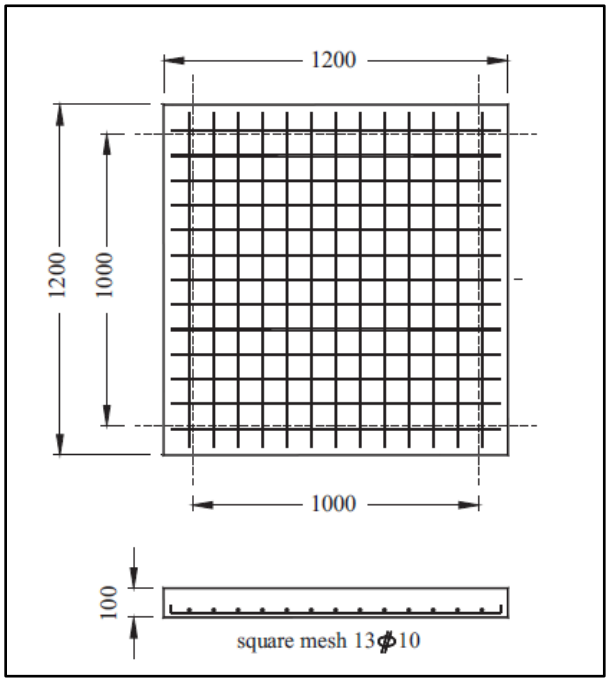

Figure (2.7): Details of slab reinforcement [10]

Four strengthened slabs were tested and compared with control one. The illustration of the preparing the specimen shown in Figure (2.8)

(a) Steel plate with shear studs **(b) slab with drilled holes**

Figure (2.8): Preparing the strengthened slab [10]

This technique can be considered a merge concept between two previous methods, using a suitable material for bond the plate to the tension face of slabs and using the shear studs for anchoring the plate. The steel plates were bonded to the concrete slab using an epoxy bonding and the holes around the studs were grouted using the same bonding material.

Two of the characteristics used in this study involve the plate, whereas the other two concern the anchor stud. The diameter and number of anchor studs, as well as the size and thickness of steel plate, were investigated. The Table (2.4) and Figure (2.9) summarize all of the details:

Table (2.4): properties of strengthened specimens [10].

Specimen	Plate size (mm)	Plate thickness (mm)	Stud diameter (mm)	Number of studs	f_{cu} (N/mm^2)
S-1	Control specimen, no strengthening plate				40
S-2	500 × 500	4	6	16	38
S-3	500 × 500	4	8	16	38
S-4	500 × 500	6	8	16	38
S-5	700 × 700	4	8	24	38

The major purpose of the experimental program was to examine the efficiency of employing external steel plates to strengthen reinforced concrete slabs subjected to punching shear.

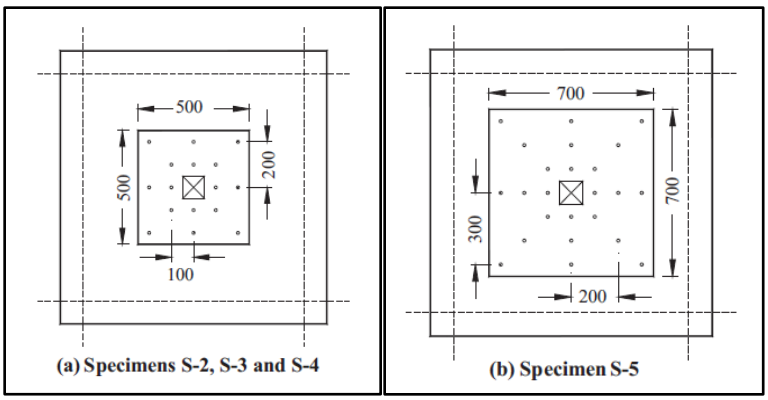

Figure (2.9): Details of strengthening steel plates [10]

Capacity of punching shear and stiffness were improved clearly in strengthened slabs. The obtained enhancements were 15 to 39 percent for punching shear capacity. The stiffness also increased since central deflection was decreased, the range of decreasing were from 44 to 60 percent. The amount of the improved performance was influenced by the plate size as well as the diameter and placement of the studs.

These parameters are more effective than steel plate thickness in increasing the punching shear capacity of reinforced concrete slabs.

The utilization of larger diameter and more studs resulted in a significant improvement in punching shear strength. According to Elbakry and Allam studies using a thicker plate had no noticeable influence on punching capacity.

2.3 Two Way Reinforced Concrete Slabs Using Self – Compacting Concrete

There is converse relationship between the compaction of fresh concrete and durability. Also, there is direct relationship between numbers of skilled workers and achieving suitable compaction. One solution for the optimal lines between these variables is the employment the self-compacting concrete. The researches began from 1980 till 1988 for success the first self-compacting concrete. Ozawa (1989), Okamura (1993) and Maekawa (1999) studied and developed this type of concrete, while the first printing of American Concrete

Institute (ACI) report was published in April 2007 under the series name (ACI 237R-07). Many researchers studied the behavior of concrete slabs using the self-compacting concrete.

Rasheed and Abduhameed (2012)[11] compared between the use of self-compacting concrete (SCC) and conventional concrete (CC) when they were used in two-way slabs. General behavior was experimentally investigated by testing six square slabs (900×450×80) mm reinforced by one layer of bar reinforcements, diameter 6 mm at each 150 mm. They were simply supported at four edges while they were loaded by sand bag over the top face of the slabs to simulate a uniform distributed load as shown in Figure (2.10). The sand bag pressed by a concentrated load at the center point by a universal testing machine. In fact, the simulation of uniform load is not suitable according to the force transfer principles. The six specimens were divided into three groups; each group represent case study about the effect of adding a synthetic fiber named polypropylene. The first two slabs had a 0% ratio, while the others had 0.07%, and 0.14% as a volume ratio.

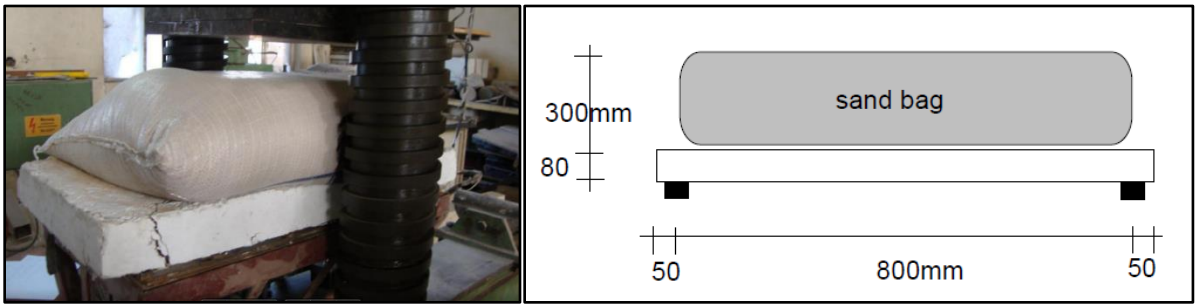

Figure (2.10): Slab loading method [11]

The fracture pattern, ultimate load, load-deflection response, and failure mechanism were used to evaluate the performance. The results indicated that the ultimate strength of SCC slabs was greater than that of CC slabs. The results also revealed that adding synthetic fibers improved the behavior and strength of slabs for both conventional and self-compacting concrete.

kumar and Chandra (2014)[12] explained the effect of shape and size of opening on reinforced concrete slabs using self-compacting concrete. Experimental program included 14 specimens 600×600×60 mm. Two specimens were cast as a reference, without opening whereas the remaining specimens had different shapes and size of openings. Every two slabs are similar, the square opening shape 50 and 150 mm while the circle opening had diameter 50 and 150 mm as shown in Figure (2.11):

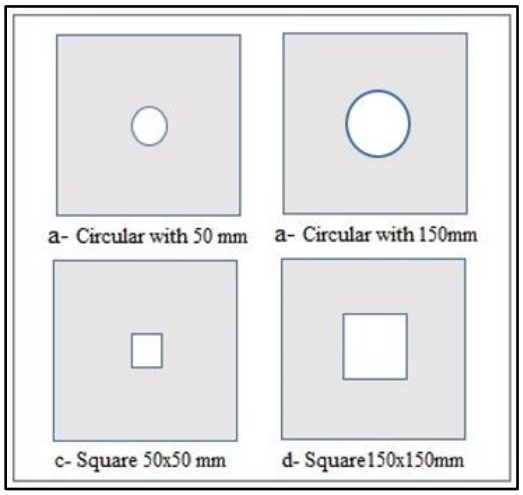

Figure (2.11): Shape and size of opening

The name and maximum load carrying capacity with corresponding deflection are clarified in Table (2.5):

Table (2.5): Summary of Flexure Test Results [12]

Name of samples	S1-1 and S1-2 (S1)	S2-1 and S2-2 (S2)	S3-1 and S3-2 (S3)	S4D-1 , S4D-2 (S4D) S4-1 , S4-2 (S4)	S5-1 and S5-2 (S5D) S5-1 and S5-2 (S5)
Shape and size of opening	Slab without opening	Square with 50x50mm	Circular with 50mm dia	Square with 150x150mm	Circular Opening 150mm dia
Average Ultimate Load (kN)	36.75	34.0	34.85	26.75 32.5 (D)	25.0 29.7 (D)
Maximum Deflection (mm)	7.50	7.2	7.62	6.65 7.33 (D)	5.96 6.57 (D)

* The D refer for diagonal reinforcement around the opening are existed

The load was subjected at four points on the top face of slabs in testing machine as can be seen in Figure (2.12). load deflection curves for the slabs with and without opening were plotted and compared.

Figure (2.12): Slab testing and loading type [12]

The results showed that a 50mm square opening reduces the slab's strength by 6%, while a circular opening reduces it by 4.10%. In addition, decrease in strength of slab with 150 mm square opening is 31.5% while for circular opening is 26.02%. moreover, the diagonal reinforcements which were provided around the opening increases the strength about 9.2% in case of 150 square opening and 16.9% in case of 150 mm circle diameter.

Patil and Harish (2015)[13] investigated the effect of adding steel fiber to high strength self-compacting concrete under partial uniform load. The experimental program included of preparing and casting eight specimens with different percentages of steel fibers and testing them. Four specimens were high-strength traditionally vibrated concrete (HSTVC) and the other four were high-strength self-compacting concrete (HSSCC). The different ratios of crimped steel fibers that were utilized (0.25, 0.50, 0.75 and 1.0) %. All specimens were square under simply supported with an effective span 900 and 1400 mm in short and

long directions respectively, the slabs extended 50 mm beyond the supports on all four sides. Thickness of slabs were 75 mm. The researchers tried to simulate the uniform load as possible as could through using sixteen load points over the top surface of the slabs, which could work as a load disperser, just like in Figure (2.13).

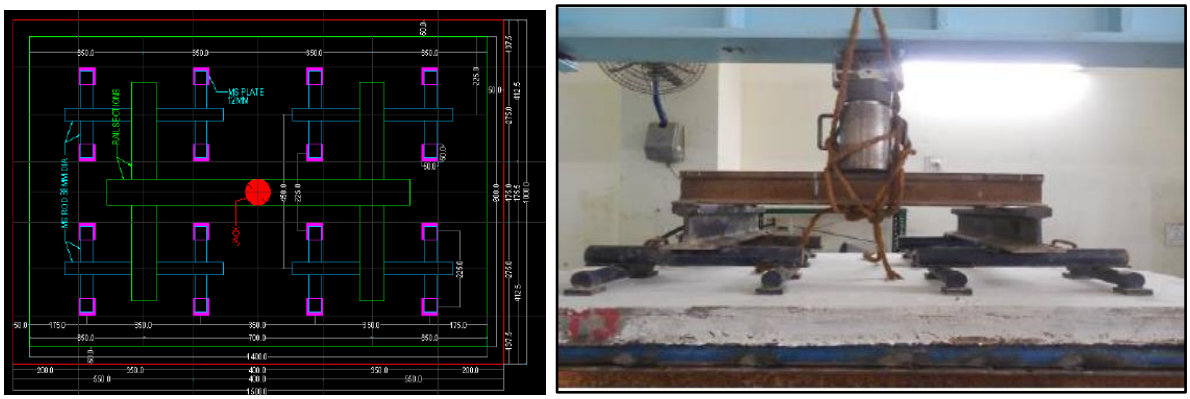

(a) Simulated (top view) **(b) Real (side view)**

Figure (2.13): distribution of load disperser (Pattern of subjected load) [13]

The results showed that the maximum resistance loads improved from 180 KN to 226 KN for HSTVC specimens and improved from 168 KN to 220 KN for HSSCC specimens while the value of deflections reduced from 17.5 mm to 16.35 mm for HSTVC and reduced from 18.89 mm to 17.22 mm for HSSCC specimens. All previous enhancement happened through increasing the percentage of steel fibers as 0.25%, 0.5%, 0.75% and 1%. These results proved that the percentage of steel fibers has a direct relationship with improvements in overall behavior when it is added to self-compacting concrete.

Ismael (2015)[14] also tested eight slabs to investigate the effect of adding steel fibers on normal-strength self-compacting concrete and compared this addition when it was used to add them in high-strength self-compacting concrete. All slabs have the same dimension of 450 × 450 × 50 mm. It is found that increasing the steel fibers in normal-strength SCC is more efficient than increasing them in high-strength SCC. When the percentage of steel fiber in

normal strength SCC increased from 0% to 0.8 percent, the first crack load, ultimate flexural strength, and ultimate deflection increased by percentages (51.4, 24.7, and 30.8) percent respectively when compared to non-fibrous SCC slab, while the increases in high strength SCC were (18.2, 19.2, and 17.1) percent respectively.

Taha Masoud et. al. (2017)[15] tried to produce light weight SCC by using expanded clay aggregate (LECA) and study the effect of using this type of concrete on behavior of slabs. Six different mixes of (LWSCC) were cast and tested to find out the values of slump flow, G-ring, and compressive strength. Based on the results obtained, the best mix was selected to study the effect of the reinforcement ratio on the behavior of (LWSCC) slabs. The investigation examines also the behavior of the (LWSCC) slabs exposed to fire.

Loading was applied by using a hydraulic jack (50-ton capacity) at two points on the top face of the slabs as it is depicted in Figure (2.14). The load was provided through the jack in small increments while a dial gauge at the center point of the slab was used to record the slab middle deflection up to failure.

Figure (2.14): Test set-up [15]

In this research, three specimens were tested and the results of the experimental tests, including flexural loads and deflection, were evaluated. Due to their larger diameter and spacing (50×50) mm, slab (S3) reinforced with wire mesh 5mm diameter obtained the highest value of ultimate load, whereas slab (S1) reinforced with wire mesh 3mm diameter obtained the lowest value of ultimate load due to their smaller diameter and spacing (30×30) mm. The failure loads of slabs (S2) and (S3) increased by 42% and 23% respectively, compared to slab (S1). The first crack load for slabs (S2 and S3) increased by 50% and 125% respectively, compared to the first crack load of slab (S1). The failure load after being subjected to fire decreased by 20%, 22%, and 26% for slabs (S1F, S2F, and S3F) respectively compared to the slabs (S1, S2, and S3). According to previous work, it can be said that the results demonstrated the possibility of obtaining a structural (LWSCC) with low density and with acceptable resistance to fire through the use of expanded clay aggregate (LECA). Also, the work showed that the failure loads of slab (S2) and (S3) increased by 42% and 23% respectively, compared to slab (S1). For the slabs (S1, S2, S3, S1F, S2F, and S3F) at the same chosen load (2.5 ton), the slabs (S1F, S2F, and S3F) deflections were increased at the mid span by about (42%, 58%, and 10%) in comparison with the control slabs (S1, S2, and S3) respectively.

2.4 Using Perforated Steel Plate in Concrete Slabs

The chemical adhesion force between concrete and steel is not enough for structural purpose so the researchers tried to provide a mechanical interlock like the replacement of plain reinforcement by deformed one. Nearly, the same things happened when using the steel plates. In 1987, a new type of shear connectors was developed by using steel plate with a suitable number of punched holes called **perfobond rib** as it is shown in Figure (2.15), which was introduced in

recognition of the unsatisfactory behavior of shear studs resulting from fatigue problems caused by live loads on composite bridges [16-22].

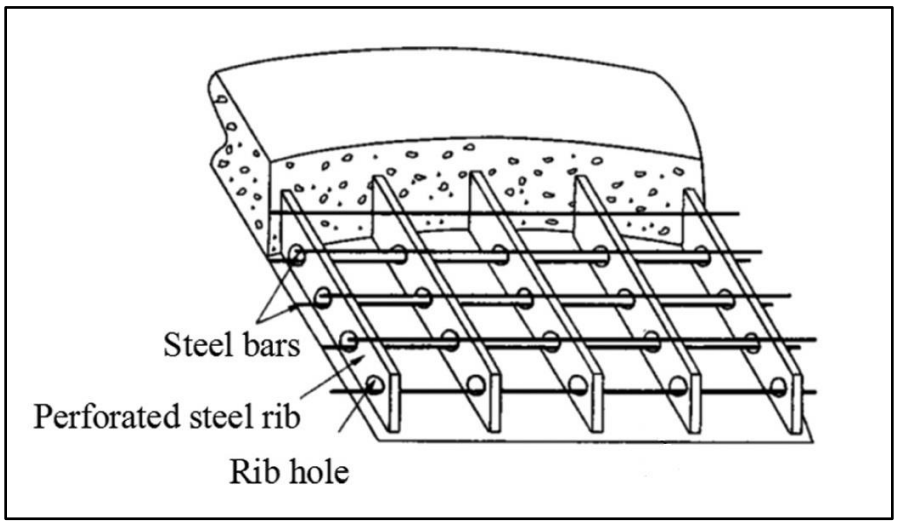

Figure (2.15): Concept of perfobond ribs [28]

Veldanda and Hosain (1992) [23] published a paper summarized the outcome information of 48 push-out specimens tested to determine the viability of utilizing perfobond rib as a type of shear connections in composite beams. The perfobond rib shear connection was described as a flat steel plate with a number of holes. The results show that perfobond rib connectors may be utilized successfully in composite beams, with test specimens showing a substantial increase in performance when extra reinforcing bars were inserted through the perfobond rib holes.

Oguejiofor and Hosain (1994) [24] conducted a parametric study of perfobond rib shear connectors, using test specimens designed to investigate the influence of various factors on the shear capacity of the connection. The main parameter was the effect of transverse reinforcement, so the study included the change of number and spacing of rib holes and concrete compressive strength. Results of 40 push-out test specimens were detected and discovered that appropriate transverse reinforcement in the highly stressed region can increase the shear capacity of the perfobond rib connector by about 70%. In general, the

perfobond behaves very stiff in service load and has good ductility in post-service load.

Kim and Jeong (2006) [25] tried to benefit from previous type of shear connectors in deck slab, the suggested deck profile is shown in Figure (2.16). The main purpose of the study was to check the validity of useing this type of shear connectors in slabs.

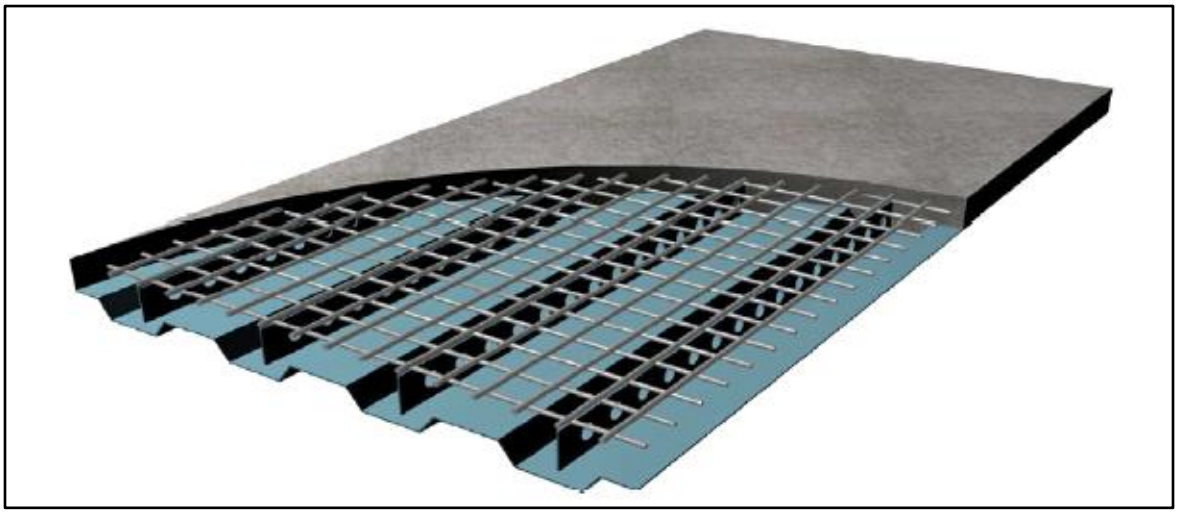

Figure (2.16): Schematics for the proposed deck profile [25]

According to test results, the perfobond ribs can be successfully and efficiently utilized for shear connection in steel–concrete composite decks, and the composite deck evaluated in this study has a ductile behavior.

In **(2009)** [26], The same authors also conducted an experimental investigation of a steel-concrete composite bridge deck slab with perfobond shear connections, as illustrated in Figure (2.17). Two deck slab specimens were statically loaded and tested to determine the ultimate load-carrying of the proposed deck slab system.

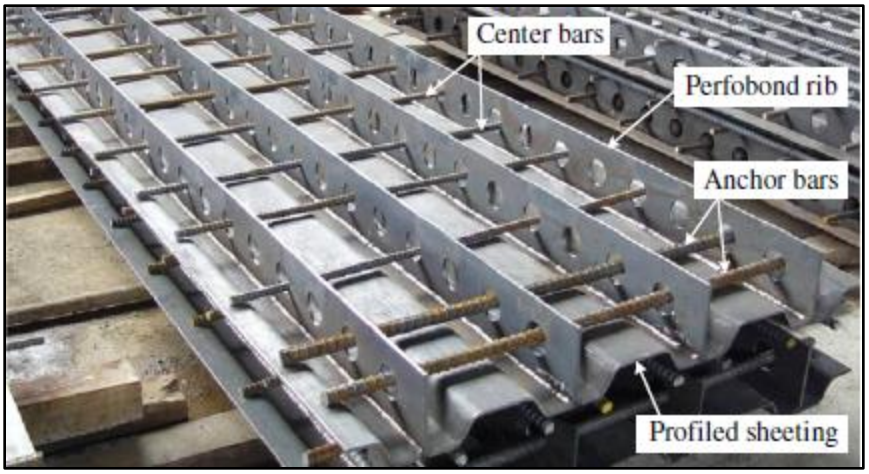

Figure (2.17): Fabrication of the suggested deck profile [26]

The test observations show that the proposed deck system's ultimate load-carrying capacity is at least 220 percent more than that of the RC deck system, and that the deck weighs about 23 percent less than the RC deck system.

Another investigation was done in 2010 by the same authors [27]. The primary objectives of this research were to develop a composite deck slab for girder bridges that spans longer but weighs less than a typical reinforced concrete (RC) deck slab.

Different lengths of shear span were examined for eight deck slabs, specimens encoding and adopted shear span lengths are clarified in Table (2.6).

Table (2.5): Different lengths of shear span [27]

Specimen ID	L_s
SF-1	L/5.3
SF-2	L/5.3
SF-3	L/4.0
SF-4	L/4.0
SF-5	L/3.0
SF-6	L/3.0
SF-7	L/2.0
SF-8	L/2.0
RC-1	L/4.0
RC-2	L/2.0

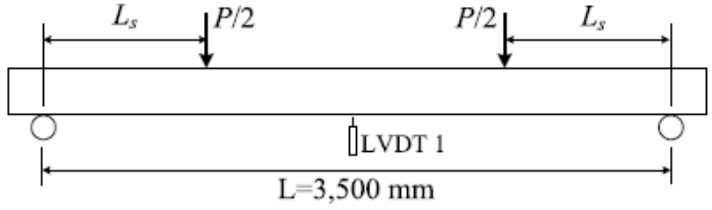

The load deflection curves are given in Figure (2.18).

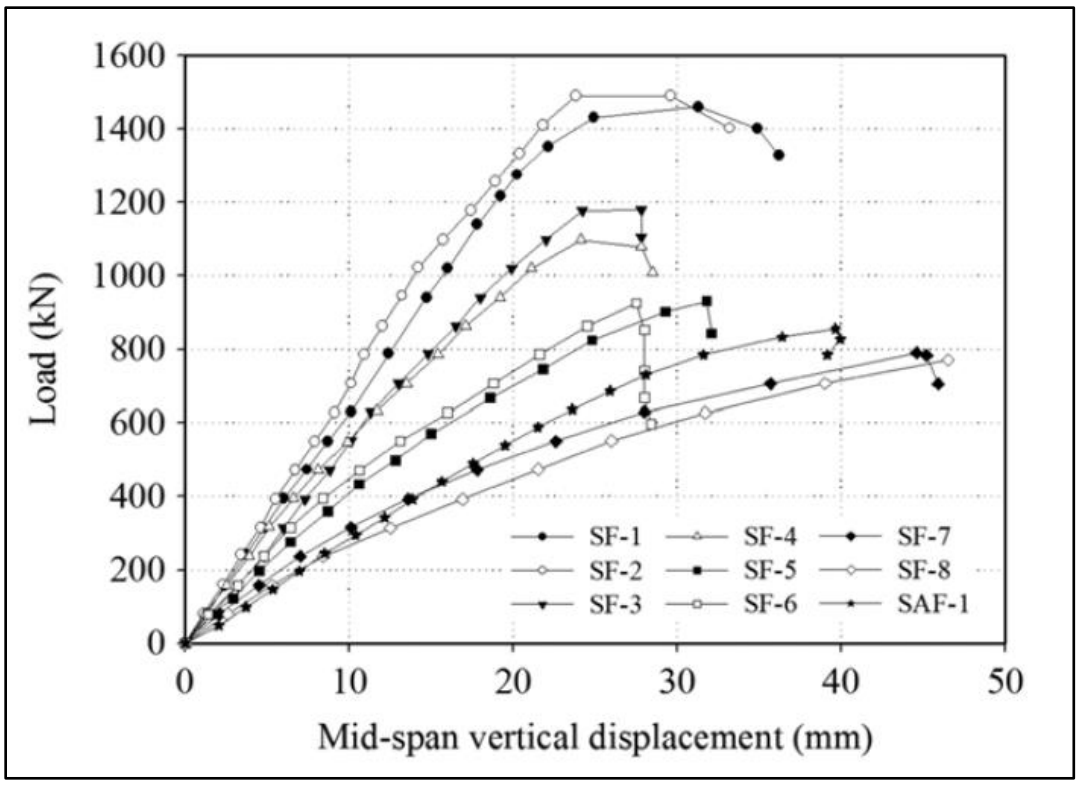

Figure (2.18): Load deflection for specimens [27]

The suggested deck system's ultimate strength and first concrete cracking load are roughly 2.5 and 7.1 times greater than those of a normal reinforced deck slab, respectively, while the deck weighs approximately 25% less than RC deck systems.

Yize Zuo et. al. (2018) [28] tried to illustrate the effect of using the perforated L-shape steel ribs on load carrying capacity when it used in two-way concrete slabs as shown in Figure (2.19).

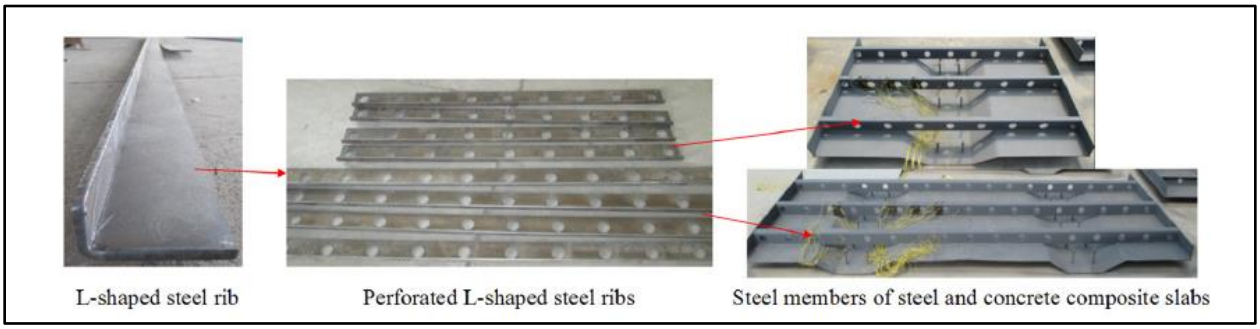

Figure (2.19): L-shaped steel ribs [28]

The experimental program consists six specimens with two types of steel ribs: L-shape and plain shape. All the samples' dimensions were equal to (1680×1200×150) mm. The study consists comparison between slabs with plain perforated ribs and L-shaped perforated ribs as given in Figure (2.20).

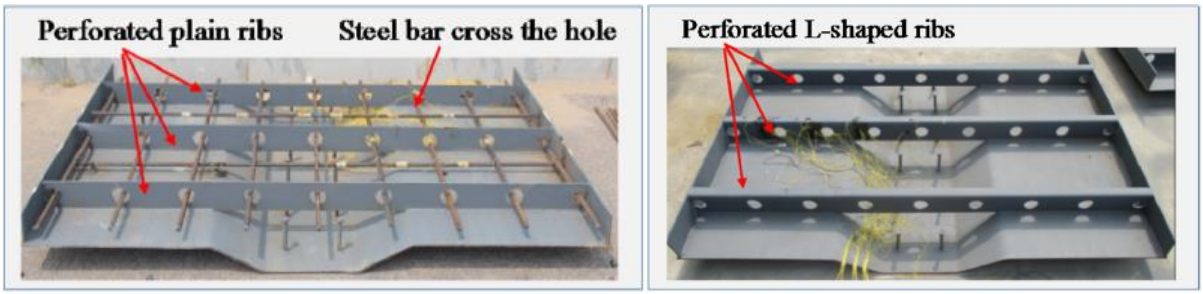

Figure (2.20): Plane versus L-shaped perforated steel ribs [28]

In general, the results prove that the perforated ribs improve flexural and shear strength of composite slabs, but the L-shaped rib was better than the plain rib when it was used in two-way concrete slabs. Perforated L-shaped ribs result in reducing the shear failure risk of composite slabs, thus having promising application.

On the other hand, **Liu and Yang (2021)** [29] tried to decrease the effect of fatigue damage and study the mechanical behavior of steel-plate-concrete composite slabs, which is shown in Figure (2.21) under low-cycle fatigue loads and static tests.

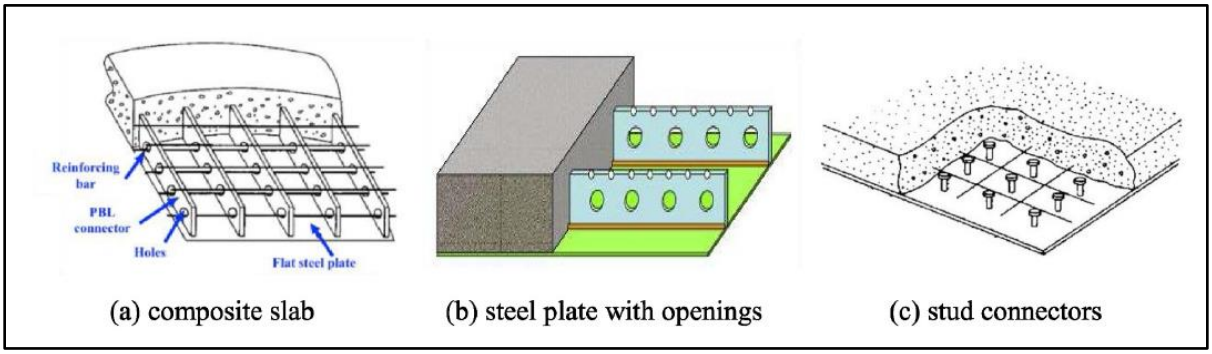

Figure (2.21): The schematic diagram of flat steel plate-concrete composite slabs [29]

The composite slab with steel plate with openings had good interaction between the bottom steel plate and the top concrete, and strain distribution could generally agree with plane-section assumption. The shear capacity of the composite slab satisfied the requirement for prevention of slippage, and the composite slab, without fatigue fracture failure, could still develop adequate residual capacity and flexural rigidity after fatigue loads.

Regardless of the type of the structural member, some research may have some relevance to use the effect of using internal steel plates for shear reinforcement instead of traditional reinforcement bars (stirrups) on the flexural behavior of SCC beams, as well as the effect of spacing and thickness on strength [30]. In addition, other studies investigated the effect of bond behaviors of chequer steel plate in concrete beams, looking for the effect of lozenges of the chequer steel plate, the use of steel bolts, the thickness of the concrete cover on the bond behavior and the behavior of bubbled wide reinforced concrete beams with different shear steel plate spacing [31, 32]. Ibrahim et al. (2018) [33] present an experimental study on the strength of bubbled wide reinforced concrete beams with different types of shear steel plates through testing of eight specimens with dimensions of 215×560×1800 mm. In 2021, Qaddoory et al. published two papers: the first about the replacement of the main reinforcements by steel plates in reinforced concrete beams; the second paper studied the effect of using different aspect ratios of longitudinal steel plates. The steel plates were used instead of traditional steel bars with different thicknesses of 4 mm, 5 mm, and 6 mm placed vertically inside the lower part of the beam [34, 35].

2.5 Concluding Remarks

According to the previous review, there are some essential points that can be summarized as follows: -

1- There are some researchers used the steel plate for strengthening slabs and there are some techniques that were used.
2- There are other researchers studied the validity of using a special type of concrete called self-consolidating concrete in two-way slabs and the results proved that it is a good special type of concrete through several comparisons that have been done between traditional concrete and self-consolidating concrete.
3- According to the adopted "key words" that are investigated, there are no studies that use the perforated steel plate as a reinforcing system instead of the bar reinforcement under concentrated and uniform load. Put into consideration that the plate without making openings in it cannot be used as a reinforcing system, that is to give an interlock between steel plate and concrete.

Hence, the experimental study of using perforated steel plate as a reinforcing system instead of traditional reinforcement is carried out in this study, and it is considered a new technique that needs plenty of studies to stand on their advantages and disadvantages. It is necessary to use self-compacting concrete to ensure that the concrete fills all the parts of the formwork under the plates without any voids inside. In other words, the success of this study may open a new promising method for reinforcing slabs system in the future.

CHAPTER THREE
EXPERIMENTAL WORK

3.1 General

The main objective of this experimental work is to investigate how well perforated steel plates may improve the behavior of two-way slabs when they are used as a reinforcing technique. This chapter includes information about the materials utilized experimentally as well as a set of standard tests. The sequence of the actual work, which included supplying the necessary materials, laboratory tests for these materials, trial mixes with fresh and hardened tests, techniques for providing perforated steel plates, and the final objective work which concern specimens to simulate slabs reinforced by perforated steel plates, were all covered in this section.

The experimental work was carried out in the laboratories of the college of engineering / University of Kufa.

3.2 Material Properties

The main items of materials that were employed to achieve the experimental work are cement, fine aggregate, coarse aggregate, mineral admixture, chemical admixture, bar reinforcement and perforated steel plate. All these materials are described below.

3.2.1 Cement

An ordinary Portland cement was used in the work type Lafarge-Cresta. The physical and chemical properties were tested in the quality control laboratory at Kufa University. The results are summarized in appendix A.

3.2.2 Fine Aggregate

Fine aggregate was tested in the laboratory of quality control at the University of Kufa. As indicated in the diagram below, the fine aggregate satisfied the requirements of the second zone of the Iraqi standard.

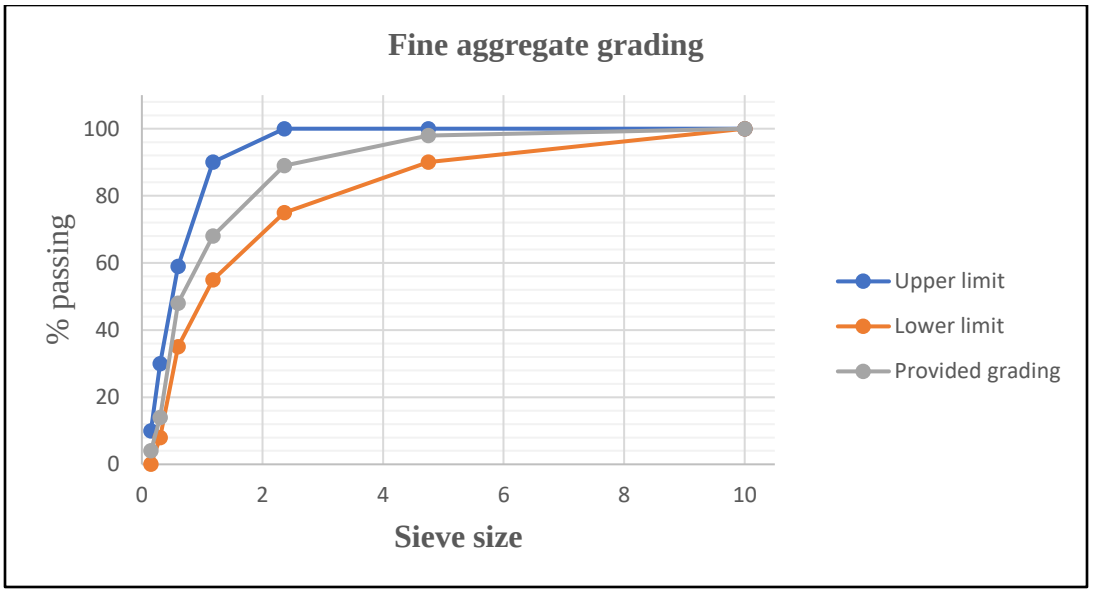

Figure (3.1): Grading of fine aggregate

Also, the ratio of clay was 3.8 % while the IQ specification specified the maximum value is 5%. Figure 3.2 shows some main steps of test.

Figure (3.2): Fine aggregate test

3.2.3 Coarse Aggregate

The coarse aggregate should be rounded as possible as can, smooth texture and a maximum size from 12 to 20 mm. For the slab models tested in the present study, the maximum size of aggregate adopted is 14 mm. Special grading was produced according to previous requirements. It is clarified in Table 3.1, a, b and c.

Table (3.1): grading of coarse aggregate

a) Iraqi specification			*b) Demand grading*			*c) Provided grading*	
Sieve	**% Passing**		**Sieve**	**% Passing**		**Sieve**	**% Passing**
37.5	**100**		**37.5**	**100**		**37.5**	**100**
20	**95-100**		**20**	**100**		**20**	**100**
14	**No requirement**		**14**	**100**		**14**	**100**
10	**30-60**		**10**	**30-60**		**10**	**32**
5	**0-10**		**5**	**0-10**		**5**	**1**

The ratio of clay in coarse aggregate was very low, it was 0.27 %, the IQ specification recommended less than 3%. Figure 3.3 illustrates the selection of test sample, sieve analysis and the clay ratio test.

a) chosen the sample of test *b) sieve test* *c) ratio of clay test*

Figure (3.3): Coarse aggregate test

3.2.4 Mineral Admixture (Silica Fume)

Silica fume is a pozzolanic material which is used to produce high-performance concrete, which can be seen in Figure 3.4. It has micro spherical particles that participate to increase the fine materials in the batch to give good cohesion and

reduce both segregation and bleeding. The ratio of using this material depends on the trial mixes.

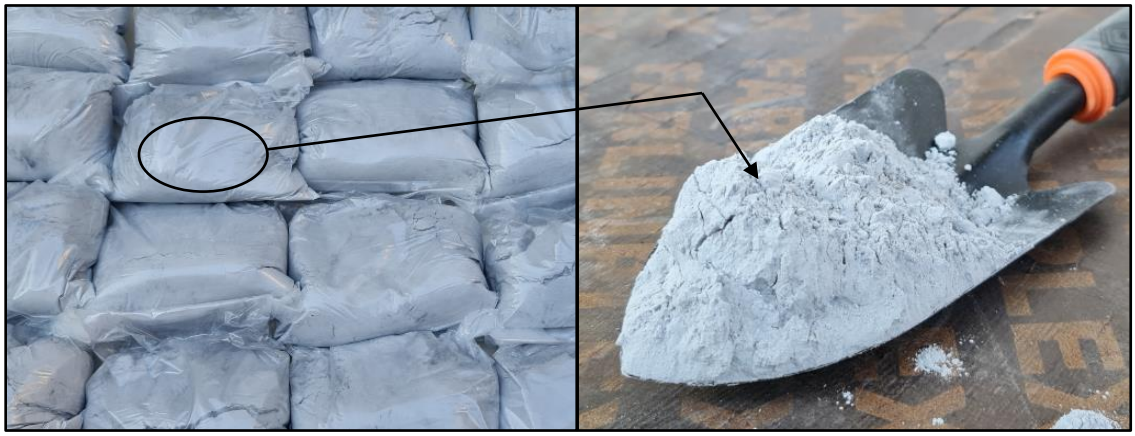

Figure (3.4): Slica Fume

3.2.5 Chemical Admixture

One of the most essential elements for achieving self-compacting concrete is using a high-performance concrete superplasticizer. The type which was used is called Glenium 54. It is compatible with all Portland cements. This type is free from chlorides and complies with ASTM C494 type A and F as shown in Figure 3.5.

The pozzolanic material is not only used to give high workability and improve the surface finishing, but also used to improve the consistency of the mix to prevent both segregation and bleeding.

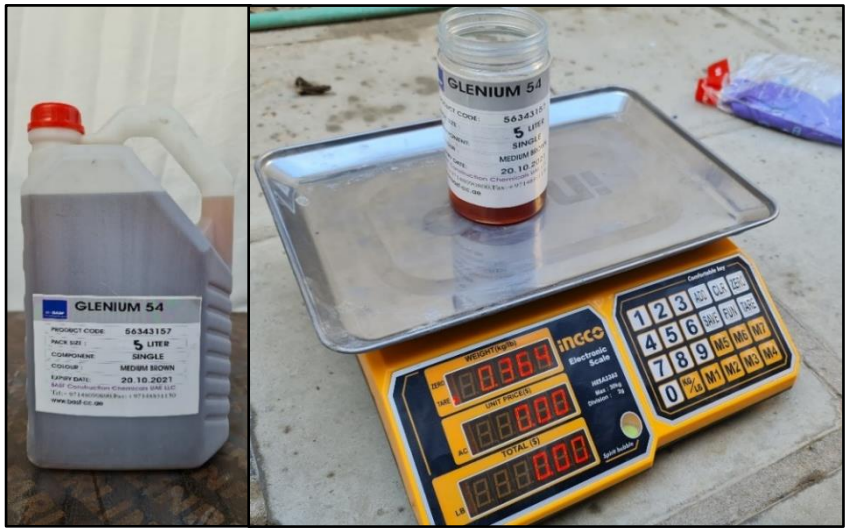

Figure (3.5): Glenium 54

3.2.6 Steel Reinforcing System

Two types of reinforcing systems were discussed in the present work which were used for reinforcing concrete slabs; the traditional method by steel bar and the proposed method by perforated steel plate.

3.2.6.1 Traditional Reinforcement

In this project, deformed steel bars with a diameter of 6 mm were employed. The yield tensile test was performed at the materials laboratory in the College of Engineering / Materials Engineering department at the University of Kufa (see Figure 3.6). The testing equipment included a computerized control system, and all results could be seen on the computer screen or exported to an excel sheet. The utilized bars have an average yield tensile strength of 590 MPa and an average ultimate strength of 878 MPa.

Figure (3.6): Steel bar testing

Next, Figure 3.7 shows the stress strain diagram for one of these selected specimens' bars.

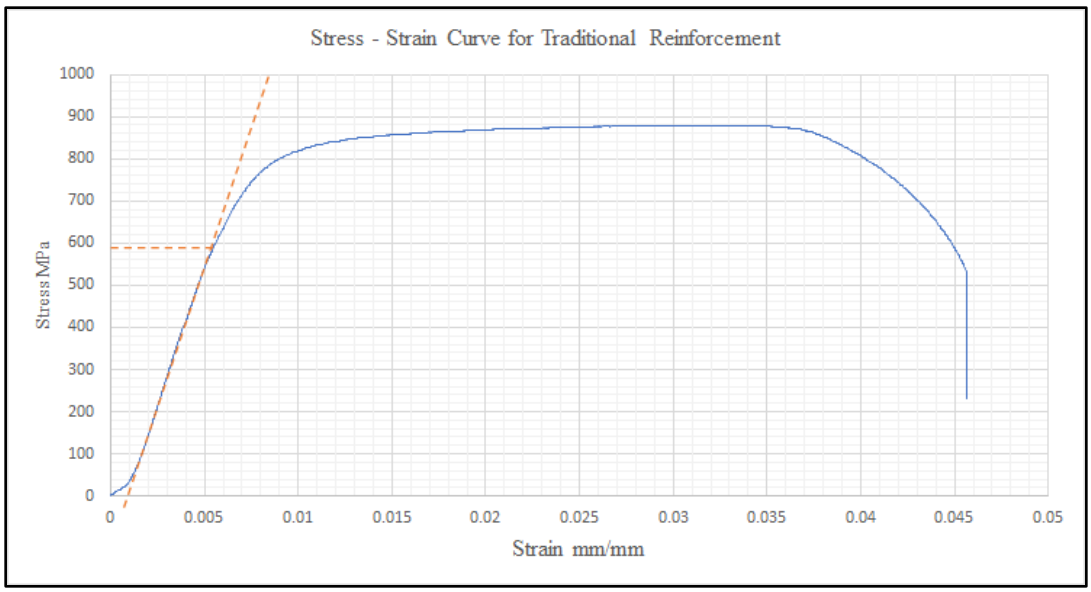

Figure (3.7): Stress strain diagram for traditional reinforcement

3.2.6.2 Perforated Steel Plate

In early stage, a sample from a plate was obtained to do a pre-calculation in order to determine the appropriate opening size. The samples were taken from an Iranian steel plate with an actual thickness of 1 mm, measured by micrometer, which can be noticed in Figure (3.8). According to the test, the average yield strength is 280 MPa, whereas the ultimate strength is 473 MPa.

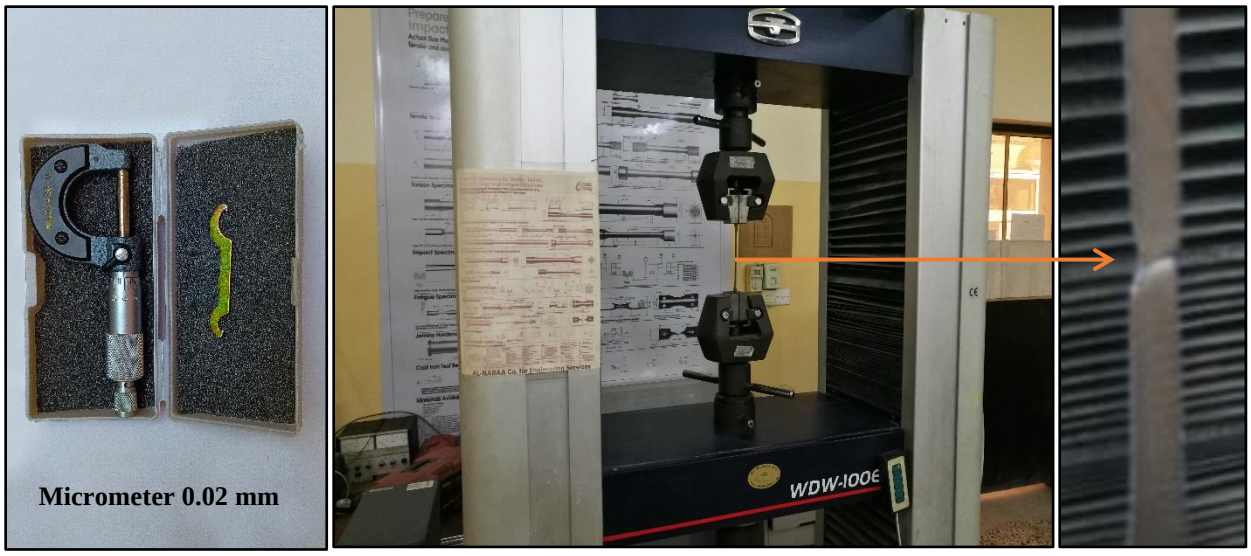

Figure (3.8): Testing of steel plate

The results were very suitable for making a perforated plate that has an equivalent property of traditional reinforcement. The two samples were tested according to ASTM E8 / E8M – 16a requirements [36], see Figure 3.9.

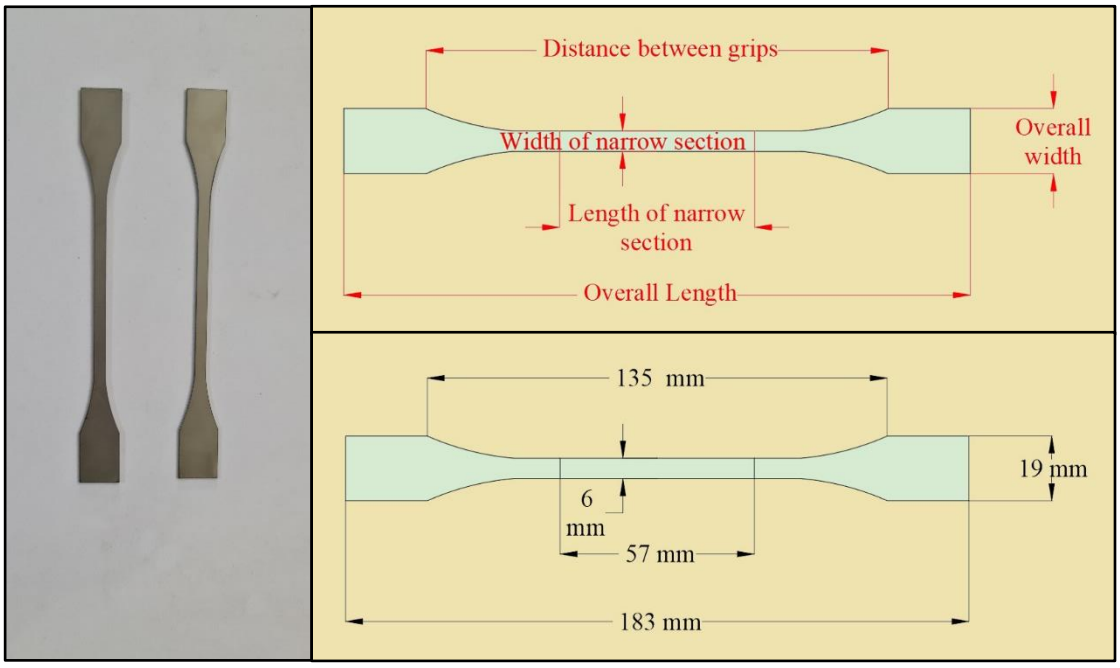

Figure (3.9): Test samples of steel plate

The stress-strain diagram for one tested specimen is clarified in Figure 3.10.

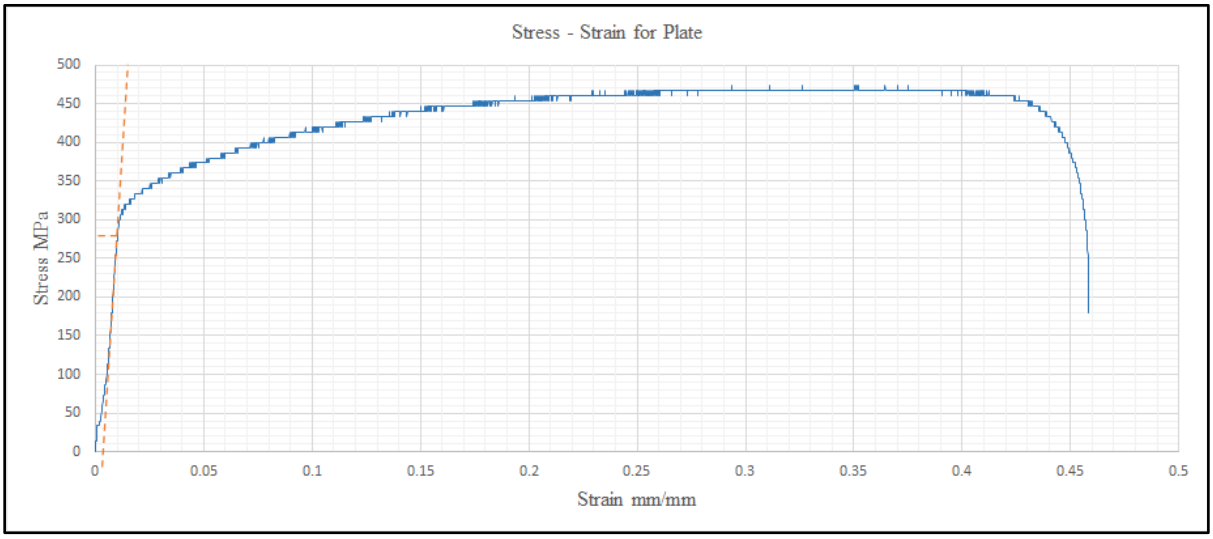

Figure (3.10): stress strain curve for steel plate

3.2.6.3 Preparing the Perforated Steel Plate

The openings of the plates were made by a Fiber Laser Cutting Machine (XQL-1330) in the Imam Ali Holy Shrine – CNC department.

The machine (XQL-1330) is computerized-controlled and very accurate. The positioning accuracy is less than 0.1 mm/m. All details concerning the machine are clarified in Appendix B. The input data and all details of the required opening were previously prepared and drawn by the Auto Cad program and fed to the machine.

Three main shapes were made: circle, octal and square shapes as shown in Figure 3.11.

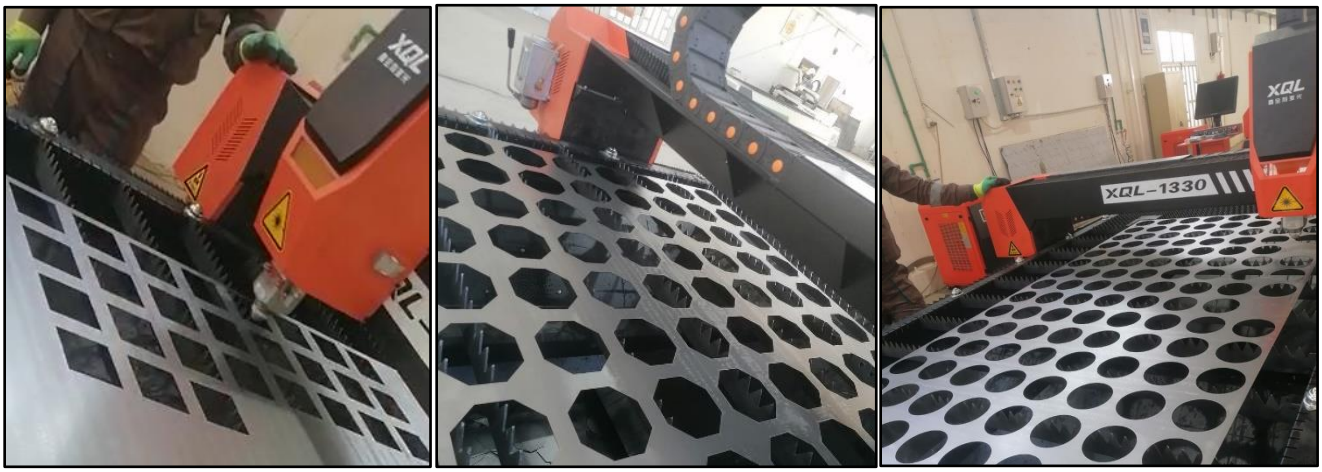

(a) Square openings **(b) Octagonal openings** **(c) Circular openings**

Figure (3.11): Shapes of opening

Each shape has three sizes; small (Opening Aspect Ratio, OAR, = 3.26×10-3), medium (Opening Aspect Ratio, OAR, = 8.17×10-3) and large openings (Opening Aspect Ratio, OAR, = 32.68×10-3). Each size was duplicated, one used for reinforced slabs and tested under concentrated load and the other used for testing slabs under uniform load. All adopted shapes and sizes are documented in Figures 3.12, 3.13, and 3.14.

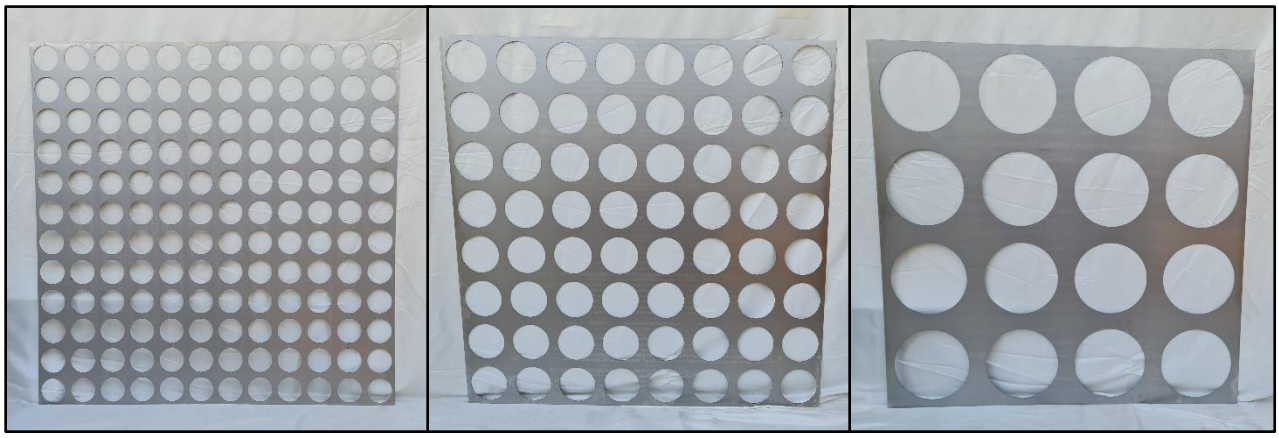

Figure (3.12): Sizes of circular openings

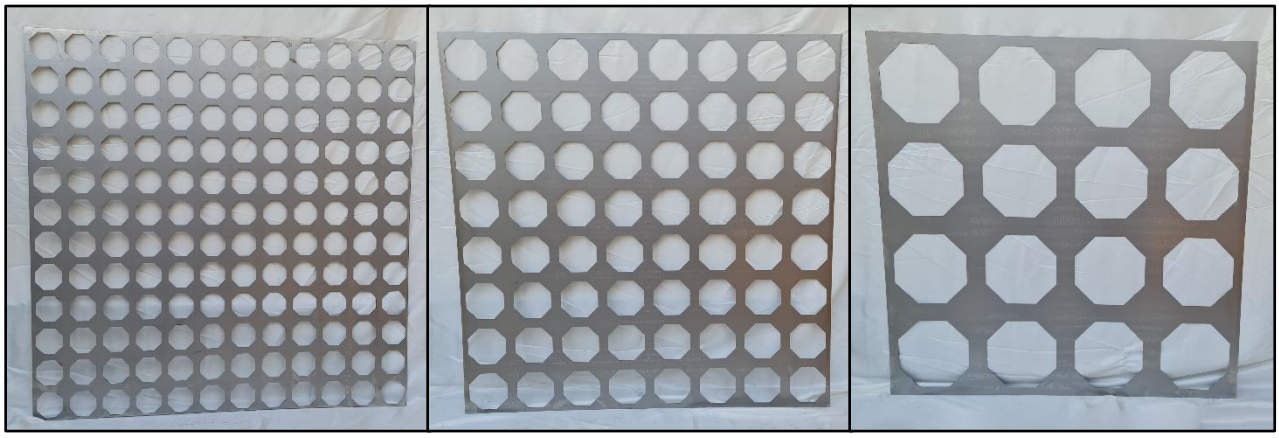

Figure (3.13): Sizes of octal openings

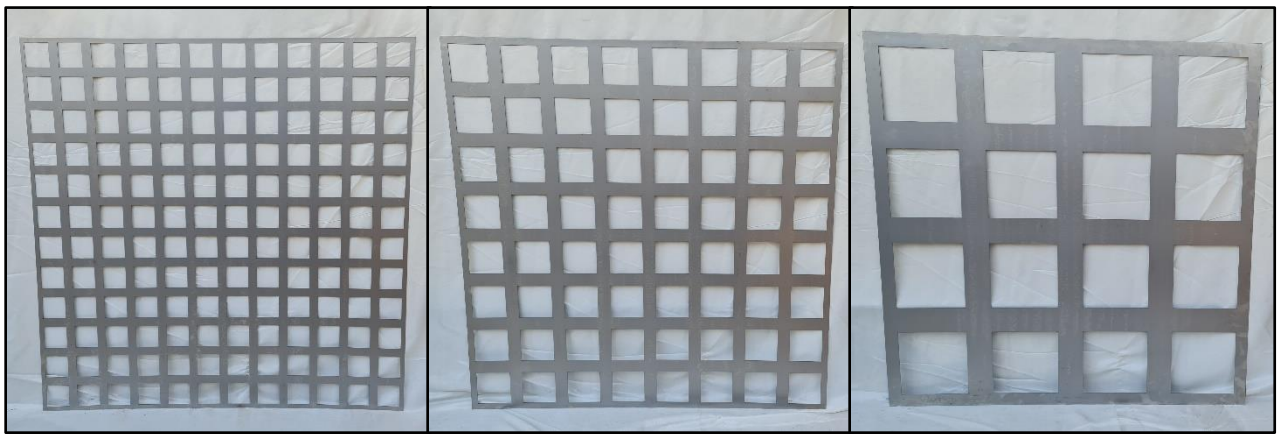

Figure (3.14): Sizes of square openings

The edges of opening were very smooth without any abnormal deformation, distortion, imperfections or irregular swelling, The details of circle, octal and rectangle shapes are shown in Figure 3.15.

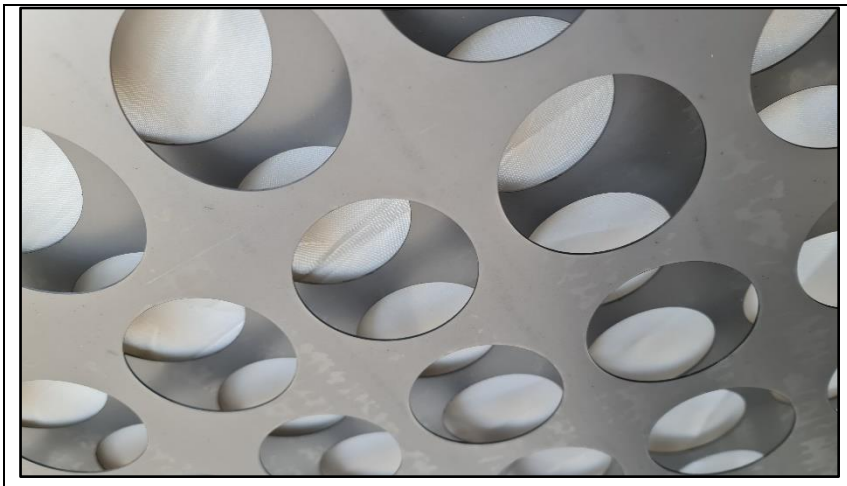

	Diameter mm	*Distance between openings mm*
Small opening	*68.0*	*15.4*
Medium opening	*102.0*	*23.0*
Large opening	*204.0*	*46*

	Side length mm	*Distance between openings mm*
Small opening	*27.4*	*17.1*
Medium opening	*41.1*	*25.7*
Large opening	*82.3*	*51.3*

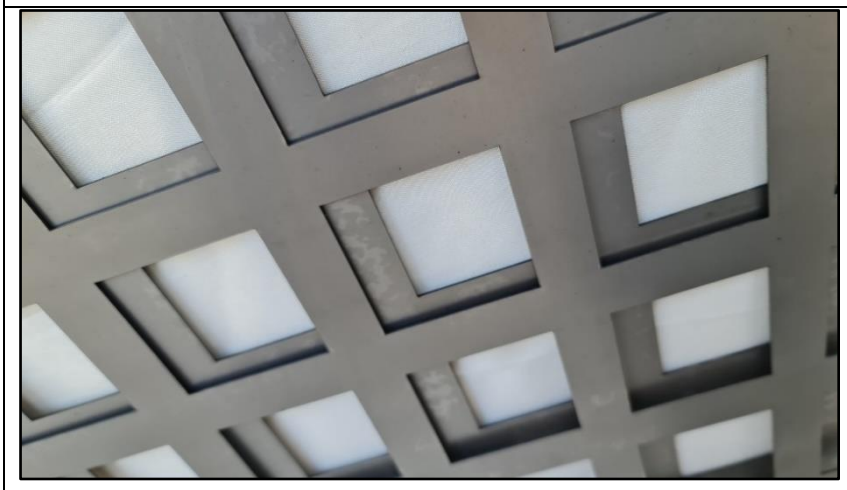

	Side length mm	*Distance between openings mm*
Small opening	*60.2*	*23.1*
Medium opening	*90.4*	*34.6*
Large opening	*180.8*	*69.2*

Figure (3.15): Details of openings

Notes: Small openings = 12×12 or 144 holes
Medium openings = 8×8 or 64 holes
Large openings = 4×4 or 16 holes
Overall plate dimensions = (1000×1000×1) mm

3.2.7 water

All concrete operations were carried out with tap water provided by the Iraqi national net system.

3.3 Trial Mixes of SCC and Mix Proportion

Before the mixing process, all the ingredients were weighted and backed into the plastic vessel. The mixing is carried out in a drum type, XCORT. It has specification clarified in Figure (3.16). The duration of mixing will depend on these specifications and it will be clarified in item 3.4.

Figure (3.16): Type and specification of drum

Before starting to mix, it is necessary to keep the mixer clean, moist and free of water.

Three important roles should be provided in SCC: filling ability, passing ability and stability [37-39]. Figure (3.17) shows several failed mixes in previous required roles that happened in some trial mixes.

(a) **(b)**

Figure (3.17): Failure trial mixes

(a) satisfy the filling and passing ability but it is failed in stability
(b) satisfy the stability but it is failed in filling and passing ability

After that, three succeed mixes that obtained, Figure (3.18), and their proportion illustrated in Table (3.4). A common range of slump flow for self-compacting concrete is (450 to 760) mm [3]. This test is for checking the filling ability. The J-ring test is used to check the passing ability while the Visual Stability Index (VSI) test is used to evaluate the resistance to segregation.

(a) **(b)**

Figure (3.18): Successful trial mixes

(a) the value of slump test equal to 600 mm
(b) the value of J-ring test equal to 550 mm

Table (3.4): Proportion of trial mixes

First trial mix						
Materials	**Cement**	**Water**	**Sand**	**Gravel**	**Glenium 54**	**Silica fume**
Weight (kg)	**7.272**	**2.691**	**10.181**	**14.544**	**0.131**	**0.4**
Ratio	**1**	**0.35**	**1.4**	**2**	**0.018**	**0.05**
Second trial mix						
Materials	**Cement**	**Water**	**Sand**	**Gravel**	**Glenium 54**	**Silica fume**
Weight (kg)	**7.272**	**2.691**	**12.726**	**14.544**	**0.131**	**0.4**
Ratio	**1**	**0.35**	**1.75**	**2**	**0.018**	**0.05**
Third trial mix						
Materials	**Cement**	**Water**	**Sand**	**Gravel**	**Glenium 54**	**Silica fume**
Weight (kg)	**7.272**	**2.617**	**12.726**	**14.544**	**0.138**	**0.4**
Ratio	**1**	**0.34**	**1.75**	**2**	**0.019**	**0.05**

The first trial mix passed the three tests; slump test, j-ring test and visual stability index, but there was an uncomfortable quantity of gravel that was grouped during the j-ring test. In spite of this, the ratio of gravel was acceptable, but increasing the sand ratio in second trial mix led to get an optimal mix that passed three tests successfully. Although of decreasing the water and increasing Glenium 54 in third trial, but the second trial mix was still the best one.

3.4 Mix Procedure

The ingredients of batch have been taken special sequence to get best way for mixing and achieving self-compacting concrete as below:

1- The fine aggregate is added to the mixer with 1/3 quantity of water and mixed for 1 minute.

2- This stage consists mixing cement and silica fume with another 1/3 quantity of water and 1/3 quantity of Glenium 54, mixed for 1.5 minute.

3- After that, the whole coarse aggregate is added with the last 1/3 quantity of water, mixed for 1 minute.

4- The mixture is left for ¾ minute for rest and prepare the batch for final step.

5- The 2/3 of the leftover of the dosage of Glenium 54 is added and mixed for 1.5 minute. The mixture is then discharged. The summery of previous points shown in Figure 3.19.

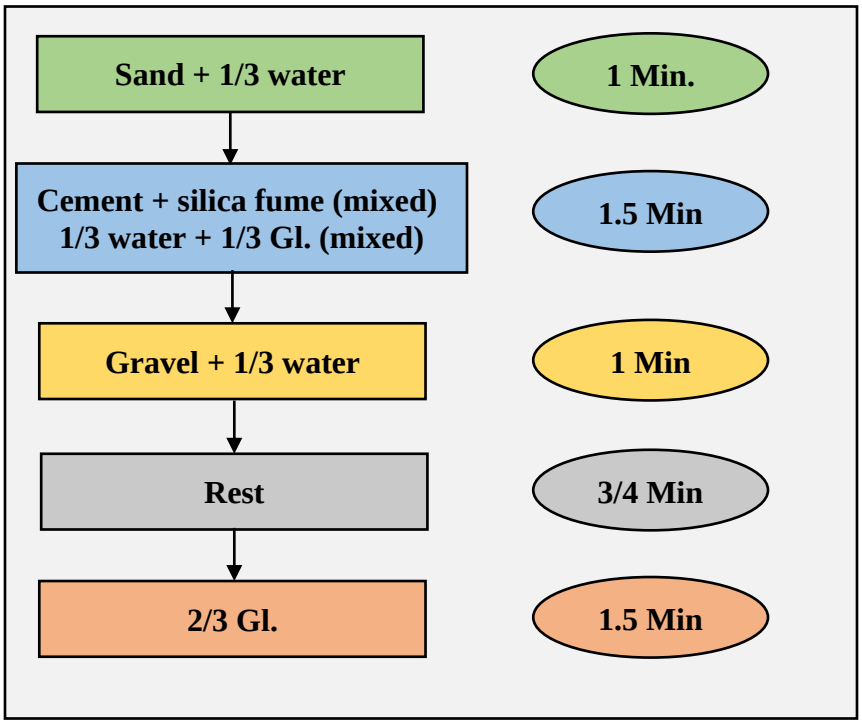

Figure (3.19): Mixing procedure

4.5 Test of Compressive Strength for Trial Mixes

The test was carried out in the laboratory of quality control at University of Kufa as shown in Figure (3.20). Six concrete cubes with three cylinders have been tested in compression testing machine for each trial mixes. The average value of results of compressive strength were:

Trial mix No. 1: average comprssive strenght for cubes were 41.91 MPa and for cylinder was 23.75 mPa.

Trial mix No. 2: average comprssive strenght for cubes were 42.58 MPa and for cylinder was 27.21 MPa.

Trial mix No. 3: average comprssive strenght for cubes were 38.43 mPa and for cylinder was 26.19 mPa.

a) Preparing the samples (Before the testing) **b) Testing the samples (During the testing)** **c) Some of the samples' failure (After the testing)**

Figure (3.20): Tests of hardened Concrete

3.6 Description of Models and Molds

The present study investigates an innovative style of reinforcing two-way slabs which is achieved by using perforated steel plate instead of traditional reinforcement. Several slabs with various kinds of openings, circular, octagonal and square shapes were adopted to compare them with the reference slab that using bar reinforcements. The other variables that were undertaken in this study were represented by changing size of opening. Large, medium and small size of openings (with same total area of openings) were discussed. There are two types of loading: concentrated and uniform. The present study is based on casting twenty specimens with a dimension of (1050 × 1050 × 60) mm, noting that the concrete cover will be 15 mm. Methodology of test and other details will be mentioned elsewhere. The following designation system is used

I. Type of loading: the Co refer to concentrated load test and Un refer to the uniform load test.

II. The perforated steel plate will be as PSP and traditional reinforcement will be Re.

III. The small, medium and large opening for the circular shape will be C1, C2 and C3 respectively.

IV. The small, medium and large opening for the octagonal shape will be O1, O2 and O3 respectively.

V. The small, medium and large opening for the square shape will be R1, R2 and R3 respectively.

According to previous descriptions, the cases adopted in this study under concentrated load are:

1- Re-Co: slab reinforced with a minimum amount of traditional steel bars, which is equal to $0.0018\ A_g$ [1].

2- PSPC1-Co: slab reinforced by perforated steel plate with small circular openings, 12×12 openings.

3- PSPC2-Co: slab reinforced by perforated steel plate with medium circular openings, 8×8 openings.

4- PSPC3-Co: slab reinforced by perforated steel plate with large circular openings, 4×4 openings.

5- PSPO1-Co: slab reinforced by perforated steel plate with small octagonal openings, 12×12 openings.

6- PSPO2-Co: slab reinforced by perforated steel plate with medium octagonal openings, 8×8 openings.

7- PSPO3-Co: slab reinforced by perforated steel plate with large octagonal openings, 4×4 openings.

8- PSPR1-Co: slab reinforced by perforated steel plate with small square openings, 12×12 openings.

9- PSPR2-Co: slab reinforced by perforated steel plate with medium square openings, 8×8 openings.

10- PSPR3-Co: slab reinforced by perforated steel plate with large square openings, 4×4 openings.

Likewise, the cases adopted in this study under uniform load will be:

1- Re-Un: slab reinforced with a minimum amount of traditional steel bars, which is equal to 0.0018 Ag [1].

2- PSPC1- Un: slab reinforced by perforated steel plate with small circular openings, 12×12 openings.

3- PSPC2- Un: slab reinforced by perforated steel plate with medium circular openings, 8×8 openings.

4- PSPC3- Un: slab reinforced by perforated steel plate with large circular openings, 4×4 openings.

5- PSPO1- Un: slab reinforced by perforated steel plate with small octagonal openings, 12×12 openings.

6- PSPO2- Un: slab reinforced by perforated steel plate with medium octagonal openings, 8×8 openings.

7- PSPO3- Un: slab reinforced by perforated steel plate with large octagonal openings, 4×4 openings.

8- PSPR1- Un: slab reinforced by perforated steel plate with small square openings, 12×12 openings.

9- PSPR2- Un: slab reinforced by perforated steel plate with medium square openings, 8×8 openings.

10- PSPR3- Un: slab reinforced by perforated steel plate with large square openings, 4×4 openings.

Figure (3.21) shows the cross section of the reference slab and slabs reinforced by perforated steel plate.

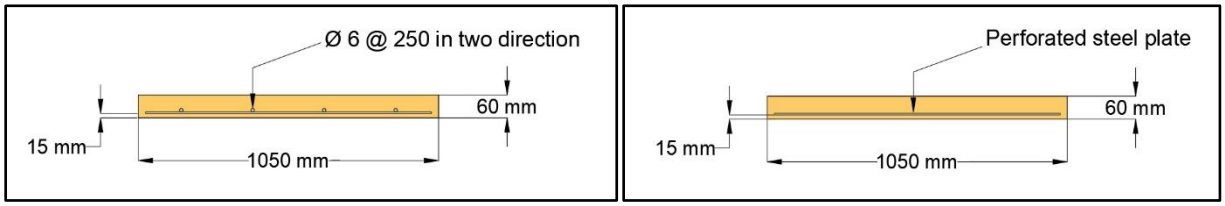

a) Reference slab **b) slab reinforced by perforated steel plate**

Figure (3.21): Details of the adopted slabs

With respect to the molds, they were fabricated by using wood called a Medium Density Fiber (MDF) as shown in Figure (3.22). They have fair face surfaces of four sides and on base, The molds were cleaned form the dust and greased before casting.

Figure (3.22): Ply wood molds of slab models

3.7 Casting and Curing the Specimens

All the required materials were prepared according to the second trial mix as stated in Table (3.4). The rotary mixer that was mentioned earlier was utilized, and one batch was used to cast each slab model with control specimens. No compaction was performed because the type of concrete that was used was SCC. Figure (3.23) illustrates the preparation of materials and casting of models.

a) Materials preparation

b) Leveling the mold

C) Checking the SCC

D) Casting the specimens

E) Encoding the specimens

Figure (3.23): Casting the specimens

3.8 Instruments and Testing Procedure of Slab Models

All slab types were subjected to monotonic loads up to ultimate load in a universal testing machine with a capacity of 2000 kN. Figure (3.24) displays the universal machine which is accessible at the Structural Laboratory in the College of Engineering/Civil Engineering Department at the University of Kufa.

Figure (3.24): Universal Testing Machine

3.8.1 Supporting and Loading Condition

Each slab model was prepared to apply the test in a rigid steel frame that served as a supporting system and was welded to the top face of the testing machine base. The touching area between the slabs and the frame was a steel strip with a width of 50 mm and a thickness of 5 mm along the slab's edge, which was then overlaid with compressed rubber to simulate the slabs resting on a brick wall as shown in Figure (3.25).

Figure (3.25): Supporting under the slab's specimens

The load conditions were concentrated load and uniformly distributed load. The concentrated load subjected by applying a central load of 150×150 mm applied to the top face of the slabs. On the other hand, there was a special methodology for achieving the uniformly distributed load approach. It consisted of using a rigid manufactured piston. The sequence of this approach has been done by using a container over the slab's models, it was a steel box opened from the top and bottom with an inner dimension of 910×910×100 mm and the thickness of the used plate was 3 mm, as it is clarified in Figure (3.26).

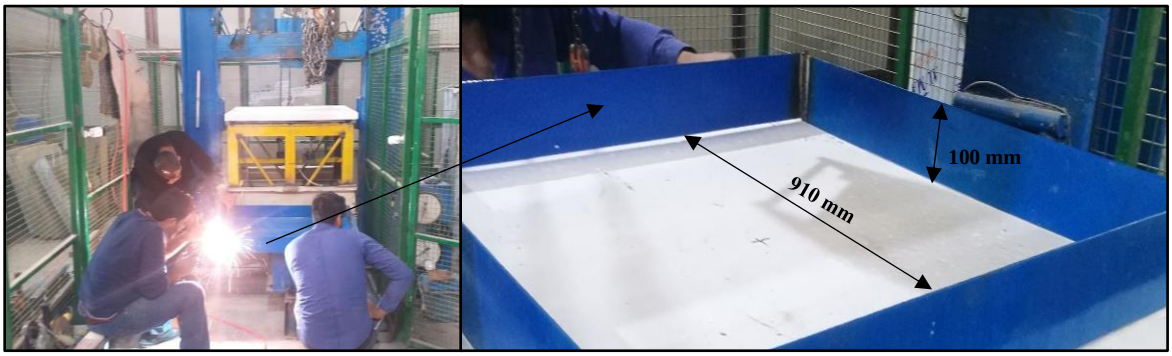

Figure (3.26): Manufacturing of sand's container

The container was utilized to fill it with sand. The inner surfaces are covered by a sheet of Nylon to make it easier to remove the sand after the test, just like in Figure (3.27).

Figure (3.27): Covering the inner sides by Nylon sheet

The using layer of sand, about 70 mm thick, over the top surface of the slab helps to distribute the weight evenly throughout the slab's top surface. After laying the sand in the container, a sufficient flattening, measuring the thickness in many different positions to reach for good leveling of sand as it is illustrated in Figure (3.28).

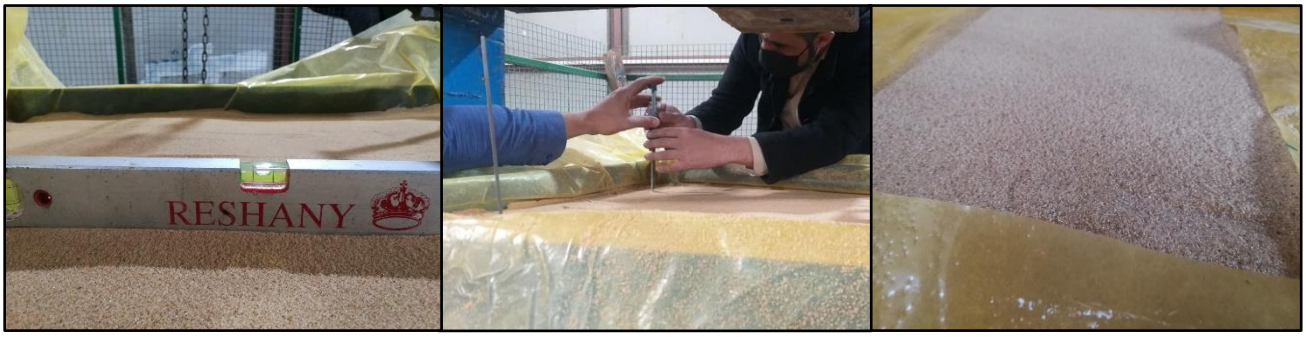

Figure (3.28): Leveling the sand

A 900×900×6 mm base plate would be set on top of the sand layer, and a rigid steel frame would be placed above the base plate, as it is stated in Figure (3.29).

a) Base plate **b) Rigid frame**

Figure (3.29): Manufacturing of rigid piston

For more illustration about the position of the base plate, see Figure (3.30) after the removal of the sand container and rigid frame.

Figure (3.30): Position of the base plate

Figure (3.31) shows the scheme of the rigid piston to clarify the whole sequence of all its components.

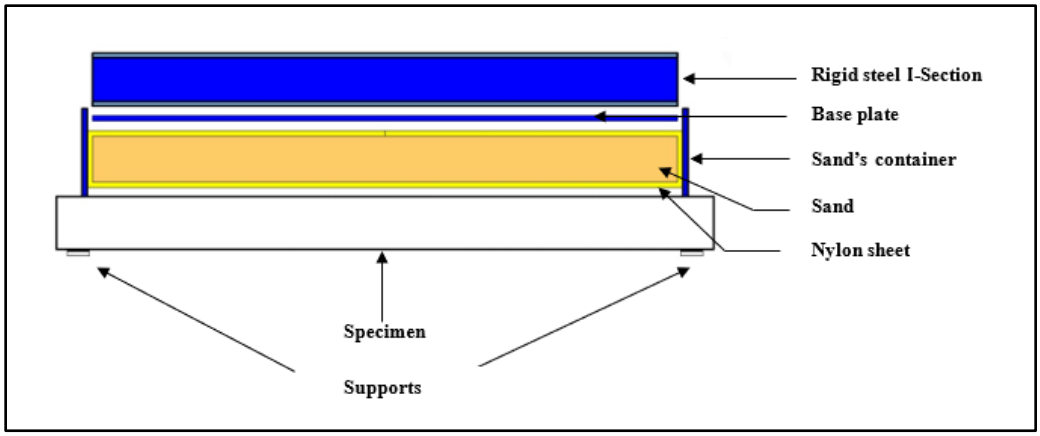

Figure (3.31): The schematic diagram of a rigid piston

3.8.2 Deflections at Different Locations of the Slab

The deflections were measured by an electronic dial gauge of 50 mm capacity and 0.001 mm accuracy. Three vertical dial gauges were used as presented in Figure (3.32); one at the center point. The other is placed at quarter point. The last one is placed at the center of the diagonal direction of a quarter slab.

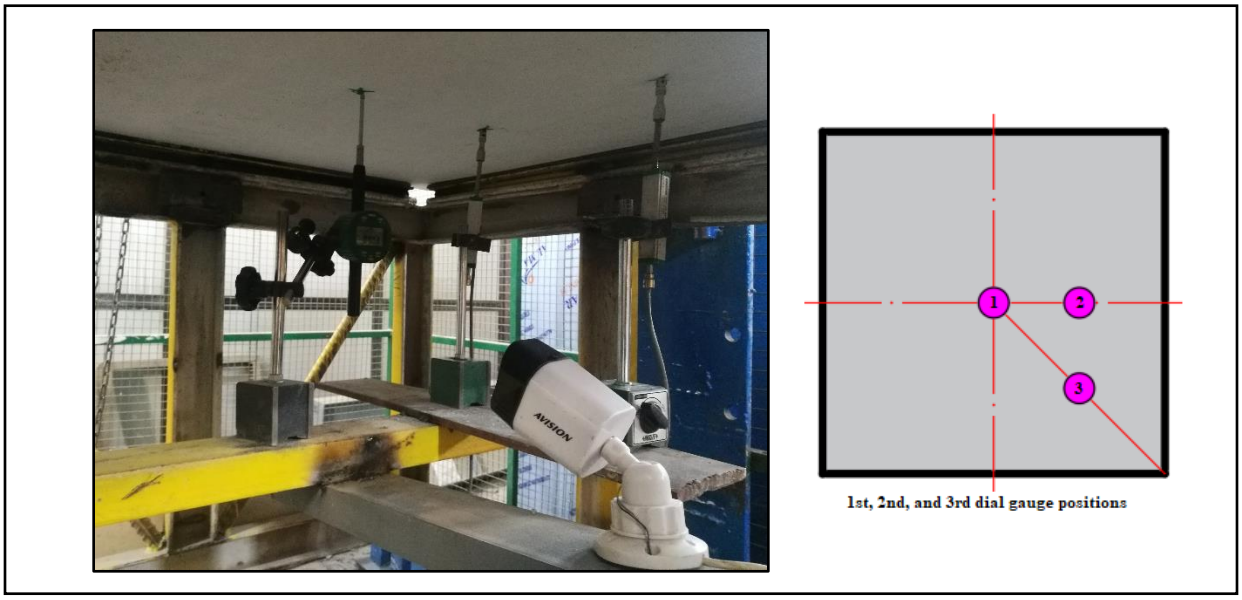

Figure (3.32): Location of the dial gauges

3.8.3 Investigating Cracks Width and Cracks Pattern

The cracks were detected and drawn in three stages. These phases describe the progression of loading from zero to ultimate load. The crack width and crack pattern were specified in each stage by using an optical crack meter type MG 10081-2, as shown in Figure (3.33), and crayon. To make it much easier to notice the cracks and measure their width, the slab surfaces were painted white.

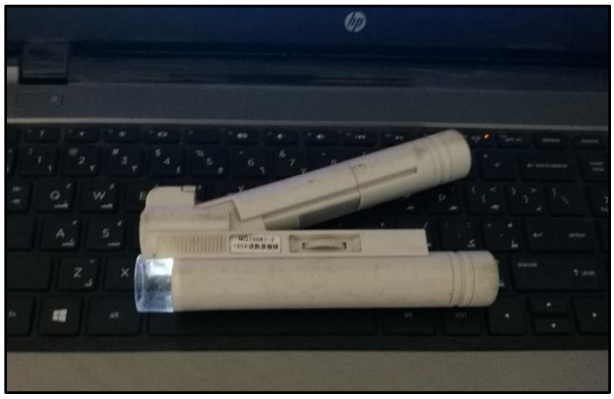

Figure (3.33): Optical crack meter type MG 10081-2

3.8.4 Controlling System of the Test

A system of surveillance cameras was used to record all models' testing. It includes four cameras of type **AVISION**, such as in the Figure (3.34). Two of these record the central dial gage and the load indicator. The other two cameras monitored and recorded the overall models from opposite corners during the test. These four cameras were connected together and switched on simultaneously. All the data is saved in DVR, which can be used to examine the results at any time after the test.

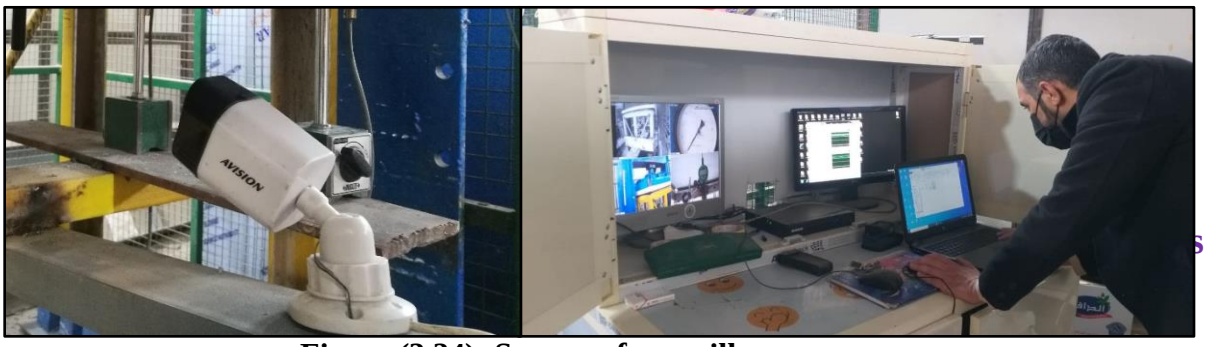

Figure (3.34): System of surveillance camera

CHAPTER FOUR
EXPERIMENTAL RESULTS AND DISCUSSION

4.1 Introduction

The illustration of all experimental results will be presented in this chapter. It included the results of tests of twenty slab models, ten samples were tested under a concentrated load while the others were tested under a uniform load. One of each ten samples was reinforced by traditional reinforcement, since the other nine were reinforced by perforated steel plate. The load deflection behavior was recorded at three main points; at the center, quarter point and diagonal quarter point. The cracks were investigated from the initial visible crack load till the failure load. The crack width was measured at the initial visible crack load, at a load approximately twice the initial visible crack load and measured at the final load. The crack pattern was also specified. Finally, this chapter will introduce the computerized mapping Figures that explain the growth cracks in tested samples in three main stages. Hence, all of these results will be reviewed one by one and compared with the referenced one reinforced by traditional reinforcement.

4.2 Properties of Concrete

The slab models were cured by sprinkling water and covered by nylon sheets; the concrete cubes were cured under the same situation. The first six concrete cubes were taken from the first work day and they are specified for models tested under concentrated load. The other six cubes represent the second work day and they are specified for models tested under uniform load. Two days between the first and second work days. The results of compressive strength show that there is no noticeable difference between them, it is due to high-quality control of casting and close ages of concrete cube. The ages of six concrete cubes would take from samples tested under concentrated load are 84 days, while the

ages of the other six concrete cubes are 82 days which is specified for samples tested under uniform load. Table (4.1) shows the results of compressive strength.

Table (4.1): Compressive strength for uniform and concentrated batch (cubic samples)

Cubes from concentrated batch Tested on the day of slabs testing		**Cubes from uniform batch** Tested on the day of slabs testing	
Cube No.	**Compressive strength MPa**	**Cube No.**	**Compressive strength MPa**
1	**41.89**	**1**	**43.82**
2	**39.08**	**2**	**47.56**
3	**48.34**	**3**	**47.02**
4	**42.85**	**4**	**37.00**
5	**46.44**	**5**	**46.90**
6	**47.36**	**6**	**45.34**
Average	**44.32**	**Average**	**44.60**

Note: other concrete cylinders were tested for every batch and their results were clarified in Table (4.2):

Table (4.2): Compressive strength for uniform and concentrated batch (cylindrical samples)

Cylinder from concentrated batch Tested on the day of slabs testing		**Cylinder from uniform batch** Tested on the day of slabs testing	
Cylinder No.	**Compressive strength MPa**	**Cylinder No.**	**Compressive strength MPa**
1	**30.13**	**1**	**32.08**
2	**32.47**	**2**	**28.41**
3	**34.57**	**3**	**29.72**
Average	**32.39**	**Average**	**30.07**
Cylinder No.	**Splitting test MPa**	**Cylinder No.**	**Splitting test MPa**
1	**3.793**	**1**	**3.931**
2	**3.091**	**2**	**3.587**
3	**3.961**	**3**	**3.951**
Average	**3.615**	**Average**	**3.823**

4.3 General Results of Experimental Works

Twenty slabs were tested in the laboratory of Structural Higher Studies at the engineering college of the University of Kufa. The results will be classified into four main parts: ultimate load, maximum deflection, load deflection curve, and cracking behavior (including the pattern and width of cracks).

4.4 Ultimate Load and Maximum Deflection

The ultimate load and maximum deflection were investigated and their results are clarified below:

4.4.1 Ultimate Load and Maximum Deflection for Models Under Concentrated Load

All results concerning the ultimate load and maximum deflection for slabs models under concentrated load are recorded and summarized in Table (4.2).

Table (4.3): Ultimate load and maximum deflection for models under concentrated load

No.	Opening shape	OAR (Opening Aspect Ratio)	Models	Ultimate load kN	% Load increasing	Max. deflection mm	Deflection at service load [2] mm
1	Traditional reinforcement	---	Re-Co	19.5	*Reference*	17.168	2.115
2	Circular opening	3.62×10^{-3}	PSPC1-Co	31	58.97	24.84	0.868
3		8.17×10^{-3}	PSPC2-Co	34.5	76.92	25.289	1.43
4		32.6×10^{-3}	PSPC3-Co	28	43.59	22.903	2.206
5	Octagonal opening	3.62×10^{-3}	PSPO1-Co	32.5	66.67	27.711	2.268
6		8.17×10^{-3}	PSPO2-Co	35.5	82.05	28.125	1.925
7		32.6×10^{-3}	PSPO3-Co	30	53.85	22.484	3.188
8	Square opening	3.62×10^{-3}	PSPR1-Co	35	79.49	27.888	2.178
9		8.17×10^{-3}	PSPR2-Co	36	84.62	27.054	1.188
10		32.6×10^{-3}	PSPR3-Co	31.5	61.54	30.653	1.248

[2] **The deflection at the service live load level (service load equal to 65% of ultimate load) is compared with the limitations of ACI 318-19 for immediate deflection for flat roofs due to service live load (Lc/c/180 = 5.28 mm).**

The technique of using perforated steel plate in two-way concrete slabs shows a significant enhancement in ultimate load. All shapes, circular, octagonal and square gave ultimate load more than the reference slab which was reinforced by bar reinforcements. The medium size of the openings for each shape (for the same ratio of openings' area to total plate area) displays the optimal resistance. It was more than the reference slab about 76.92%, 82.05%, and 84.62% for medium size of circular, octagonal and square shapes. The rest percent can be noticed in Table (4.3). However, the square shape of openings gives ultimate load more than octagonal and circular because it provides most related simulation of reinforcements in both orthogonal directions. In addition, this technique is considered an enhanced method for distributing steel along the cross section of slabs as a smeared method.

4.4.2 Ultimate Load and Corresponding Deflection for Models Under Uniform Load

Table (4.4) shows the results of ultimate load and maximum deflection for slabs models under uniform load.

Table (4.4): Ultimate load and maximum deflection for models under uniform load

No.	Opening shape	OAR (Opening Aspect Ratio)	Models	Ultimate load kN	% Load increasing	Max. deflection mm	Deflection at service load [3] mm
1	Traditional reinforcement	---	Re-Un	148	*Reference*	20.687	2.863
2	Circular opening	3.62×10^{-3}	PSPC1-Un	152.5	3.04	12.768	2.688
3		8.17×10^{-3}	PSPC2-Un	183	23.65	25.337	3.549
4		32.6×10^{-3}	PSPC3-Un	150	1.35	19.421	<u>5.502</u>

[3] **The deflection at the service live load level (service load equal to 65% of ultimate load) is compared with the limitations of ACI 318-19 for immediate deflection for flat roofs due to service live load ($L_{c/c}/180$ = 5.28 mm). The underlined number is out of the recommended provision by ACI 318-19.**

Table (4.4): Ultimate load and maximum deflection for models under uniform load (continue)

No.	Opening shape	OAR (Opening Aspect Ratio)	Models	Ultimate load kN	% Load increasing	Max. deflection mm	Deflection at service load [4] mm
5	Octagonal opening	3.62×10^{-3}	PSPO1-Un	158	6.76	17.584	1.263
6		8.17×10^{-3}	PSPO2-Un	178	20.27	22.978	5.273
7		32.6×10^{-3}	PSPO3-Un	155	4.73	21.713	<u>7.408</u>
8	Square opening	3.62×10^{-3}	PSPR1-Un	160	8.11	14.014	2.328
9		8.17×10^{-3}	PSPR2-Un	205	38.51	25.897	5.056
10		32.6×10^{-3}	PSPR3-Un	161	8.78	24.758	<u>6.913</u>

In two-way concrete slabs, a large increase in ultimate load is obtained by using perforated steel plate. The ultimate load was higher in all forms, including circular, octagonal, and square, than in the reference slab, which was reinforced by classical reinforcement (bars). For each form of openings, the medium size of the openings provides the best resistance. For medium size circular, octagonal, and square shapes, it was greater than the reference slab by around 23.65%, 20.27%, and 38.51% respectively. Others can be shown in Table (4.4). Again, square openings provide greater ultimate load than octagonal and circular openings since it allows for the most accurate simulation of reinforcements in both main orthogonal directions.

4.5 Load Deflection Curves

4.5.1 Load Deflection Curves for Models Under Concentrated Load

This article will be divided into three sections as: section devoted to slabs reinforced by perforated steel plates with circular openings, slabs reinforced by

[4] The deflection at the service live load level (service load equal to 65% of ultimate load) is compared with the limitations of ACI 318-19 for immediate deflection for flat roofs due to service live load ($L_{c/c}/180$ = 5.28 mm). The underlined number is out of the recommended provision by ACI 318-19.

perforated steel plate with octagonal openings, and the last part about the slabs reinforced by perforated steel plate with square openings.

4.5.1.1 Models Reinforced by Perforated Steel plate – Circle Opening

Three diameters of circular openings in this study were considered; PSPC1-Co with a diameter of 68 mm and 12×12 openings, PSPC2-Co with a diameter of 102 mm and 8×8 openings and the last one is PSPC3-Co, 204 mm in diameter with 4×4 openings. These three different sizes of openings are all of the same total area of openings. All previous specimens were compared with reference one reinforced by steel deformed bars (Re-Co) as shown in Figures (4.1), (4.2) and (4.3) respectively.

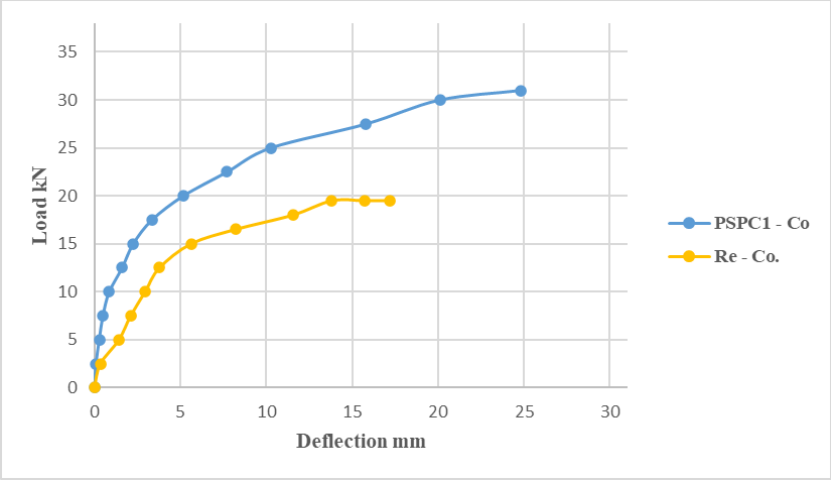

Figure (4.1): Comparison of load deflection curve for PSPC1-Co and Re-Co

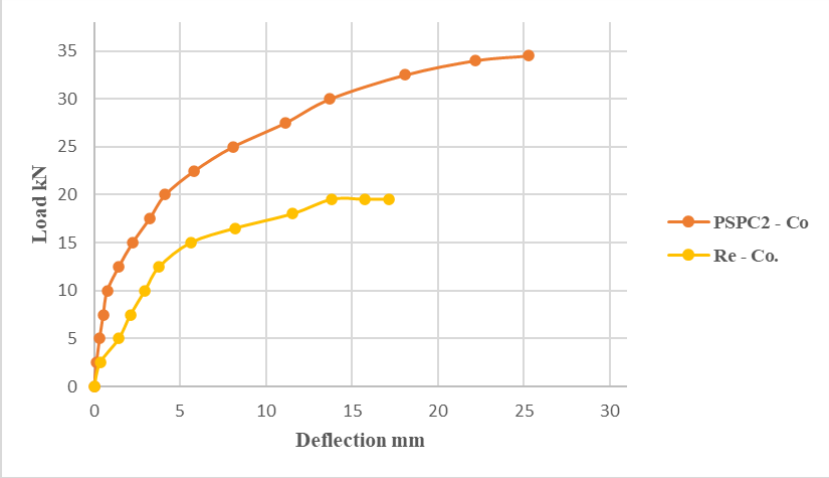

Figure (4.2): Comparison of load deflection curve for PSPC2-Co and Re-Co

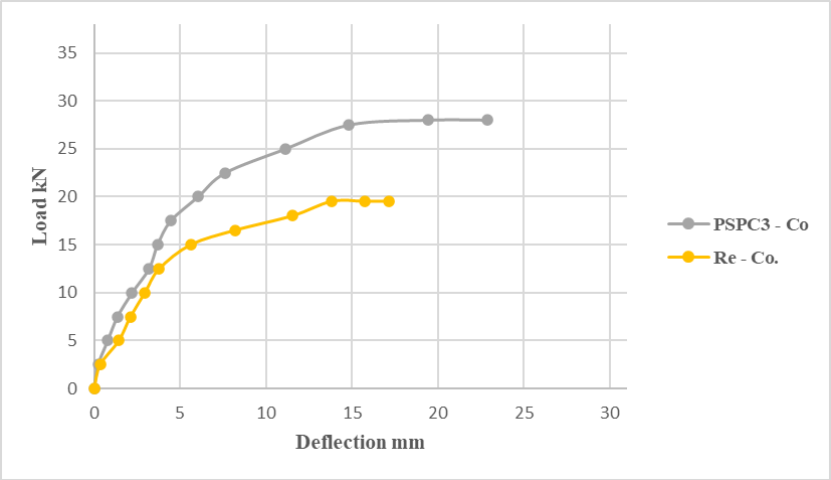

Figure (4.3): Comparison of load deflection curve for PSPC3-Co and Re-Co

It is obvious that the slabs reinforced by perforated steel plate are of more stiffness than slabs reinforced by traditional reinforcement. The ultimate load of slabs reinforced by traditional reinforcement is 19.5 kN and corresponding deflection is 13.82 mm. At this load, 19.5 kN, deflection of sample PSPC1-Co is 5.184 mm, PSPC2-Co is 4.128 while the PSPC3-Co is equal to 6.043. PSPC2-Co presents optimal size opening for stiffer slabs as shown in Figure (4.4).

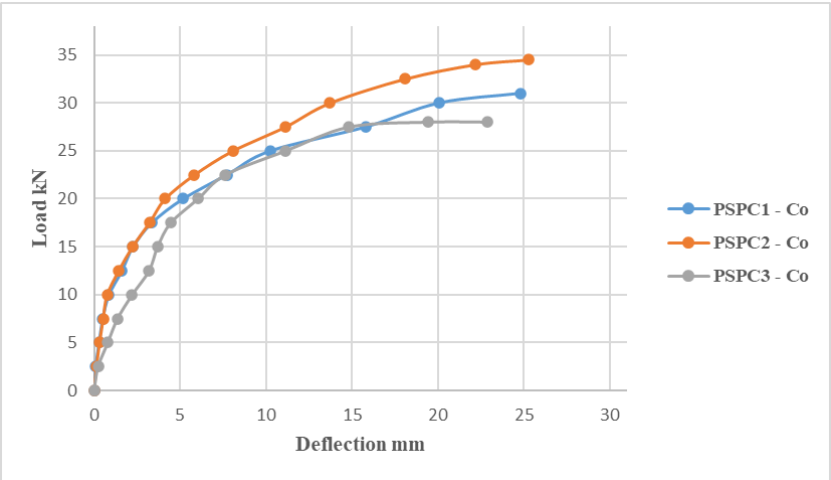

Figure (4.4): Effect of change size opening for circular shape – concentrated load

4.5.1.2 Models Reinforced by Perforated Steel Plate – Octagonal Opening

Here, the distance between opposite sides in octal shape are 66.1 mm, 99.2 mm and 198.7 mm. Category name of them were PSPO1-Co, PSPO2-Co and PSPO3-Co respectively. As clarified in Figures (4.5), (4.6), and (4.7), all prior samples were compared to the reference sample using the conventional deformed steel bars (Re-Co).

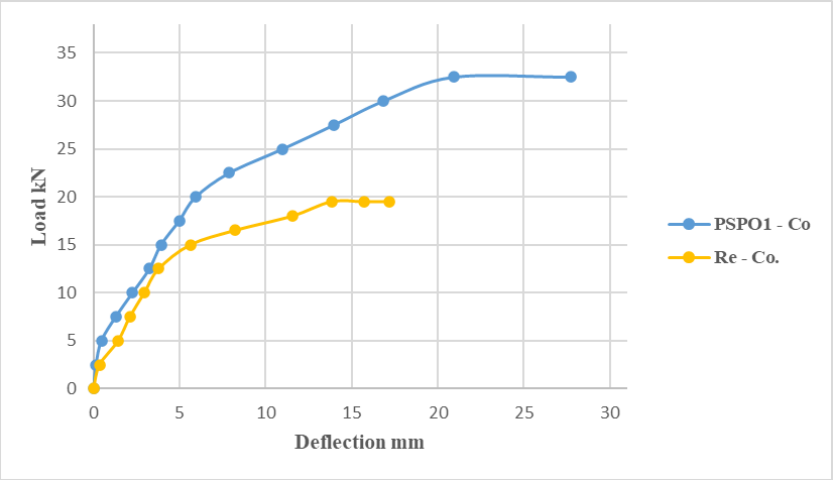

Figure (4.5): Comparison of load deflection curve for PSPO1-Co and Re-Co

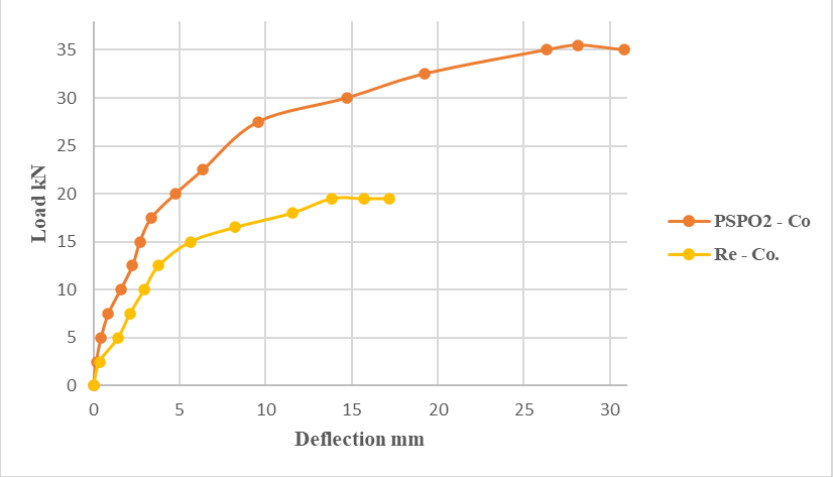

Figure (4.6): Comparison of load deflection curve for PSPO2-Co and Re-Co

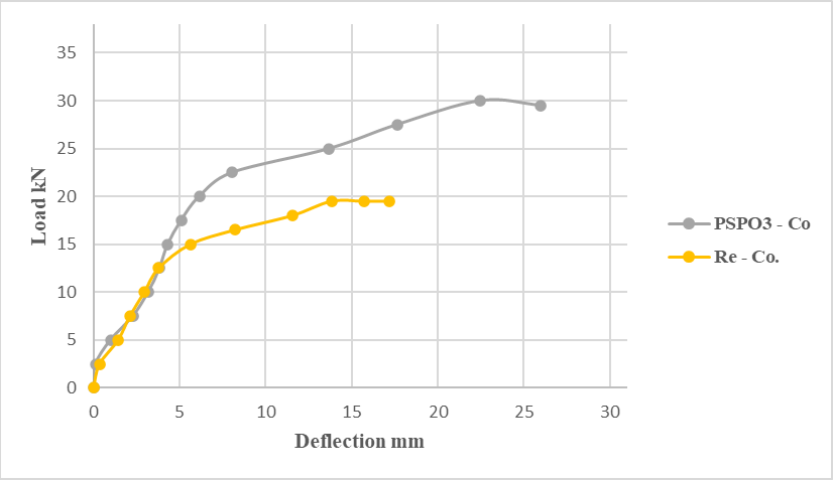

Figure (4.7): Comparison of load deflection curve for PSPO3-Co and Re-Co

The rigidity of slabs reinforced with perforated steel plate is clearly higher than that of slabs reinforced with conventional reinforcement. The deflection of slabs reinforced with conventional reinforcement is 13.82 mm at the ultimate load (19.5 kN).

PSPO1-Co has a deflection of 5.94 mm at 19.5 kN, whereas PSPO2-Co has a deflection of 4.768 mm, and PSPO3-Co has a deflection of 6.149 mm. Figure (4.8) shows how PSPC2-Co offers the most appropriate size aperture for stiffer slabs.

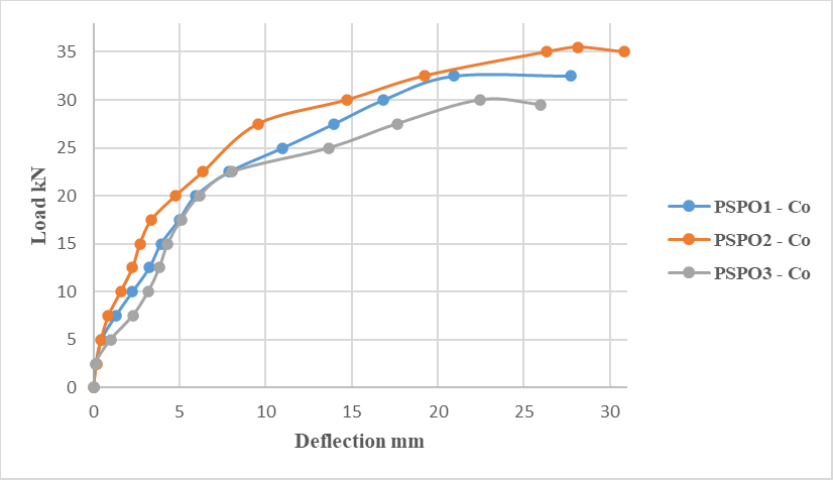

Figure (4.8): Effect of change size opening for octagonal shape – concentrated load

4.5.1.3 Models Reinforced by Perforated Steel Plate – Square Opening

The side lengths of the square forms were 60.2 mm, 90.4 mm, and 180.8 mm. PSPR1-Co, PSPR2-Co, and PSPR3-Co were their respective category names. All preceding samples were compared to the reference sample using the classical reinforcements (deformed steel bars) Re-Co, as can be seen in Figures (4.9), (4.10), and (4.11).

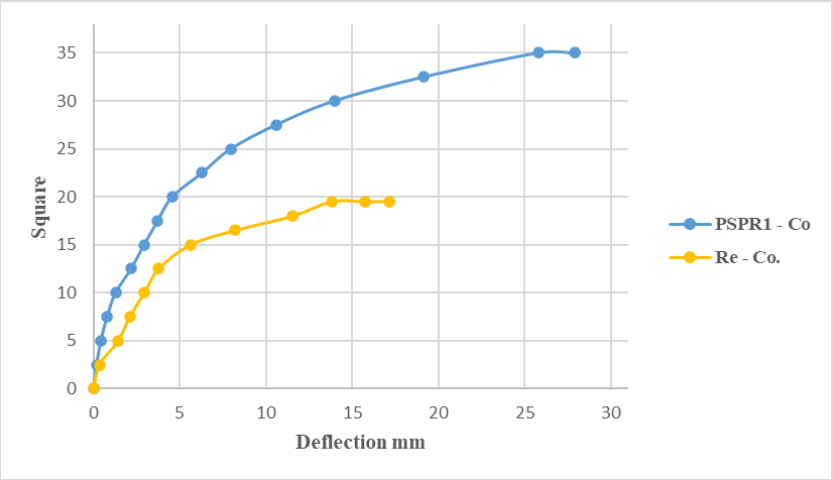

Figure (4.9): Comparison of load deflection curve for PSPR1-Co and Re-Co

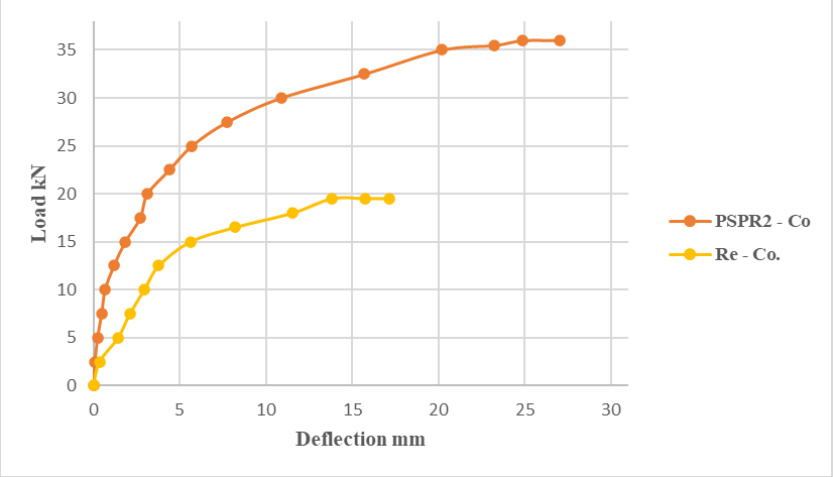

Figure (4.10): Comparison of load deflection curve for PSPR2-Co and Re-Co

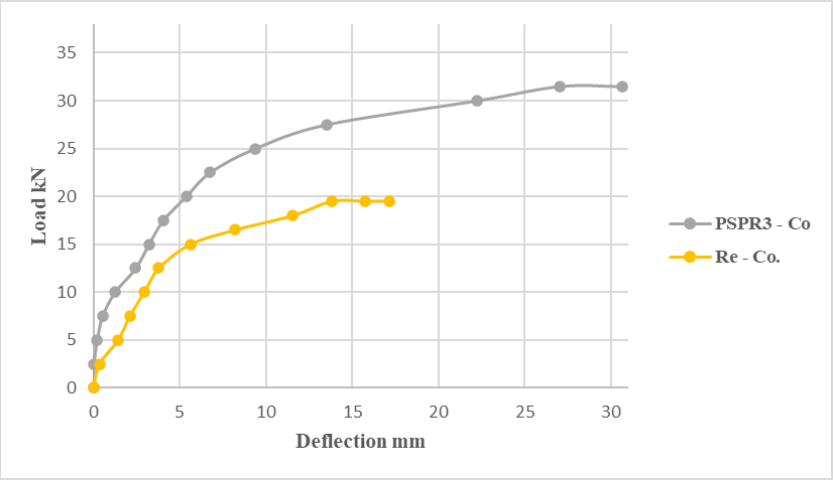

Figure (4.11): Comparison of load deflection curve for PSPR3-Co and Re-Co

The stiffness of slabs reinforced using perforated steel plate is significantly higher than slabs reinforced with traditional reinforcement. At the ultimate load for conventionally reinforced slabs deflects 13.82 mm since the PSPR1-Co, PSPR2-Co and PSPR3-Co deflect 4.568 mm, 3.128 mm and 5.379 mm respectively. As demonstrated in Figure 4.12, PSPC2-Co offers the optimum size openings.

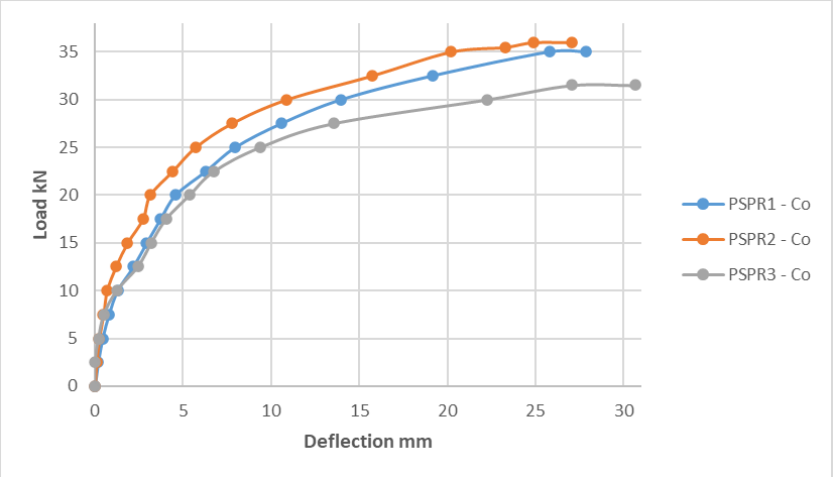

Figure (4.12): Effect of change size opening for square shape – concentrated load

4.5.1.4 Discussion About the Effect of Opening Shape – Concentrated Load

Three shapes were discussed in experimental work and each shape has three sizes. The small size represents 12×12 openings, each opening has an area

equal to 36 cm^2, moderate size indicates 8×8 openings, area of one opening is 81 cm^2, the large openings equivalent to 4×4 with an area equal to 32 cm^2.

Experimental results proved that the shape of the opening is slightly effective on the load-deflection curve. However, the square shape is the best among all the shapes discussed, this fact can be seen in Figures (4.13), (4.14), and (4,15).

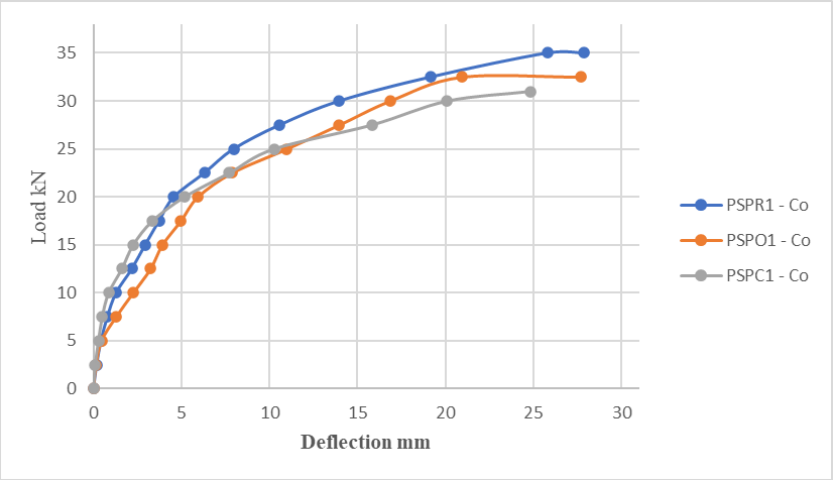

Figure (4.13): Effect of opening shape – small size – concentrated load

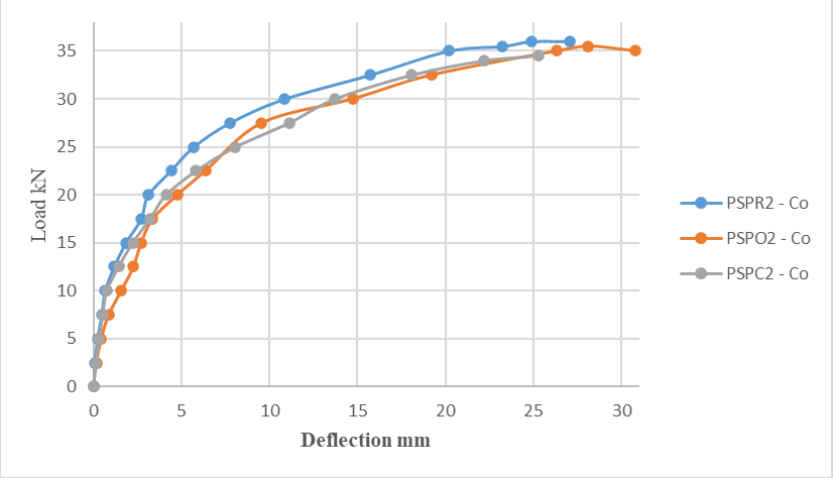

Figure (4.14): Effect of opening shape – moderate size – concentrated load

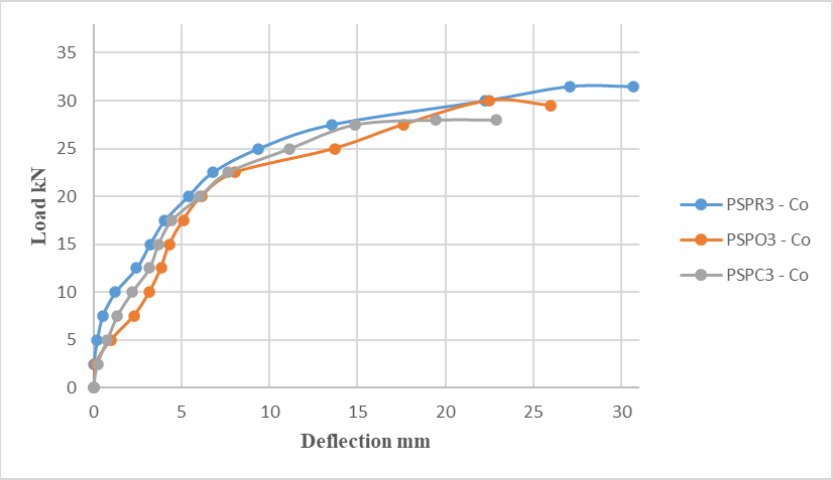

Figure (4.15): Effect of opening shape – large size – concentrated load

4.5.2 Load Deflection Curves for Models Under Uniform Load

The same pervious division which was considered in case of concentrated load, the next parts will be comprised of three sections: slabs reinforced with perforated steel plates with a circular hole, slabs reinforced with perforated steel plates with an octagonal hole, and slabs reinforced with perforated steel plates with a square hole.

All details of previous ten slabs will be repeated here except the nature of loading, A uniform load will be subjected here.

4.5.2.1 Models Reinforced by Perforated Steel Plate – Circle Opening

PSPC1-Un, PSPC2-Un and PSPC3-Un are models reinforced by perforated steel plates with circular openings which have a diameter of 68 mm with 144 openings, 102 mm with 64 openings and 204 mm with 16 openings respectively. All previous samples had the same amount of steel. Figures (4.16), (4.17) and (4.18) described how the load deflection curve behaved for them when compared to a reference curve reinforced with deformed steel bars.

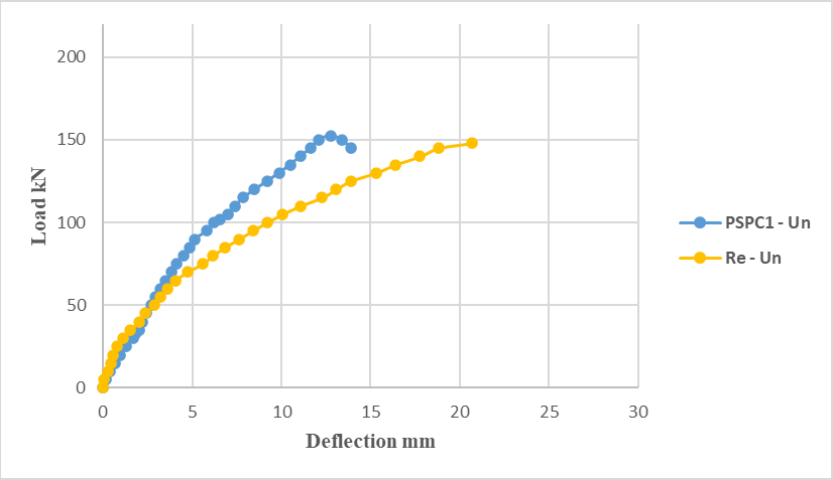

Figure (4.16): Comparison of load deflection curve for PSPC1-Un and Re-Un

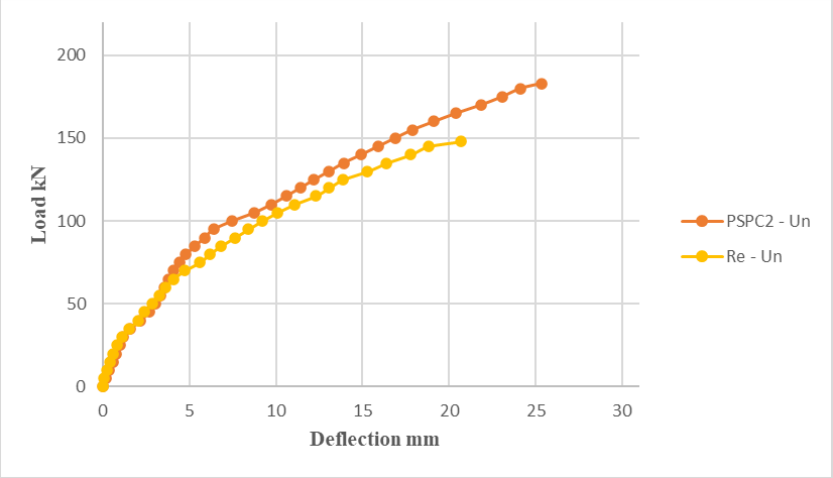

Figure (4.17): Comparison of load deflection curve for PSPC2-Un and Re-Un

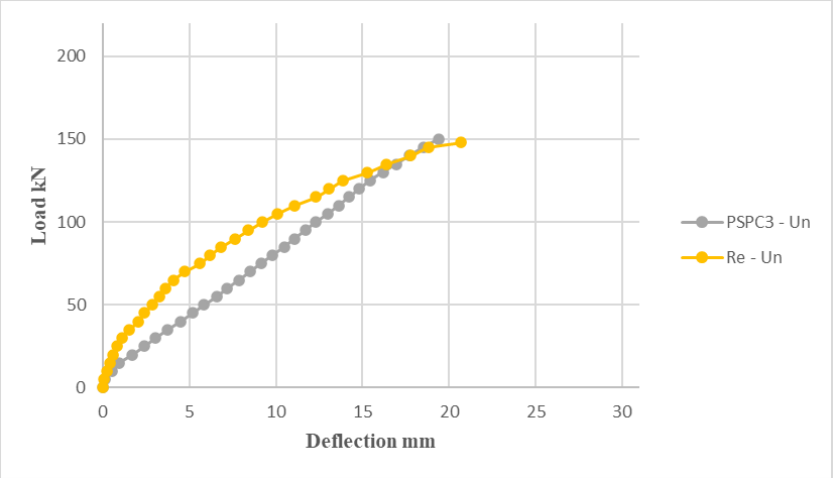

Figure (4.18): Comparison of load deflection curve for PSPC3-Un and Re-Un

All PSPC1-Un, PSPC2-Un, and PSPC3-Un samples give more ultimate load than sample reinforced with conventional reinforcement. However, the number of openings has a significant effect on slab stiffness. The smallest number of large holes indicates that there is less interlock between the steel plate and the concrete, whereas the failure occurred due to plate-to-concrete slippage. When there are a lot of openings, there is greater interlock and stiffness.

PSPC2-Un has an appropriate number of holes that provide better rigidity than a traditional slab and the highest ultimate load of all variants. Figure (4.19) clarifies all prior interpretations.

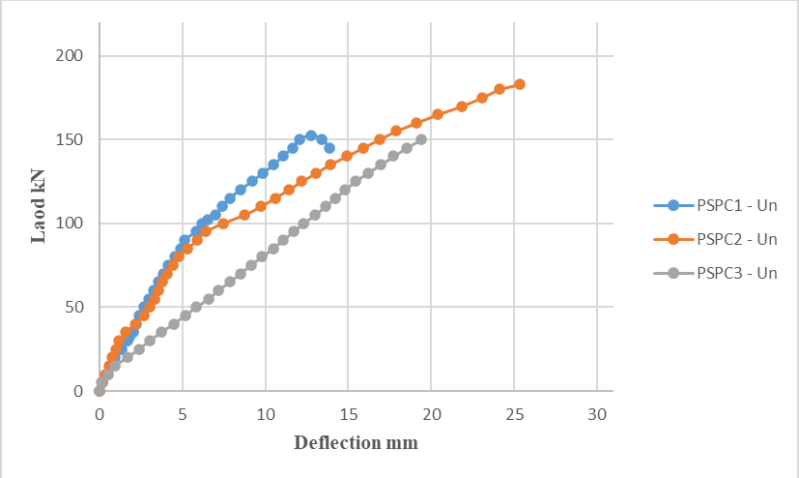

Figure (4.19): Effect of change size opening for circular shape – uniform load

4.5.2.2 Models Reinforced by Perforated Steel Plate – Octal Opening

For the perforated steel plate with an octagonal shape, the comparison between the (PSPO1-Un, PSPO2-Un, PSPO3-Un) and the reference (Re-Un) has been plotted in Figures (4.20), (4.21) and (4.22) respectively.

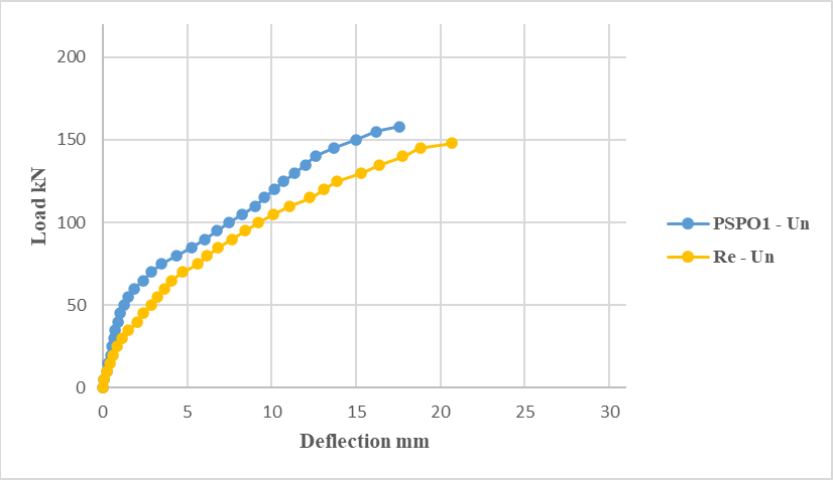

Figure (4.20): Comparison of load deflection curve for PSPO1-Un and Re-Un

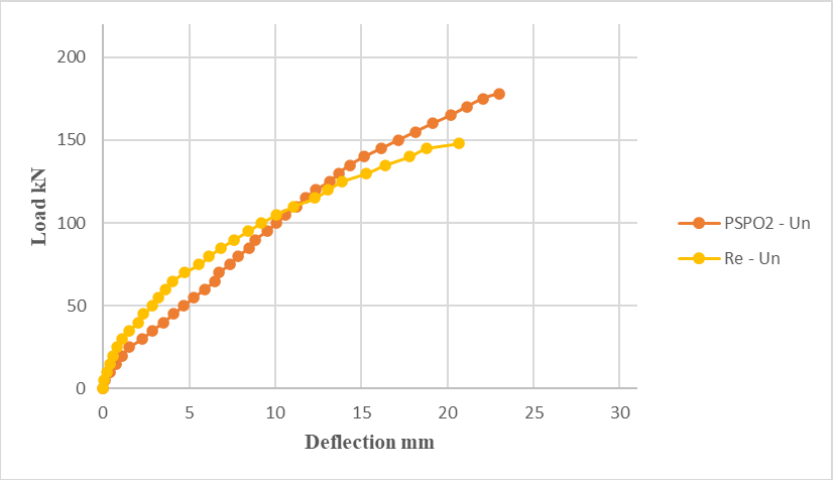

Figure (4.21): Comparison of load deflection curve for PSPO2-Un and Re-Un

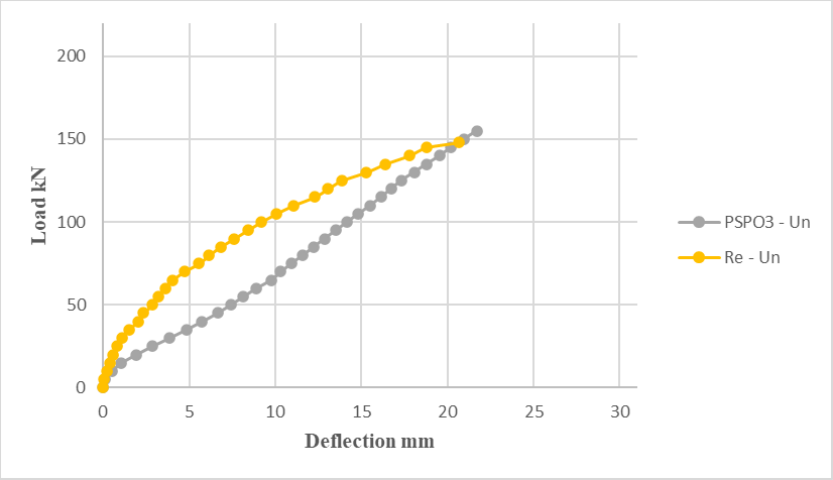

Figure (4.22): Comparison of load deflection curve for PSPO3-Un and Re-Un

The numbers of openings play a main domain for slabs rigidity in perforated steel reinforcing system. PSPO2-Un has considered an adequate number of openings which give rather more rigidity than the classic slab and maximum load among all models. All the previous explanations are clear in Figure (4.23).

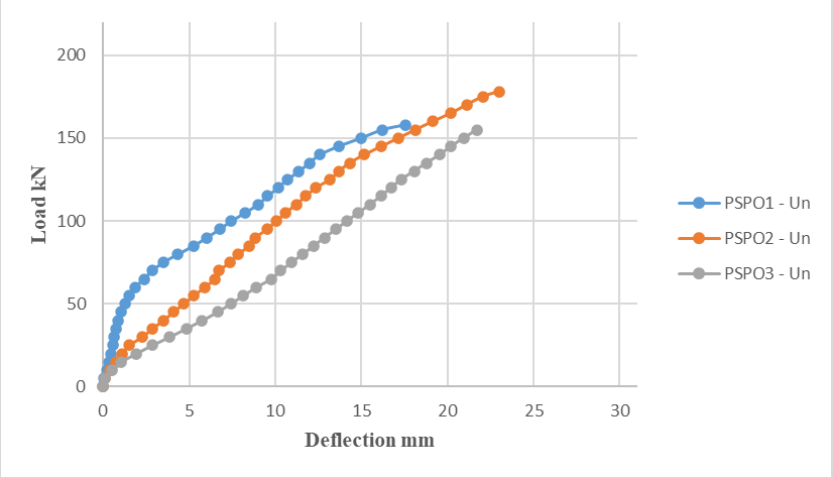

Figure (4.23): Effect of change size opening for octagonal shape – uniform load

4.5.2.3 Models Reinforced by Perforated Steel Plate – Square Opening

The last group of square perforated steel plates with the reference, bar reinforcing system, has been illustrated in Figures (4.24), (4.25) and (4.26).

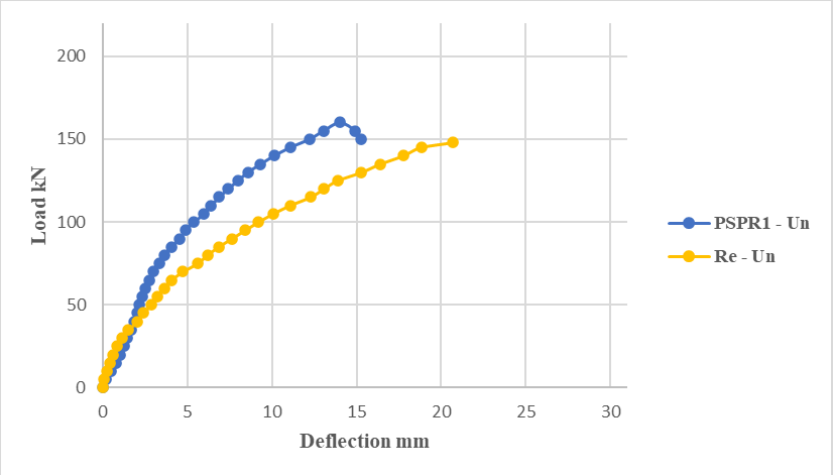

Figure (4.24): Comparison of load deflection curve for PSPR1-Un and Re-Un

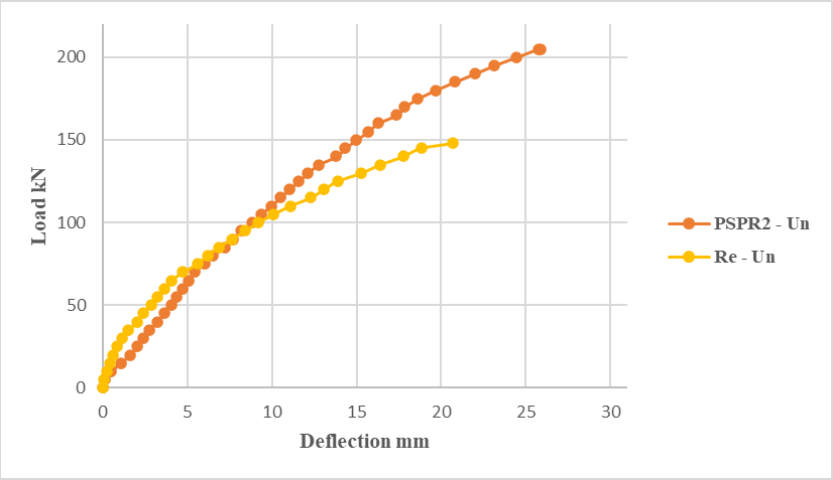

Figure (4.25): Comparison of load deflection curve for PSPR2-Un and Re-Un

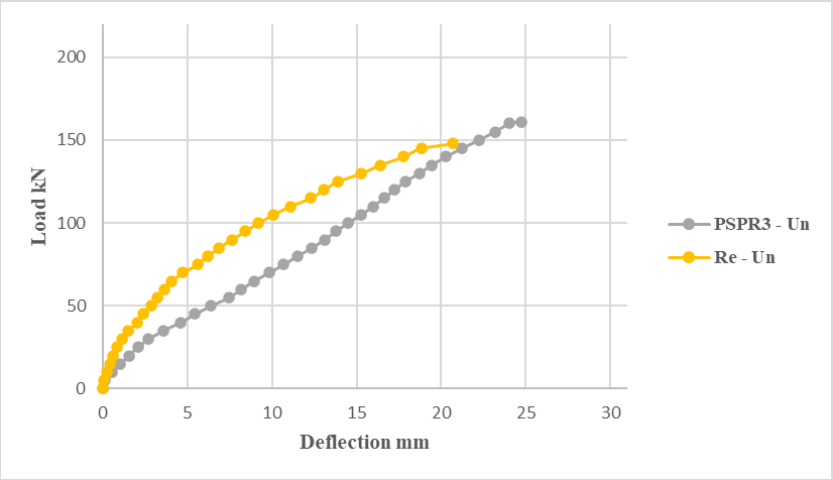

Figure (4.26): Comparison of load deflection curve for PSPR3-Un and Re-Un

In spite of the PSPR1-Un shows rigidity more than others but the PSPR2-Un offers higher ultimate load capacity and enhanced rigidity when it compared with the traditional method of reinforcing. The reduce of openings' number will reduce the interlock between concrete and steel plate. The effect of changing size opening for square shape under uniform load is shown in Figure (4.27).

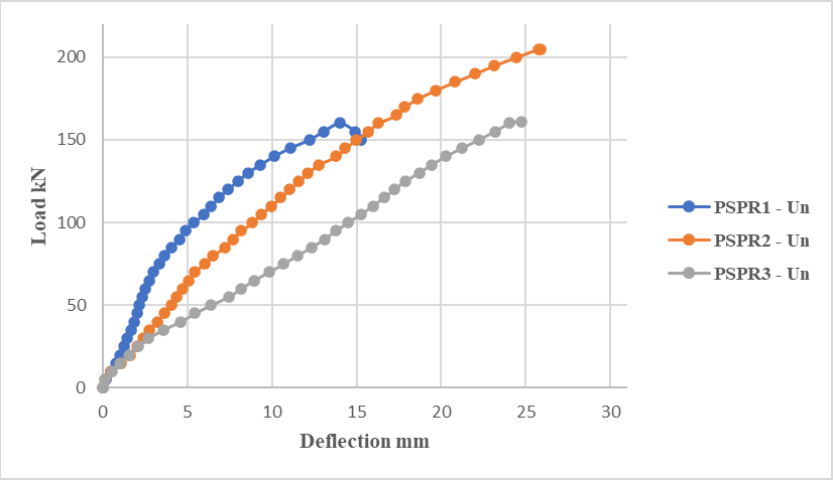

Figure (4.27): Effect of change size opening for square shape – uniform load

4.5.2.4 Discussion About the Effect of Opening shape – Uniform Load

Approximately, there is no clear effect of the opening shape. All circular, octagonal and square shapes have the same behavior as shown in Figures (4.28), (4.29) and (4.30), however, square shape displays ultimate load rather more than other shapes. It is about (4.69) % and (1.25) % more than circular and octagonal respectively when the openings 12×12, and the percentage increasing of ultimate load equals to (10.73) % and (13.17) % for 8×8 openings. In 4×4 openings it was (6.83) % and (3.73) % respectively.

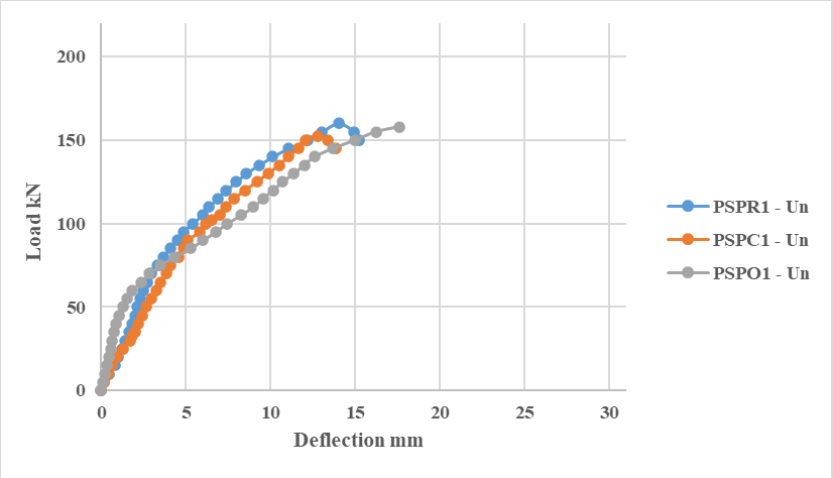

Figure (4.28): Effect of change shape opening – small size – uniform load

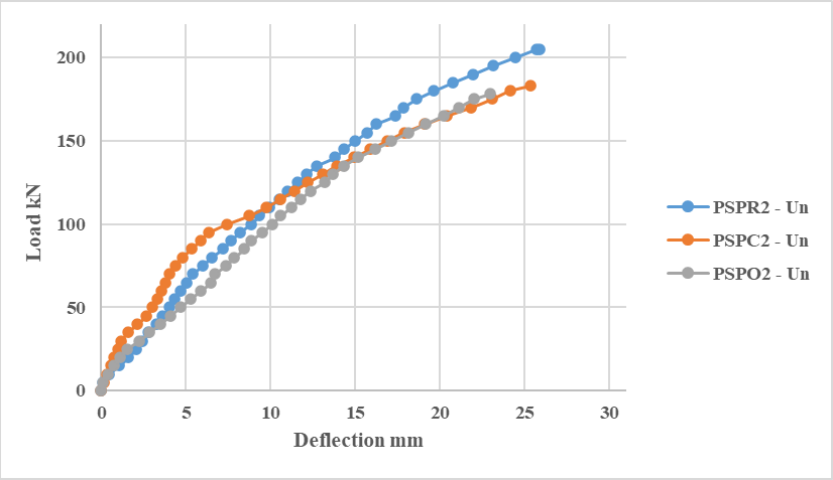

Figure (4.29): Effect of change shape opening – moderate size – uniform load

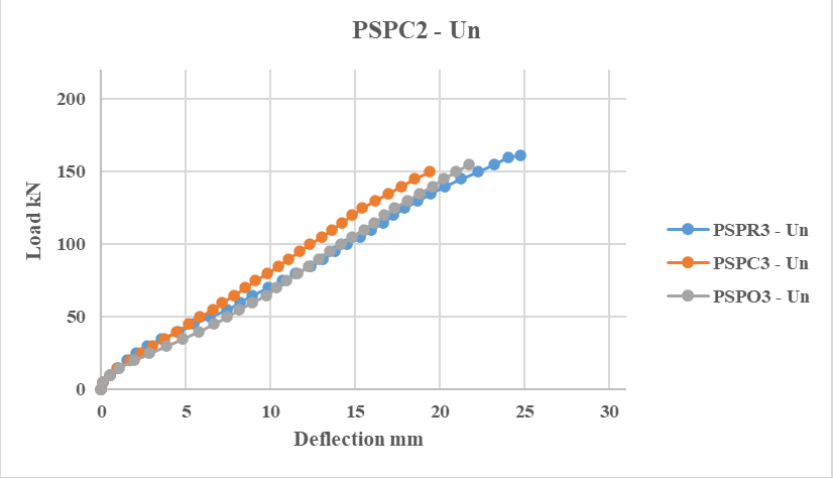

Figure (4.30): Effect of change shape opening – large size – uniform load

4.6 Cracking Behavior

Here, a strategy was adopted to focus the light on the development of cracks and how the cracks began in the tension face and how they increased in both types of loading. It consists of three main stages. The first stage began from zero load until the first visual crack appeared. All these cracks will be sketched in green. The cracks of the second stage are sketched in blue and it takes approximately twice the load of the first stage. The final stage continues till failure and the most suitable color for this stage is red. At each stage, the crack width was recorded.

Compression face cracks were drawn in red after the slabs were loaded and before they were moved. When the slabs were lifted, more cracks appeared, especially in the compression face. These cracks were not apparent before because they were either hidden or micro cracks, but when the slabs moved or lifted, they became visible, as a result, these cracks were neglected.

Finally, computerized Mapping for every stage was prepared and drawn.

4.6.1 Cracking Behavior for Models Under Concentrated Load

The concentrated load was applied gradually until the first crack happened. The first crack was still invisible because it was in a micro stage. The load would be continued till the first crack became visible, then the crack width was specified. During periods of increased load, several cracks began to form at the tension face throughout the slab, progressively increasing in number, becoming wider, and moving upwards as noted across four sides of slab models. As the load was raised, the rigidity of the structure deteriorated, and the mode of failure occurred: flexure – punching.

The three stages concerning the development of cracks for the slabs Re-Co, PSPC1-Co, PSPC2-Co, PSPC3-Co, PSPO1-Co, PSPO2-Co, PSPO3-Co, PSPR1-Co, PSPR2-Co and PSPR3-Co are clarified in Figures (4.31), (4.32), (4.33), (4.34), (4.35), (4.36), (4.37), (4.38), (4.39), (4.40) respectively (in tension face).

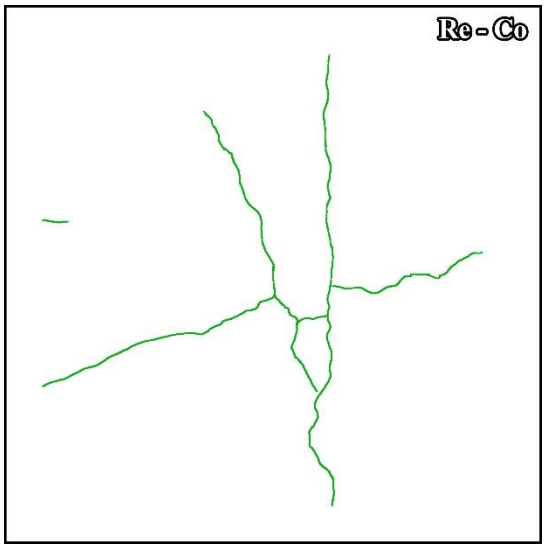

Computerized Mapping
Tension Face – First Stage
Load: 10 kN
Crack Width: 0.482 mm

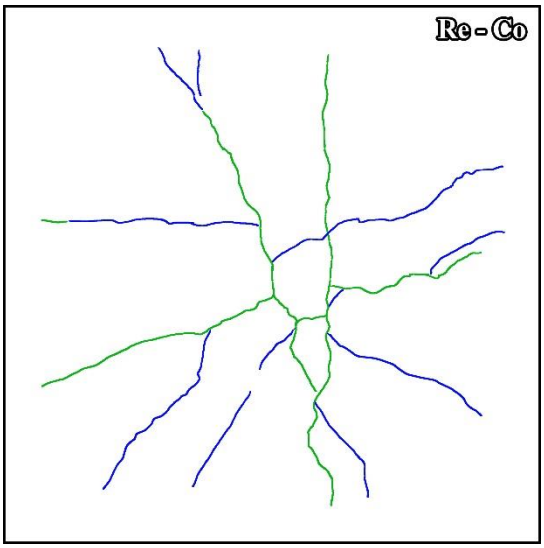

Computerized Mapping
Tension Face – Second Stage
Load: 15 kN
Crack Width: 3.17 mm

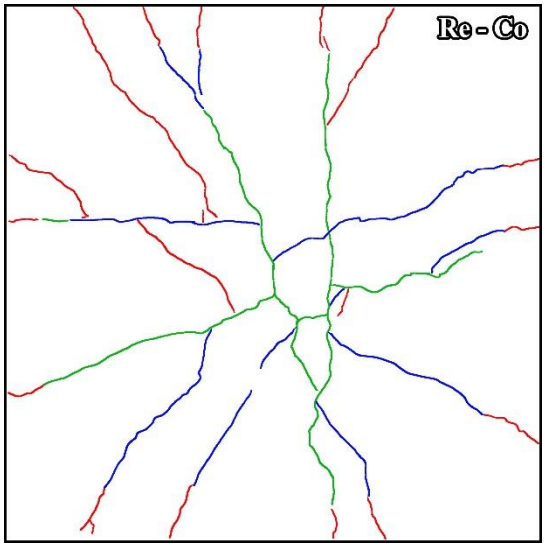

Computerized Mapping
Tension Face – Third Stage
Load: 19.5 kN
Crack Width: 9.52 mm

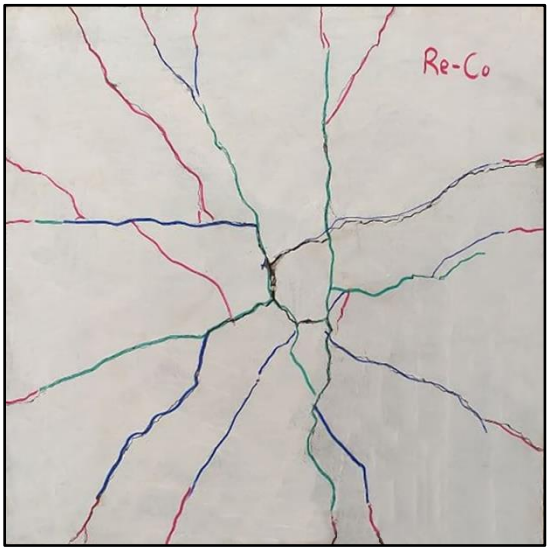

Actual Cracks
Tension Face – Third Stage
Load: 19.5 kN
Crack Width: 9.52 mm

Figure (4.31): Crack pattern for Re-Co (Tension Face)

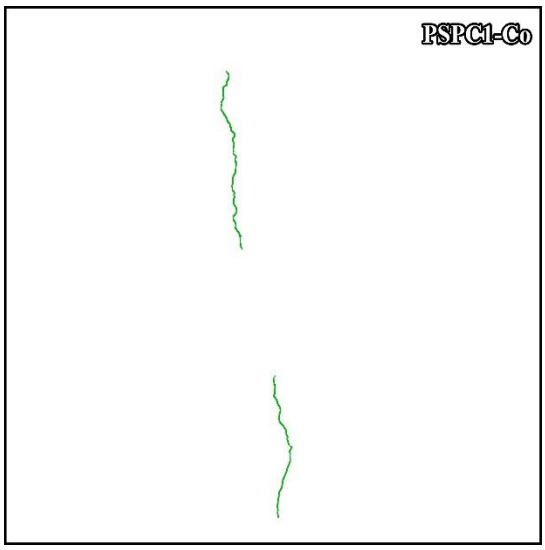

Computerized Mapping
Tension Face – First Stage
Load: 8 kN
Crack Width: 0.436 mm

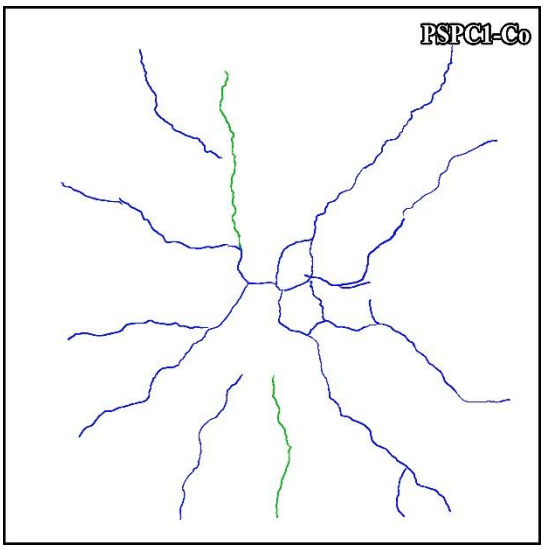

Computerized Mapping
Tension Face – Second Stage
Load: 20 kN
Crack Width: 1.59 mm

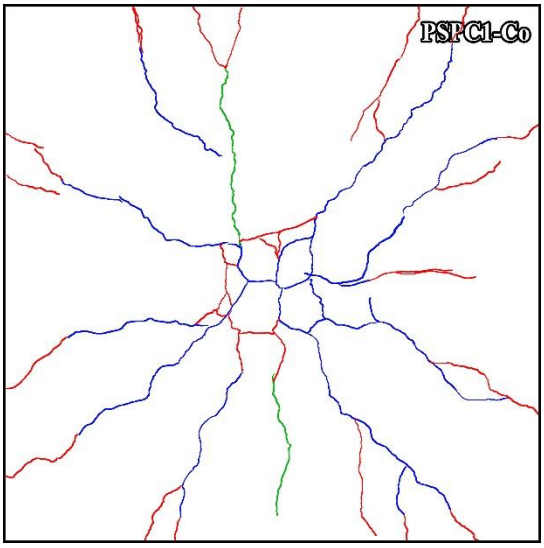

Computerized Mapping
Tension Face – Third Stage
Load: 31 kN
Crack Width: 3.55 mm

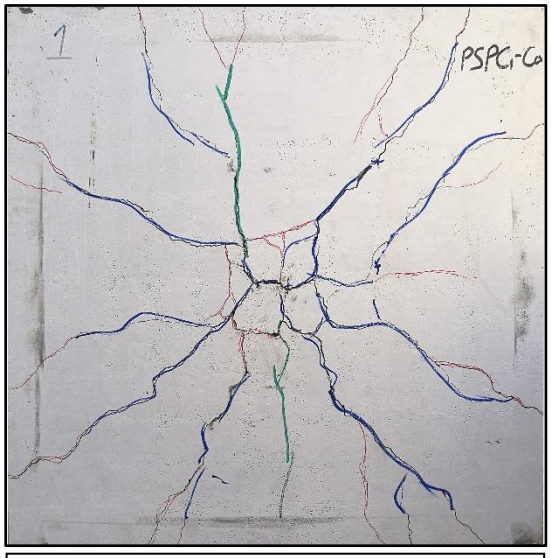

Actual Cracks
Tension Face – Third Stage
Load: 31 kN
Crack Width: 3.55 mm

Figure (4.32): Crack pattern for PSPC1-Co (Tension Face)

Computerized Mapping
Tension Face – First Stage
Load: 15 kN
Crack Width: 0.66 mm

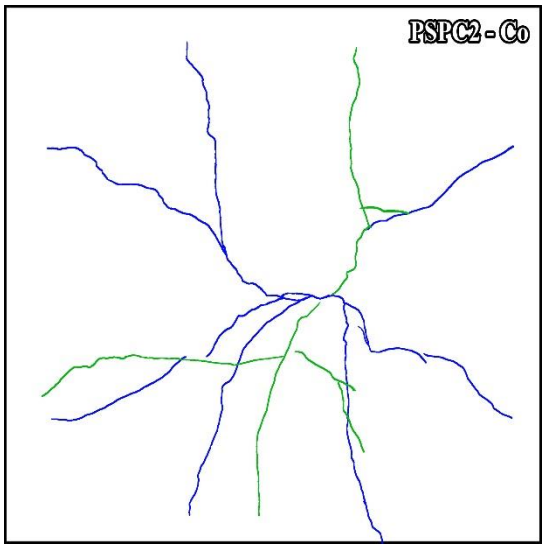

Computerized Mapping
Tension Face – Second Stage
Load: 20 kN
Crack Width: 1.26 mm

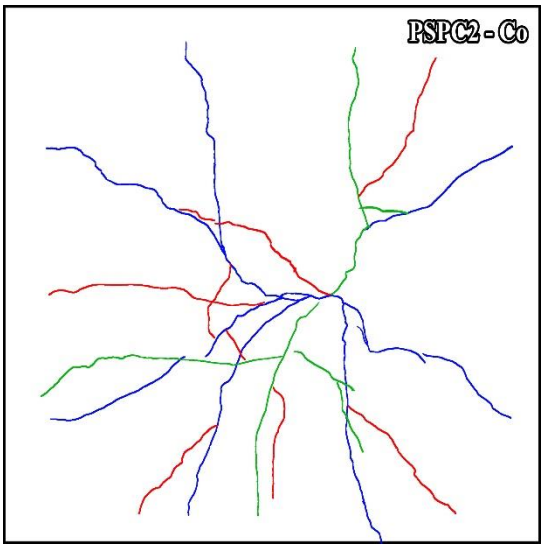

Computerized Mapping
Tension Face – Third Stage
Load: 34.5 kN
Crack Width: 3.02 mm

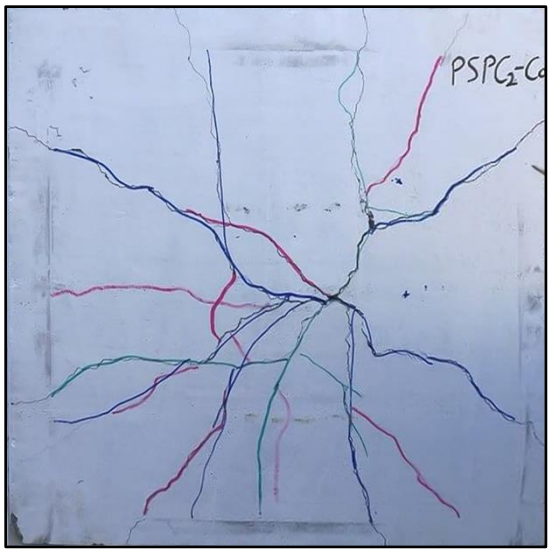

Actual Cracks
Tension Face – Third Stage
Load: 34.5 kN
Crack Width: 3.02 mm

Figure (4.33): Crack pattern for PSPC2-Co (Tension Face)

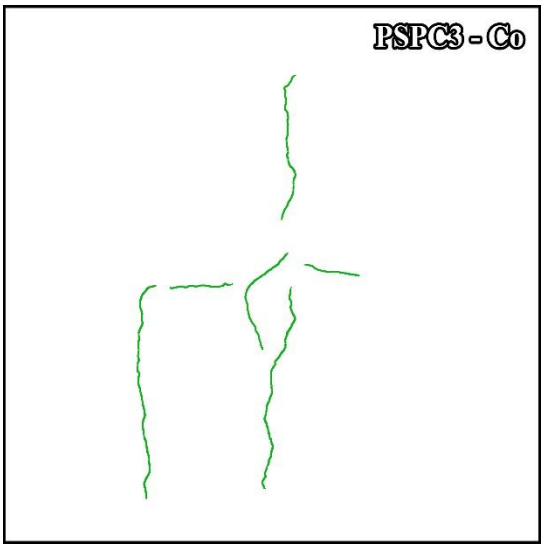

Computerized Mapping
Tension Face – First Stage
Load: 9.0 kN
Crack Width: 0.74 mm

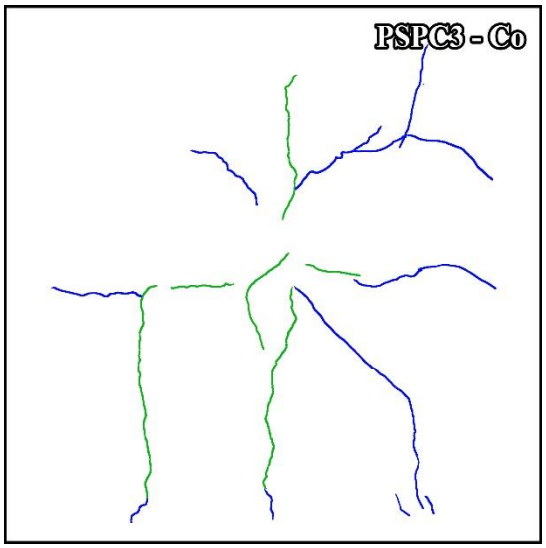

Computerized Mapping
Tension Face – Second Stage
Load: 20 kN
Crack Width: 3.05 mm

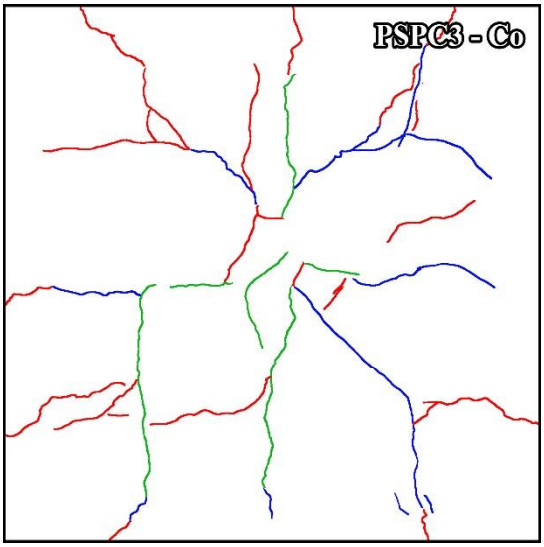

Computerized Mapping
Tension Face – Third Stage
Load: 28 kN
Crack Width: 9.79 mm

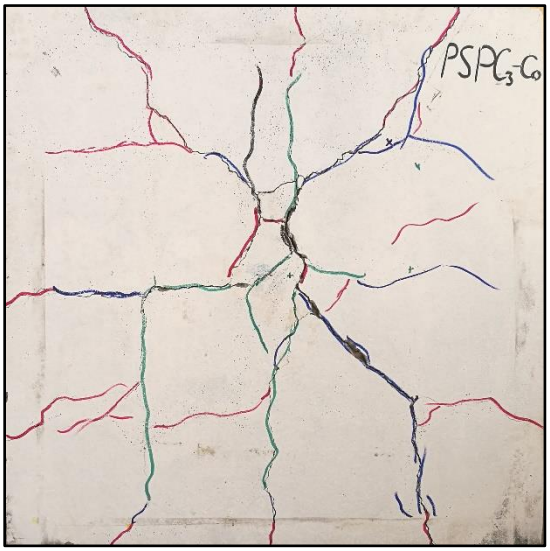

Actual Cracks
Tension Face – Third Stage
Load: 28 kN
Crack Width: 9.79 mm

Figure (4.34): Crack pattern for PSPC3-Co (Tension Face)

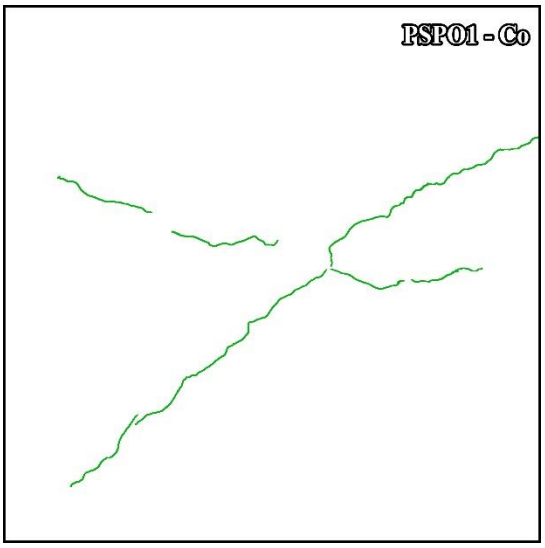

Computerized Mapping
Tension Face – First Stage
Load: 10 kN
Crack Width: 0.89 mm

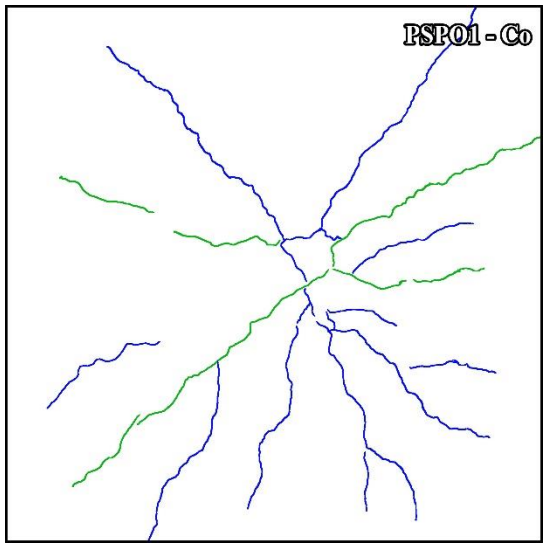

Computerized Mapping
Tension Face – Second Stage
Load: 25 kN
Crack Width: 2.42 mm

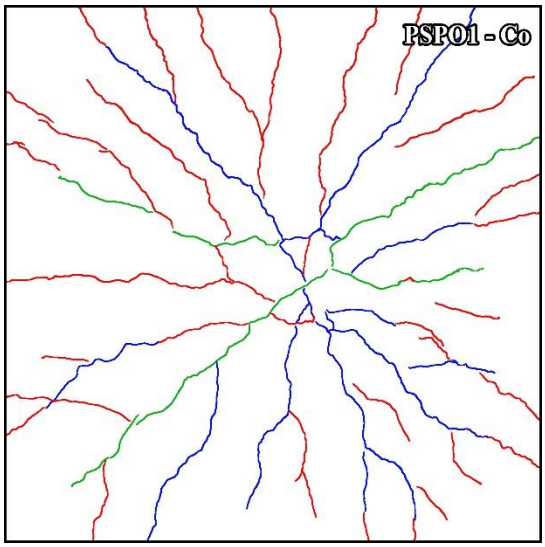

Computerized Mapping
Tension Face – Third Stage
Load: 32.5 kN
Crack Width: 3.28 mm

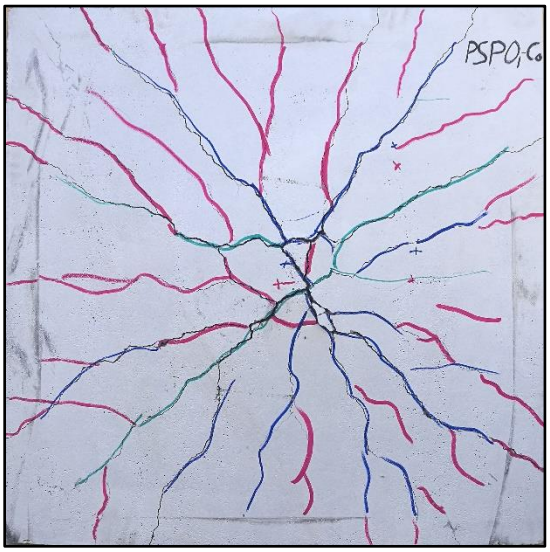

Actual Cracks
Tension Face – Third Stage
Load: 32.5 kN
Crack Width: 3.28 mm

Figure (4.35): Crack pattern for PSPO1-Co (Tension Face)

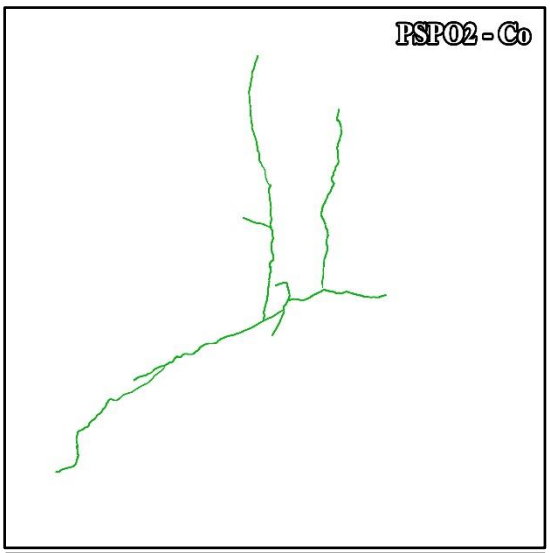

Computerized Mapping
Tension Face – First Stage
Load: 10 kN
Crack Width: 0.71 mm

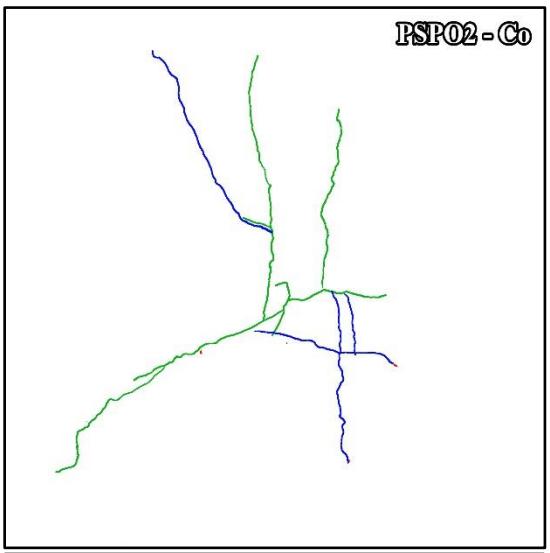

Computerized Mapping
Tension Face – Second Stage
Load: 20 kN
Crack Width: 1.84 mm

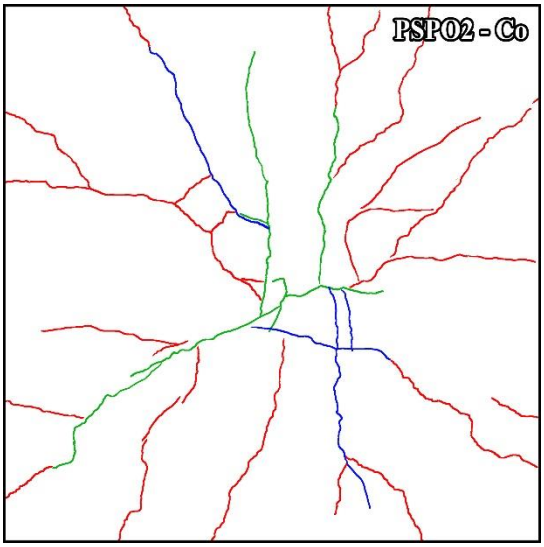

Computerized Mapping
Tension Face – Third Stage
Load: 35.5 kN
Crack Width: 4.0 mm

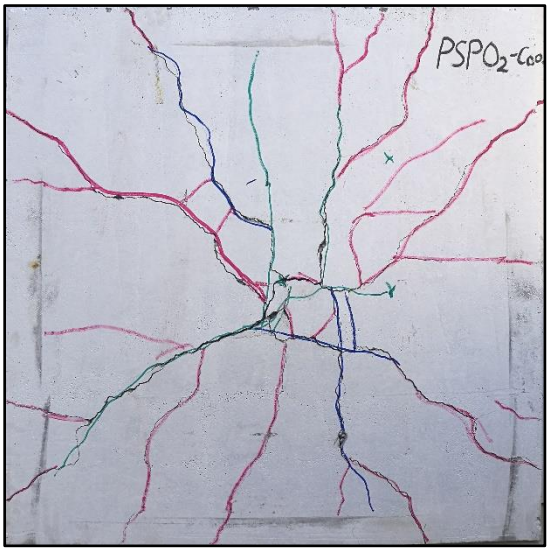

Actual Cracks
Tension Face – Third Stage
Load: 35.5 kN
Crack Width: 4.0 mm

Figure (4.36): Crack pattern for PSPO2-Co (Tension Face)

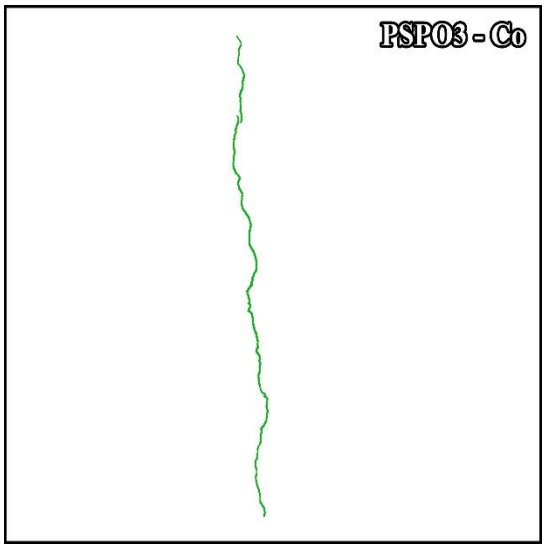

Computerized Mapping
Tension Face – First Stage
Load: 10 kN
Crack Width: 0.81 mm

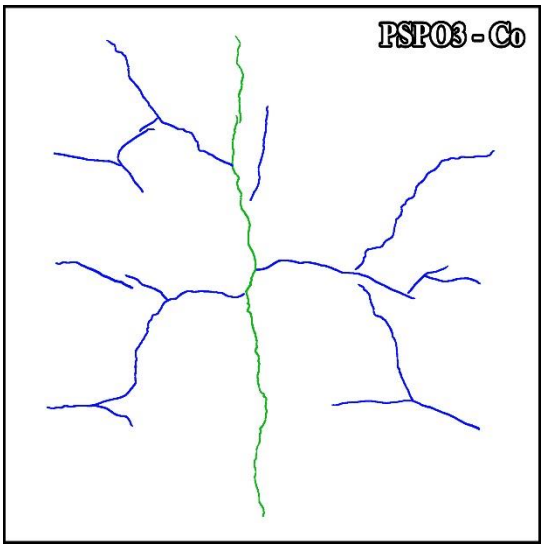

Computerized Mapping
Tension Face – Second Stage
Load: 22.5 kN
Crack Width: 2.35 mm

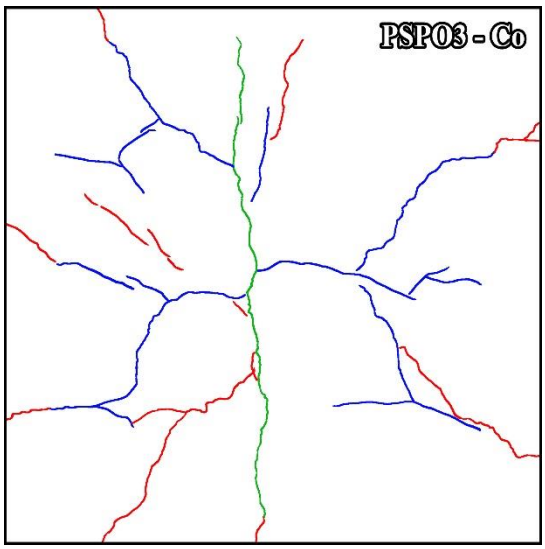

Computerized Mapping
Tension Face – Third Stage
Load: 30 kN
Crack Width: 4.11 mm

Actual Cracks
Tension Face – Third Stage
Load: 30 kN
Crack Width: 4.11 mm

Figure (4.37): Crack pattern for PSPO3-Co (Tension Face)

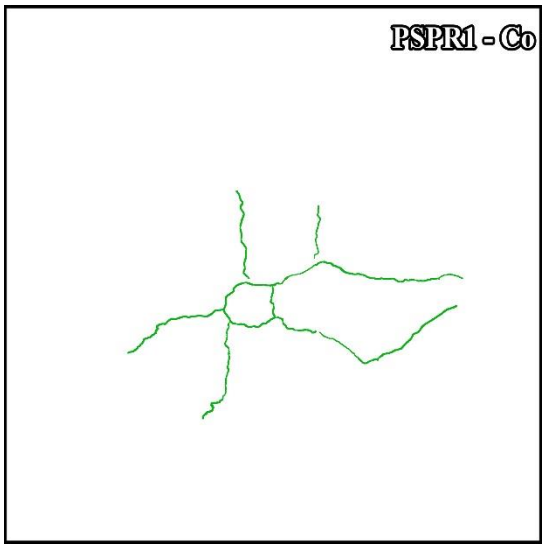

Computerized Mapping
Tension Face – First Stage
Load: 12 kN
Crack Width: 0.367 mm

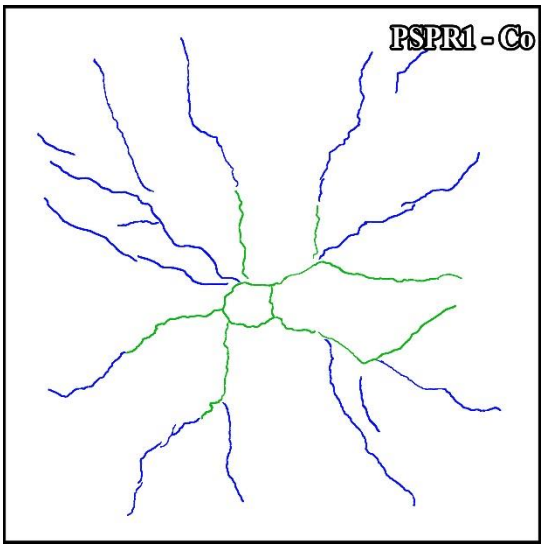

Computerized Mapping
Tension Face – Second Stage
Load: 25 kN
Crack Width: 1.54 mm

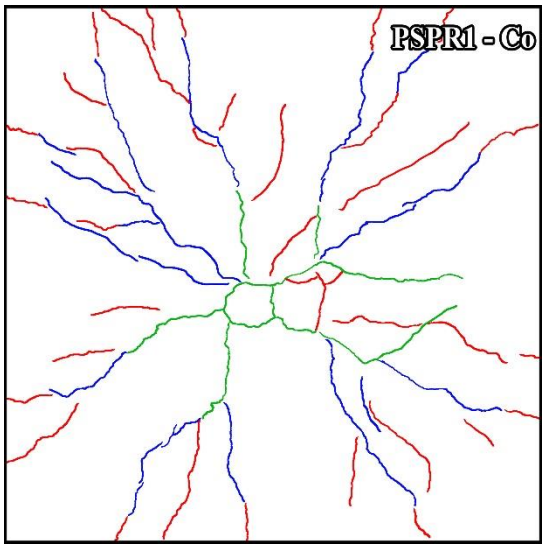

Computerized Mapping
Tension Face – Third Stage
Load: 35 kN
Crack Width: 3.46 mm

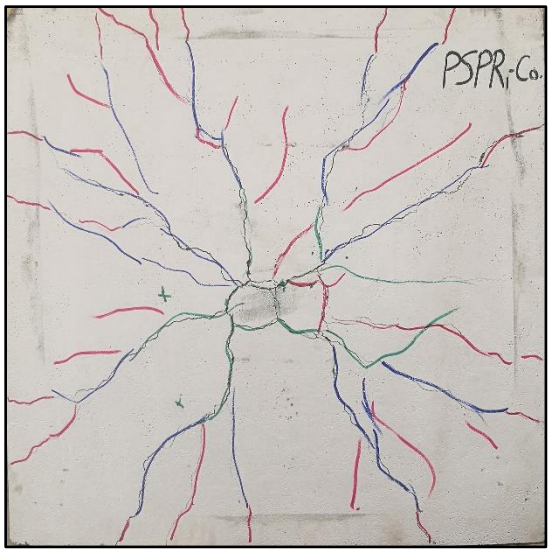

Actual Cracks
Tension Face – Third Stage
Load: 35 kN
Crack Width: 3.46 mm

Figure (4.38): Crack pattern for PSPR1-Co (Tension Face)

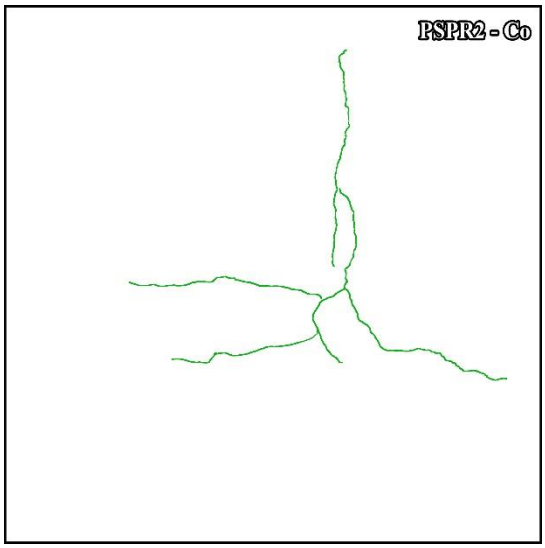

Computerized Mapping
Tension Face – First Stage
Load: 15 kN
Crack Width: 0.75 mm

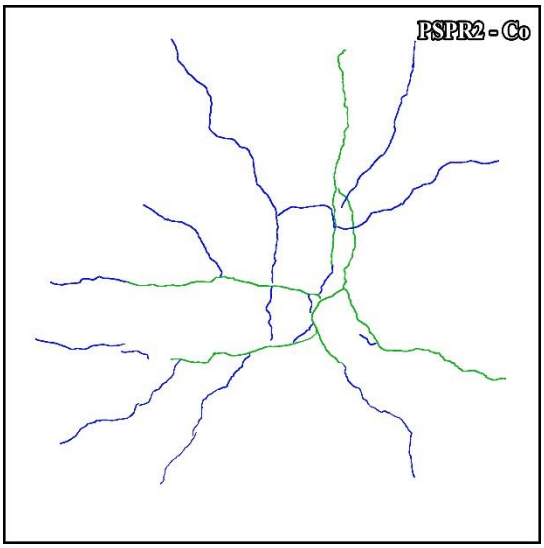

Computerized Mapping
Tension Face – Second Stage
Load: 30 kN
Crack Width: 1.78 mm

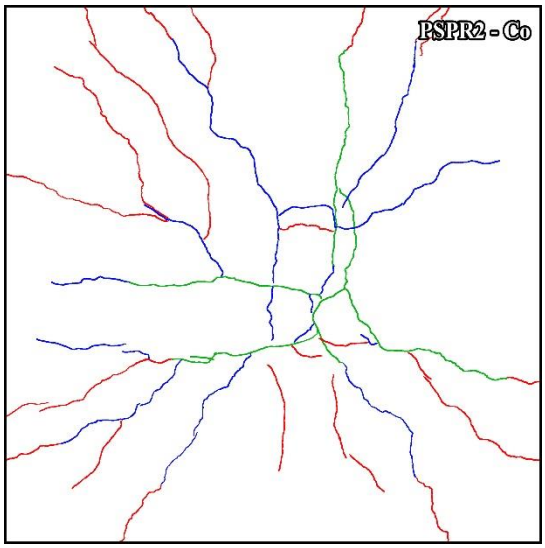

Computerized Mapping
Tension Face – Third Stage
Load: 36 kN
Crack Width: 2.87 mm

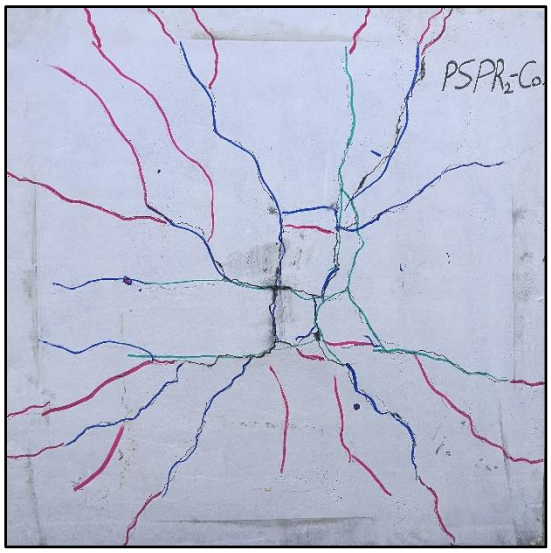

Actual Cracks
Tension Face – Third Stage
Load: 36 kN
Crack Width: 2.87 mm

Figure (4.39): Crack pattern for PSPR2-Co (Tension Face)

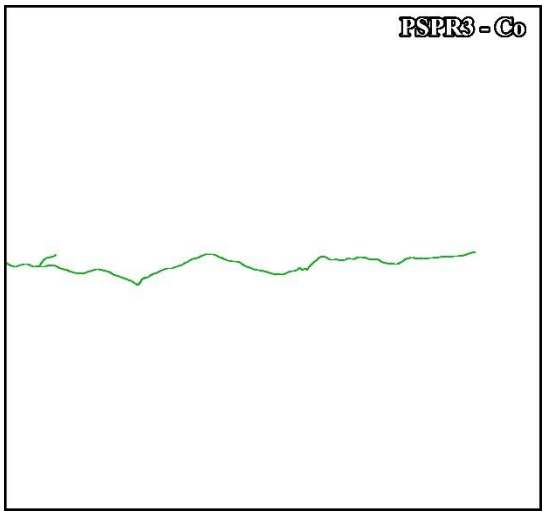

Computerized Mapping
Tension Face – First Stage
Load: 8.0 kN
Crack Width: 0.434 mm

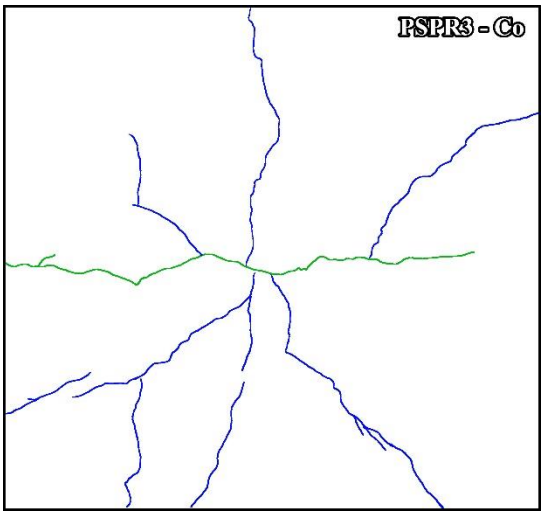

Computerized Mapping
Tension Face – Second Stage
Load: 20 kN
Crack Width: 2.09 mm

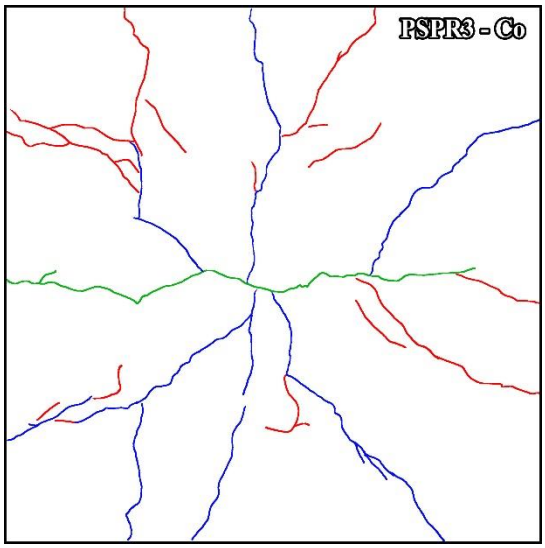

Computerized Mapping
Tension Face – Third Stage
Load: 31.5 kN
Crack Width: 5.62 mm

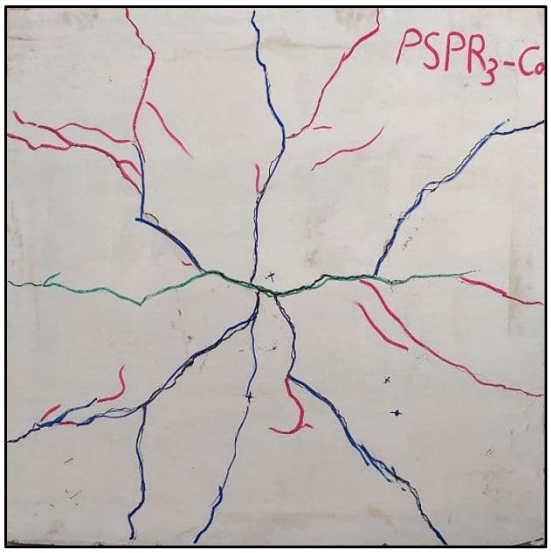

Actual Cracks
Tension Face – Third Stage
Load: 31.5 kN
Crack Width: 5.62 mm

Figure (4.40): Crack pattern for PSPR3-Co (Tension Face)

Cracks in compression face for all specimens clarified in Figures (4.41) to (4.50):

Computerized Mapping
Compression Face
Load: 19.5 kN

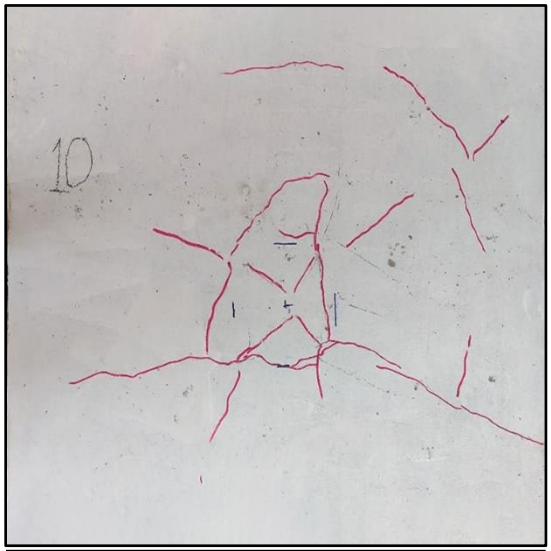

Actual Cracks
Compression Face
Load: 19.5 kN

Figure (4.41): Crack pattern for Re-Co (Compression Face)

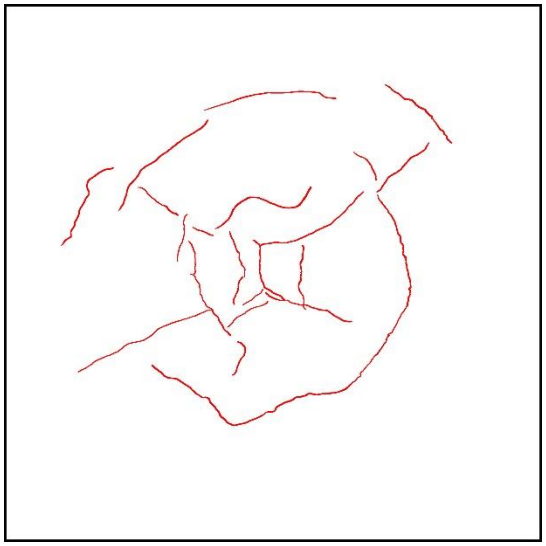

Computerized Mapping
Compression Face
Load: 31 kN

Actual Cracks
Compression Face
Load: 31 kN

Figure (4.42): Crack pattern for PSPC1-Co (Compression Face)

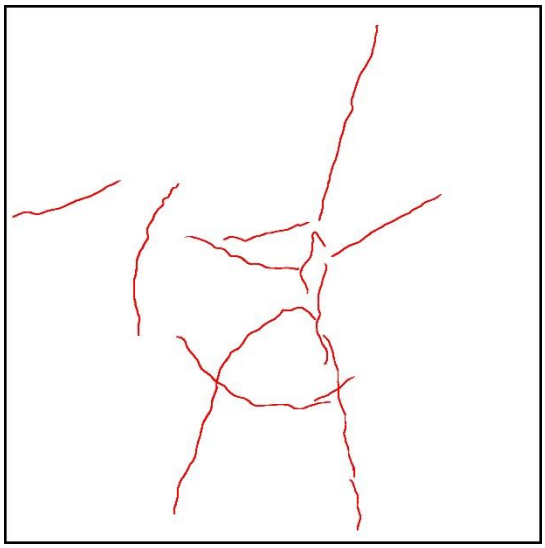

Computerized Mapping
Compression Face
Load: 34.5 kN

Actual Cracks
Compression Face
Load: 34.5 kN

Figure (4.43): Crack pattern for PSPC2-Co (Compression Face)

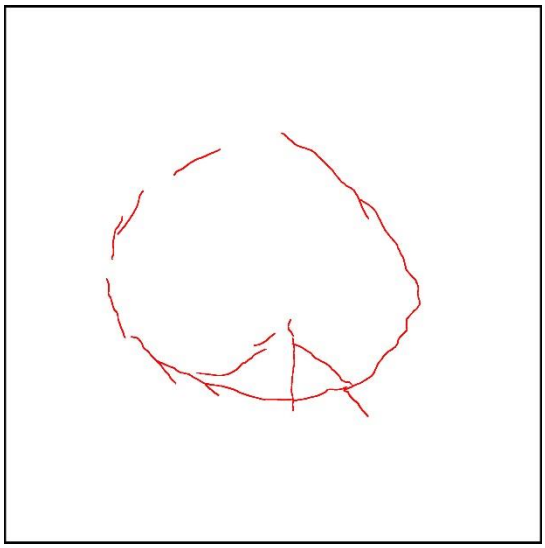

Computerized Mapping
Compression Face
Load: 28 kN

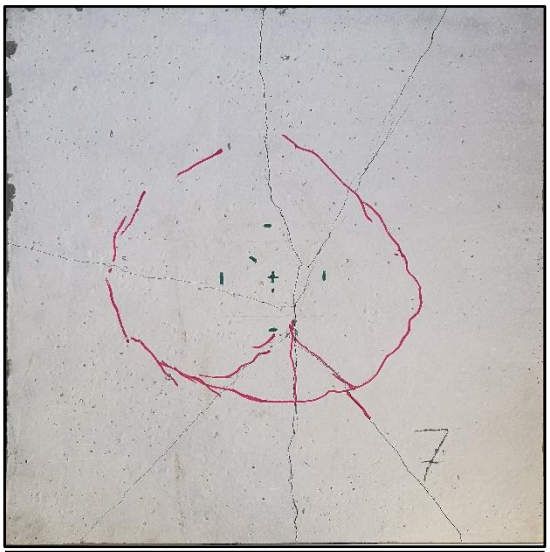

Actual Cracks
Compression Face
Load: 28 kN

Figure (4.44): Crack pattern for PSPC3-Co (Compression Face)

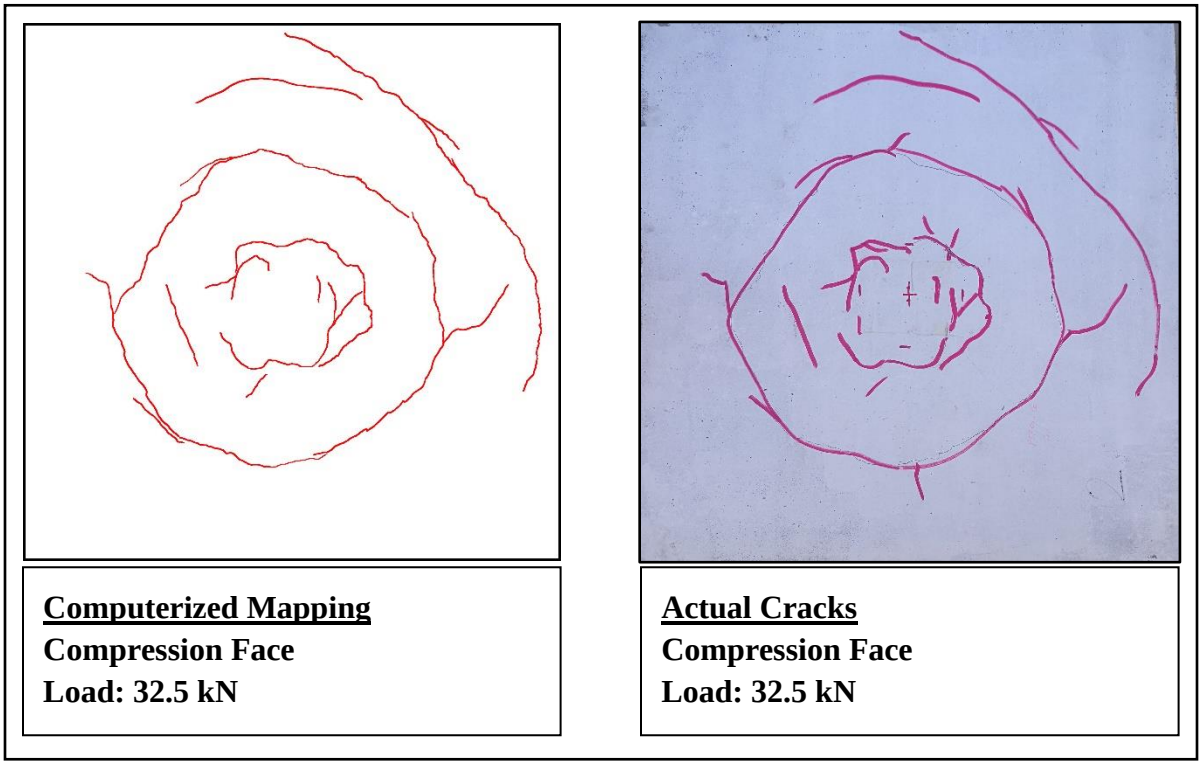

Computerized Mapping
Compression Face
Load: 32.5 kN

Actual Cracks
Compression Face
Load: 32.5 kN

Figure (4.45): Crack pattern for PSPO1-Co (Compression Face)

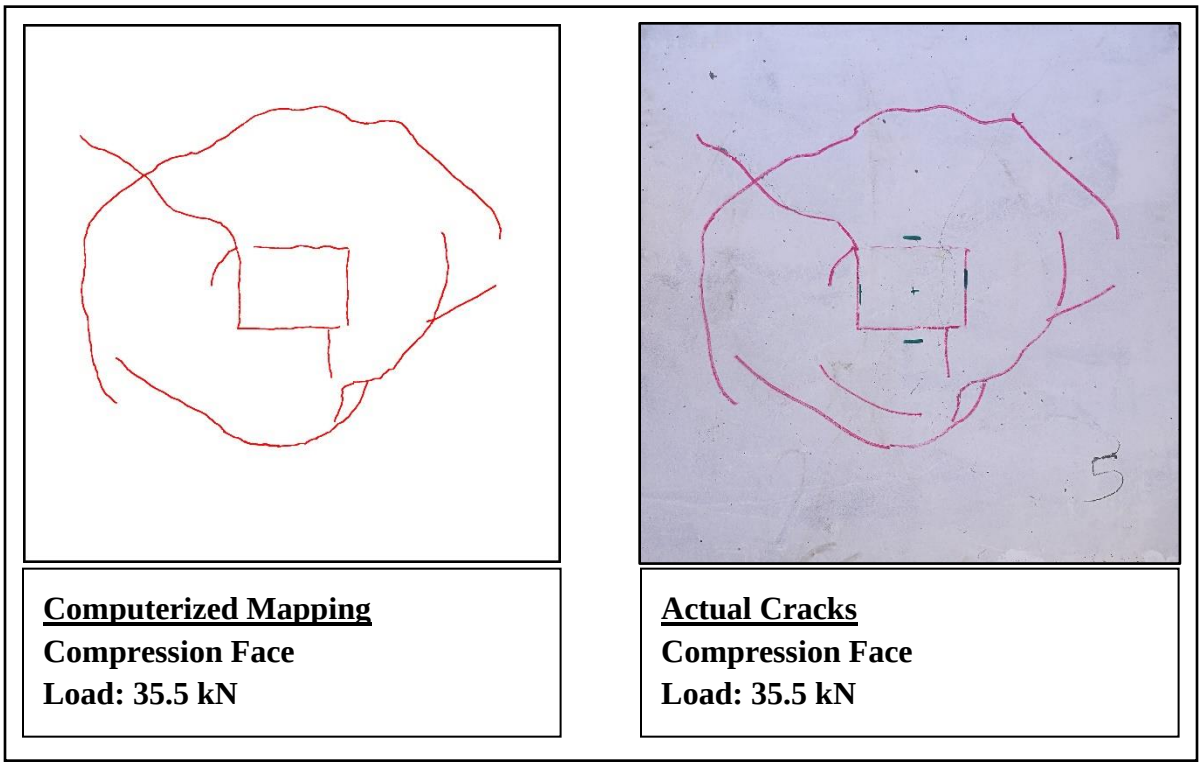

Computerized Mapping
Compression Face
Load: 35.5 kN

Actual Cracks
Compression Face
Load: 35.5 kN

Figure (4.46): Crack pattern for PSPO2-Co (Compression Face)

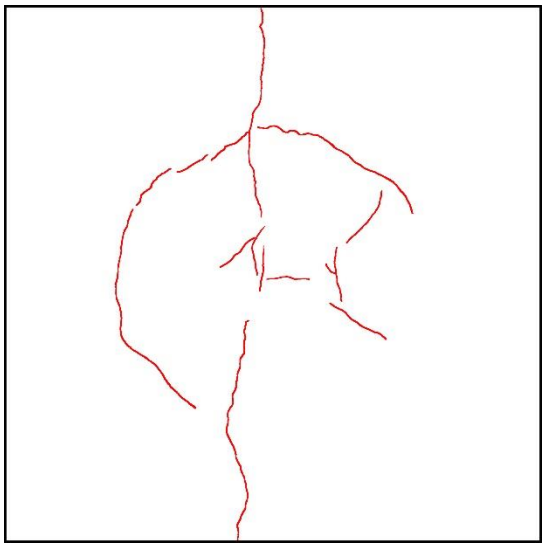

Computerized Mapping
Compression Face
Load: 30 kN

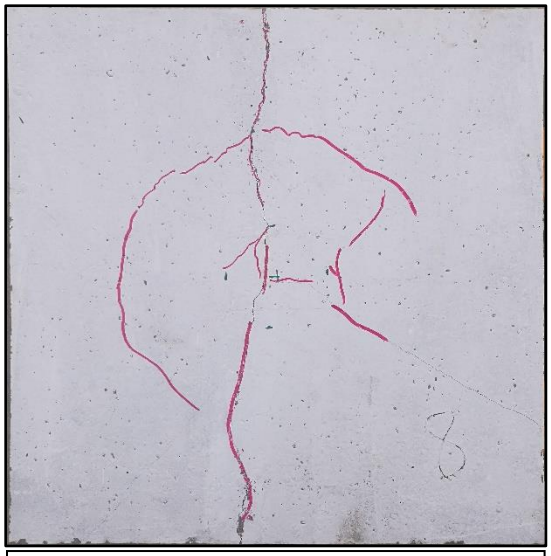

Actual Cracks
Compression Face
Load: 30 kN

Figure (4.47): Crack pattern for PSPO3-Co (Compression Face)

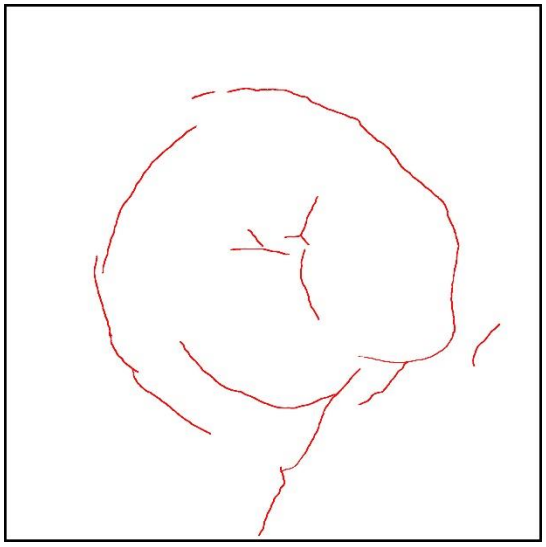

Computerized Mapping
Compression Face
Load: 35 kN

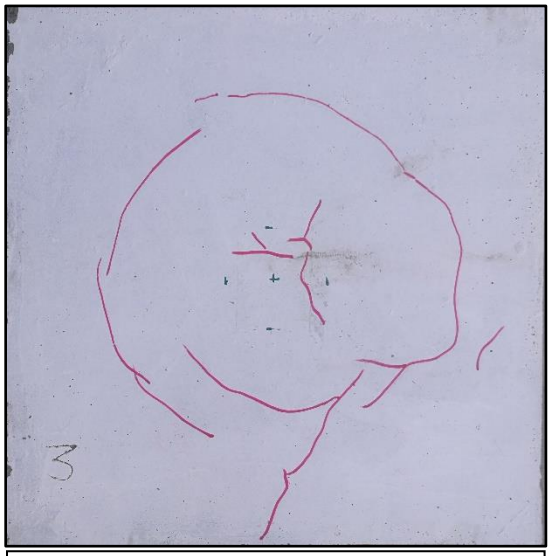

Actual Cracks
Compression Face
Load: 35 kN

Figure (4.48): Crack pattern for PSPR1-Co (Compression Face)

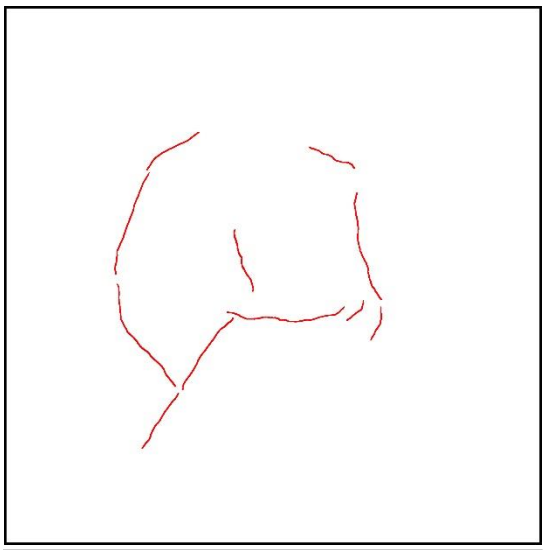

Computerized Mapping
Compression Face
Load: 36 kN

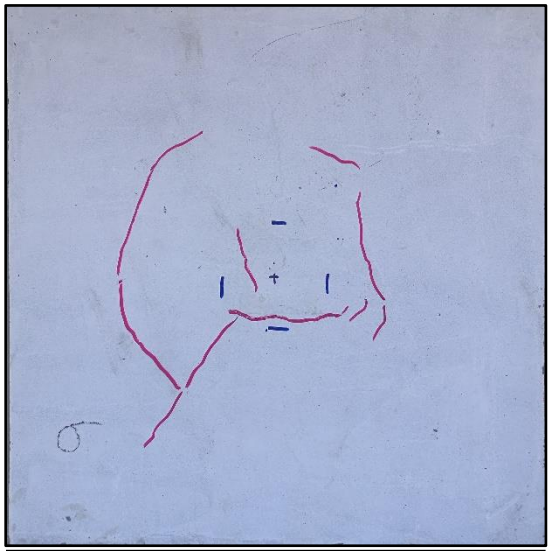

Actual Cracks
Compression Face
Load: 36 kN

Figure (4.49): Crack pattern for PSPR2-Co (Compression Face)

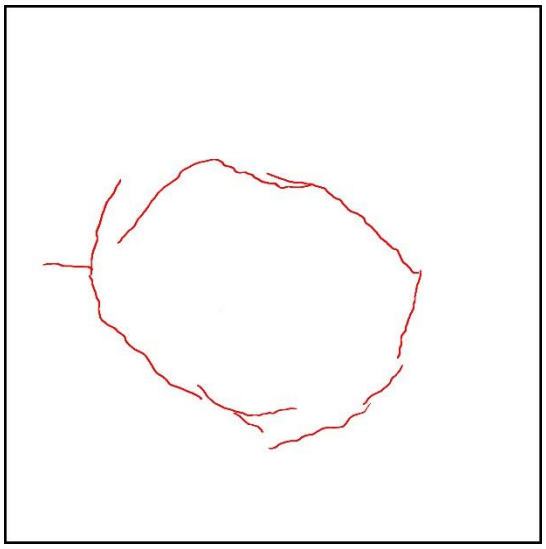

Computerized Mapping
Compression Face
Load: 31.5 kN

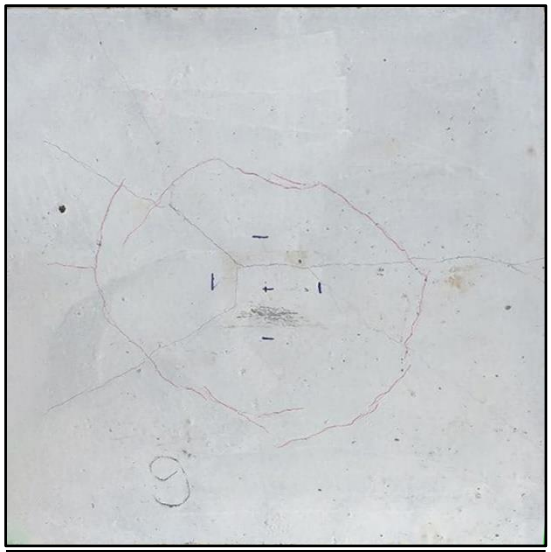

Actual Cracks
Compression Face
Load: 31.5 kN

Figure (4.50): Crack pattern for PSPR3-Co (Compression Face)

The crack behavior of perforated steel plate slabs was examined and analyzed. In general, all slabs reinforced in a circular, octagonal, or square shape produce acceptable results through comparison with a reference slab.

Because there is a vast feature of concrete in tension face without strengthening owing to the large area of opening, PSPC3-Co, PSPO3-Co, and PSPR3-Co have lesser first cracking load than Re-Co. The average of first cracking load for large opening is 9 kN and that is less than Re-Co about 10 percent.

PSPC2-Co, PSPO2-Co, and PSPR2-Co are the optimum models for initial visible cracking load resistance. These models have average initial visible cracking load greater than Re-Co by 33.3 percent.

Table (4.5) displays a summary of data collected.

Table (4.5): loads and corresponding crack's width – Concentrated load

No.	Model's name	Load kN	Crack's width mm	No.	Model's name	Load kN	Crack's width mm
1	Re - Co	10	0.482	6	PSPO2 - Co	10	0.71
		15	3.17			20	1.84
		19.5	9.52			35.5	4
2	PSPC1 - Co	8	0.436	7	PSPO3 - Co	10	0.81
		20	1.59			22.5	2.35
		31	3.55			30	4.11
3	PSPC2 - Co	15	0.66	8	PSPR1 - Co	12	0.367
		20	1.26			25	1.54
		34.5	3.02			35	3.46
4	PSPC3 - Co	9	0.74	9	PSPR2 - Co	15	0.75
		20	3.05			30	1.78
		28	9.79			36	2.87
5	PSPO1 - Co	10	0.89	10	PSPR3 - Co	8	0.434
		25	2.42			20	2.09
		32.5	3.28			31.5	5.62

4.6.2 Cracking Behavior for Models Under Uniform Load

The same general behavior can be said when it gradually increasing the uniform load till the first crack happened. Because it is at the micro stage, the initial fracture is still invisible to the eyes. The load would be applied until the first visible crack appeared, at which point the crack width would be stated. Several cracks began to form at the tension face throughout the slab during periods of high stresses, gradually growing in number, becoming wider, and spreading upwards to the four sides of the slab models. As the load was increased, the structure's stiffness decreased, and the following mechanism of failure occurred: Steel yielding causes flexural failure in tension, followed by concrete crushing in the compression zone because all specimens are reinforced by a minimum amount of steel, making the yielding of steel controlled.

The three stages involve the formation of cracks for the slabs Re-Un, PSPC1-Un, PSPC2-Un, PSPC3-Un, PSPO1-Un, PSPO2-Un, PSPO3-Un, PSPR1-Un, PSPR2-Un and PSPR3-Un are clarified in Figures (4.51), (4.52), (4.53), (4.54), (4.55), (4.56), (4.57), (4.58), (4.59), (4.60) respectively (in tension face).

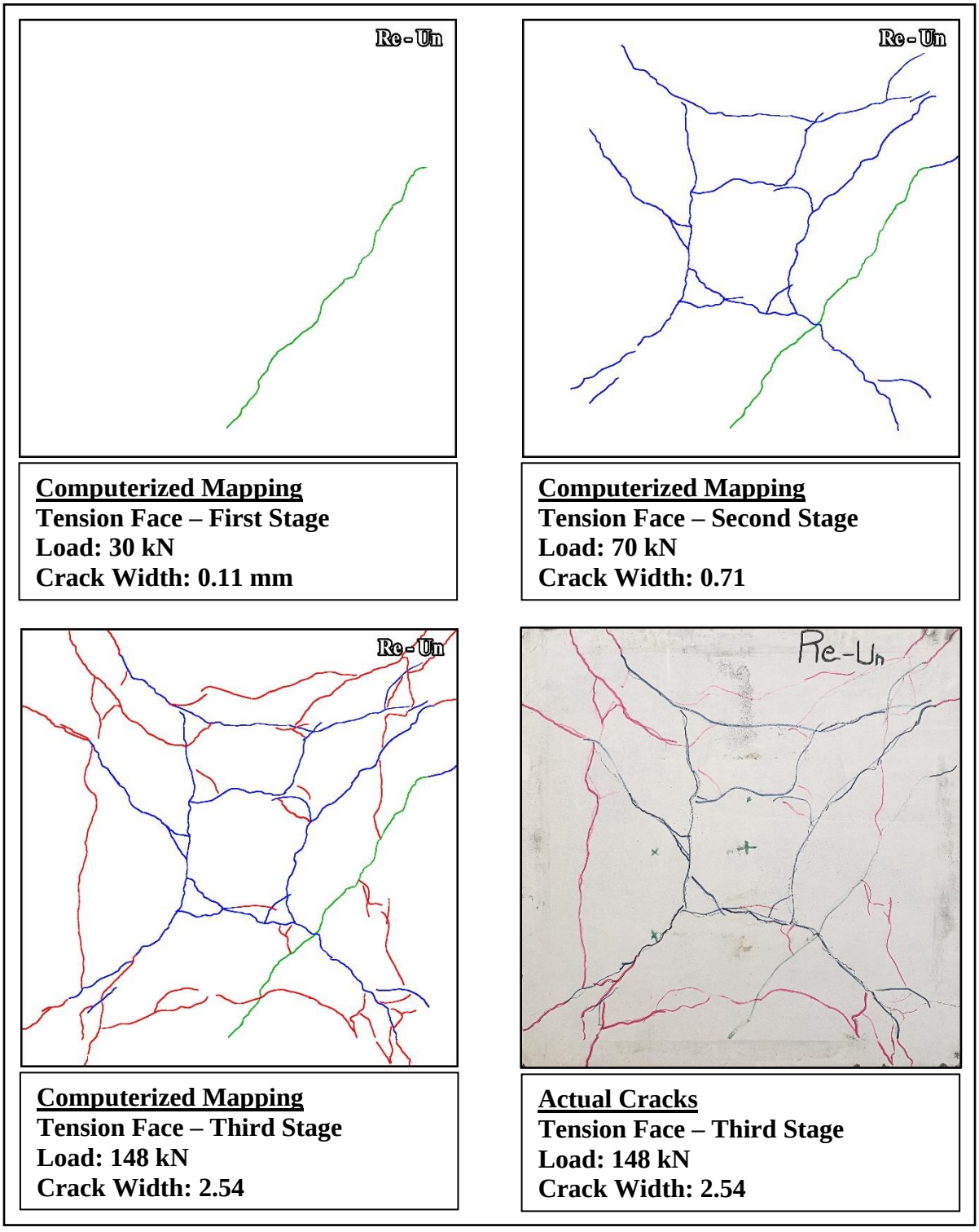

Figure (4.51): Crack pattern for Re-Un (Tension Face)

Computerized Mapping
Tension Face – First Stage
Load: 31 kN
Crack Width: 0.53 mm

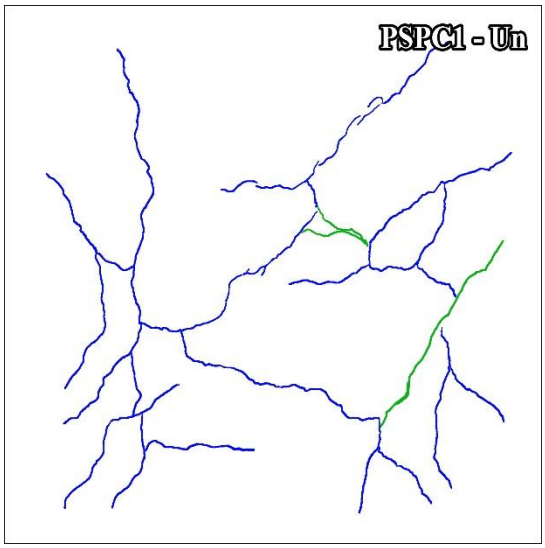

Computerized Mapping
Tension Face – Second Stage
Load: 100 kN
Crack Width: 0.84 mm

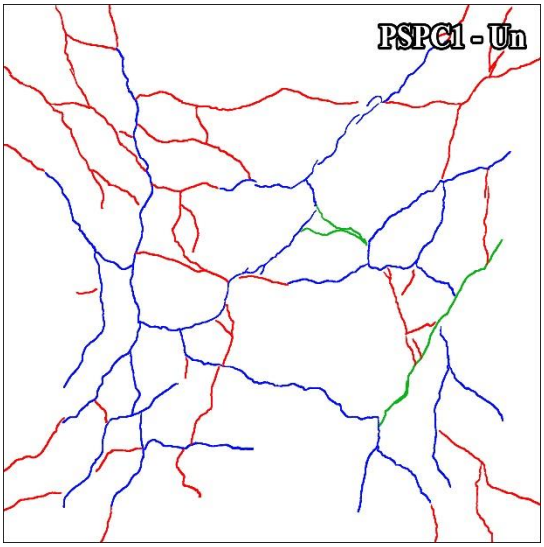

Computerized Mapping
Tension Face – Third Stage
Load: 145 kN
Crack Width: 2.29 mm

Actual Cracks
Tension Face – Third Stage
Load: 145 kN
Crack Width: 2.29 mm

Figure (4.52): Crack pattern for PSPC1-Un (Tension Face)

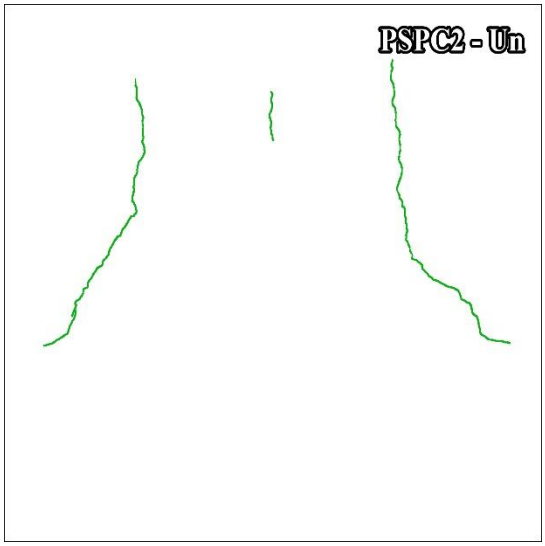

Computerized Mapping
Tension Face – First Stage
Load: 40 kN
Crack Width: 0.33 mm

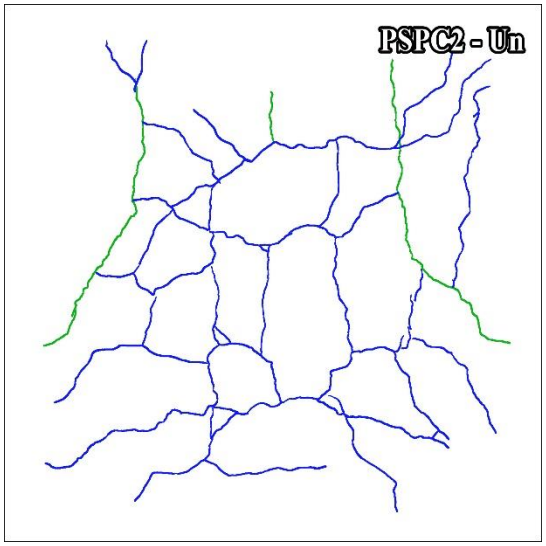

Computerized Mapping
Tension Face – Second Stage
Load: 90 kN
Crack Width: 1.31 mm

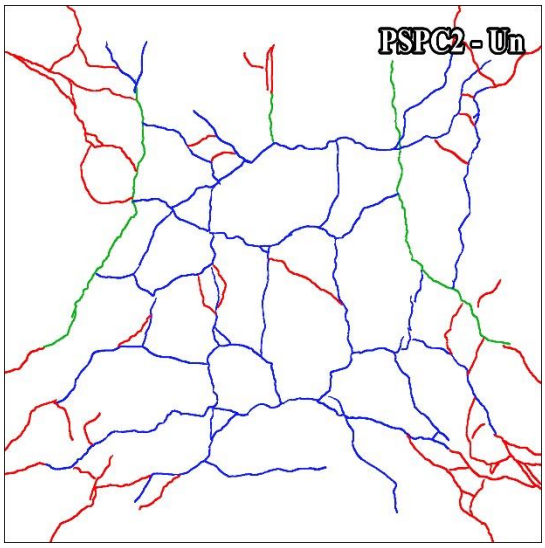

Computerized Mapping
Tension Face – Third Stage
Load: 183 kN
Crack Width: 4.00 mm

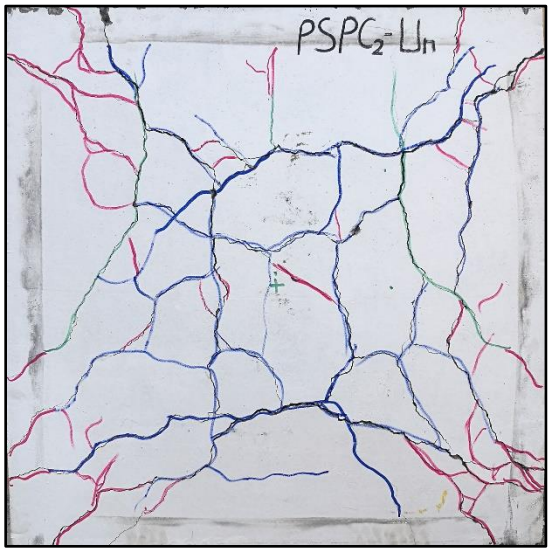

Actual Cracks
Tension Face – Third Stage
Load: 183 kN
Crack Width: 4.00 mm

Figure (4.53): Crack pattern for PSPC2-Un (Tension Face)

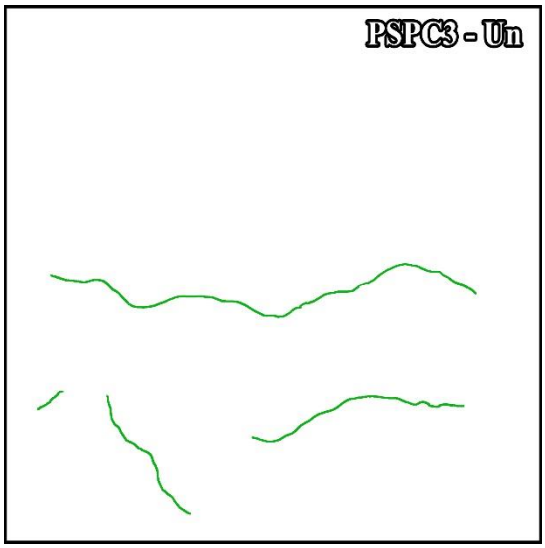

Computerized Mapping
Tension Face – First Stage
Load: 20 kN
Crack Width: 0.17 mm

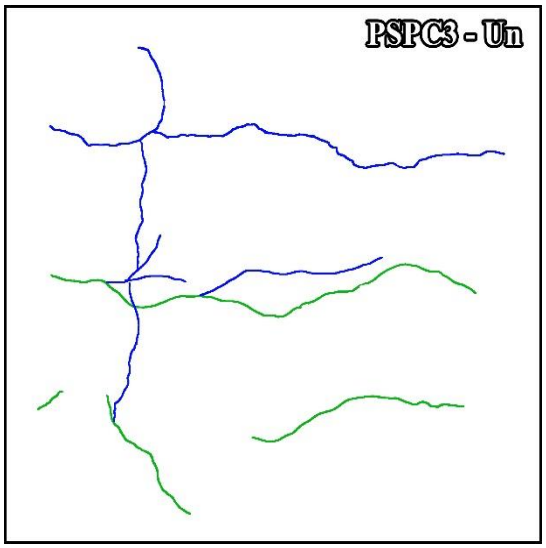

Computerized Mapping
Tension Face – Second Stage
Load: 100 kN
Crack Width: 1.41 mm

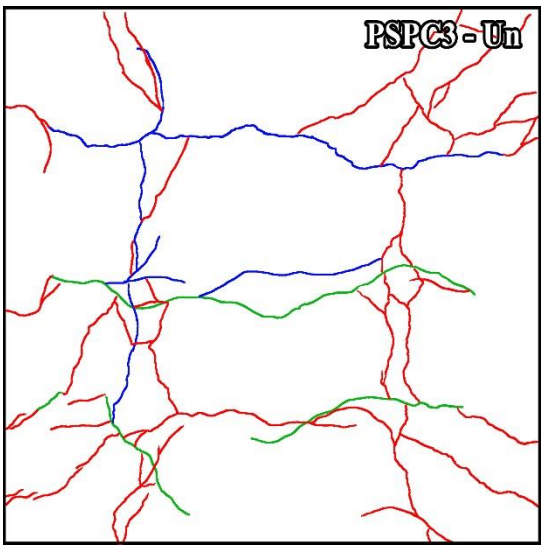

Computerized Mapping
Tension Face – Third Stage
Load: 150 kN
Crack Width: 3.24 mm

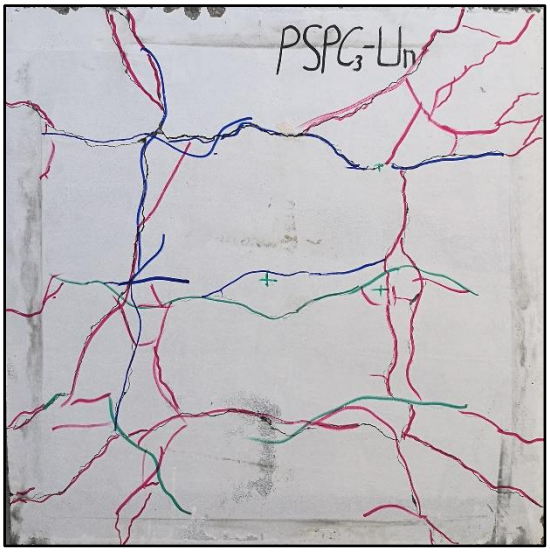

Actual Cracks
Tension Face – Third Stage
Load: 150 kN
Crack Width: 3.24 mm

Figure (4.54): Crack pattern for PSPC3-Un (Tension Face)

Computerized Mapping
Tension Face – First Stage
Load: 50 kN
Crack Width: 0.28 mm

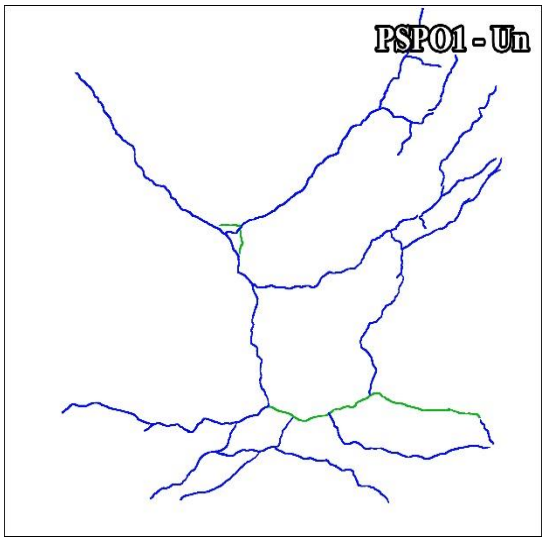

Computerized Mapping
Tension Face – Second Stage
Load: 105 kN
Crack Width: 1.66 mm

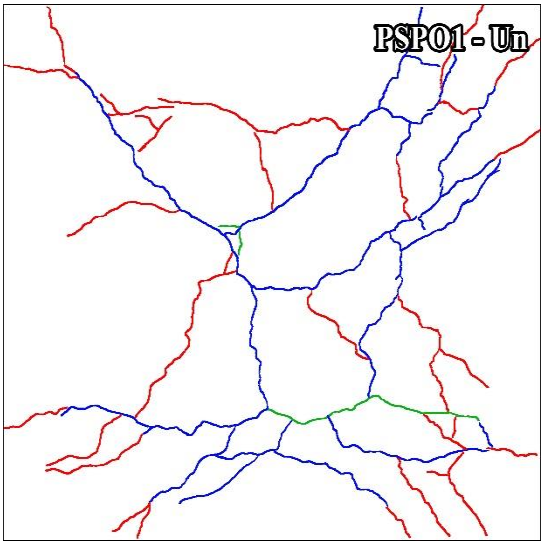

Computerized Mapping
Tension Face – Third Stage
Load: 158 kN
Crack Width: 4.48 mm

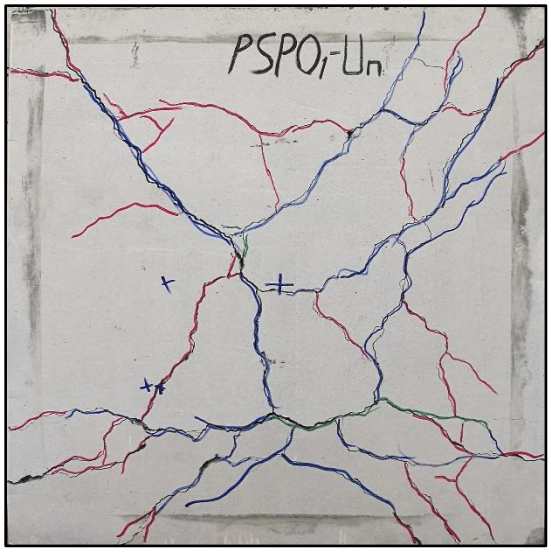

Actual Cracks
Tension Face – Third Stage
Load: 158 kN
Crack Width: 4.48 mm

Figure (4.55): Crack pattern for PSPO1-Un (Tension Face)

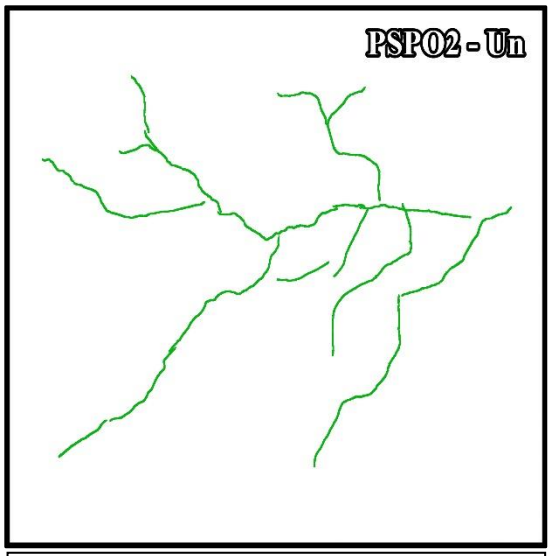

Computerized Mapping
Tension Face – First Stage
Load: 35 kN
Crack Width: 0.176 mm

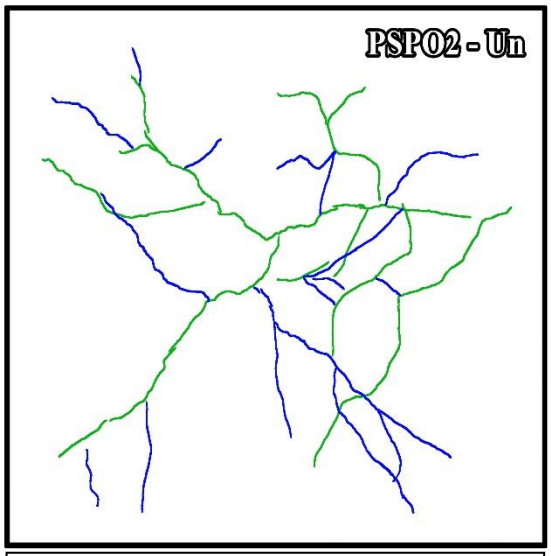

Computerized Mapping
Tension Face – Second Stage
Load: 70 kN
Crack Width: 0.593 mm

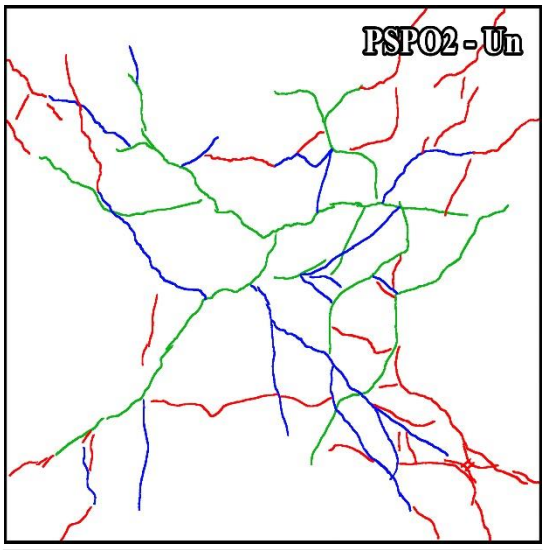

Computerized Mapping
Tension Face – Third Stage
Load: 178 kN
Crack Width: 2.01 mm

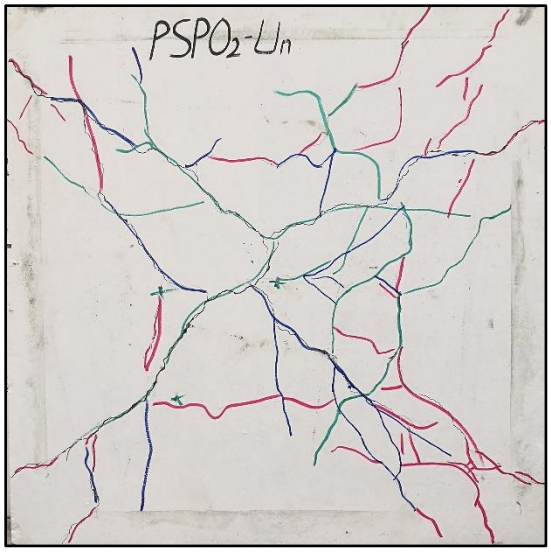

Actual Cracks
Tension Face – Third Stage
Load: 178 kN
Crack Width: 2.01 mm

Figure (4.56): Crack pattern for PSPO2-Un (Tension Face)

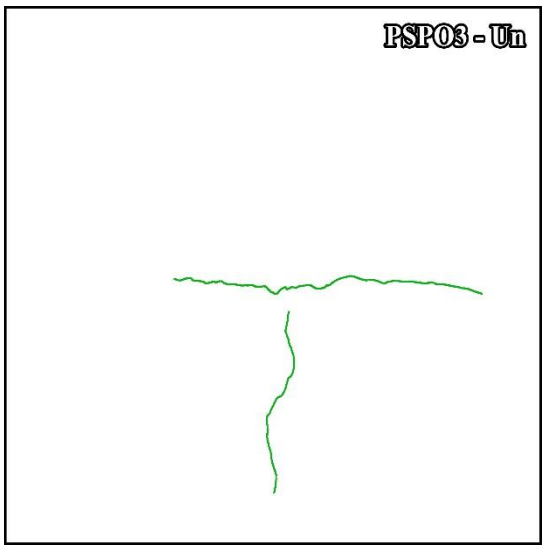

Computerized Mapping
Tension Face – First Stage
Load: 15 kN
Crack Width: 0.104 mm

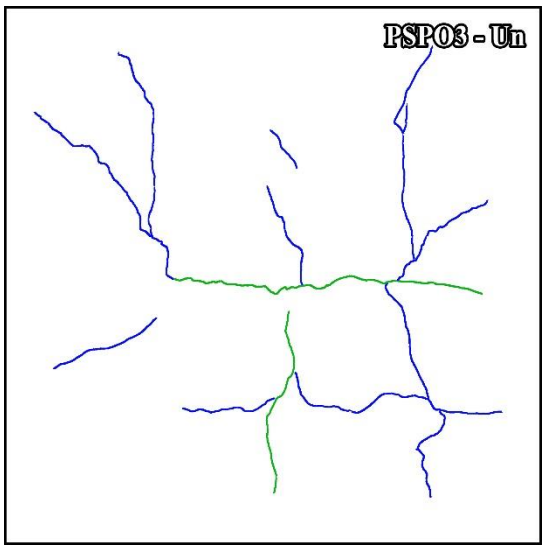

Computerized Mapping
Tension Face – Second Stage
Load: 41.5 kN
Crack Width: 0.61 mm

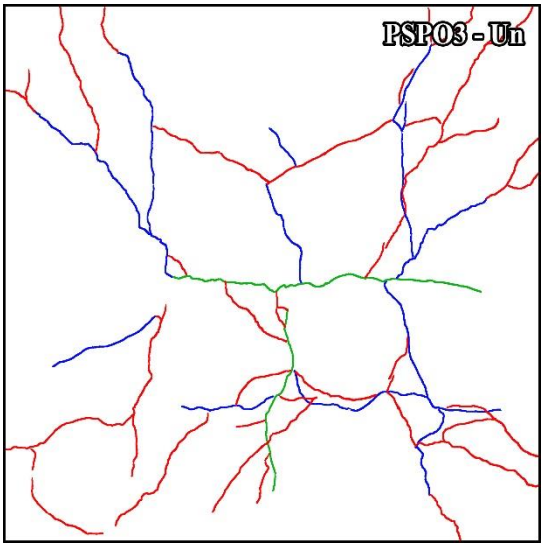

Computerized Mapping
Tension Face – Third Stage
Load: 155 kN
Crack Width: 5.13 mm

Actual Cracks
Tension Face – Third Stage
Load: 155 kN
Crack Width: 5.13 mm

Figure (4.57): Crack pattern for PSPO3-Un (Tension Face)

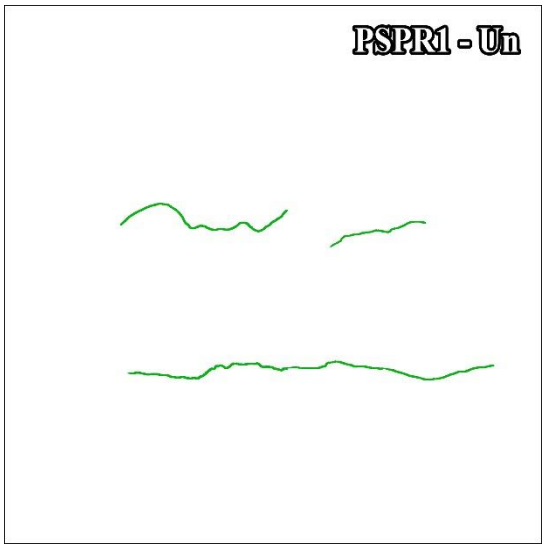

Computerized Mapping
Tension Face – First Stage
Load: 20 kN
Crack Width: 0.073 mm

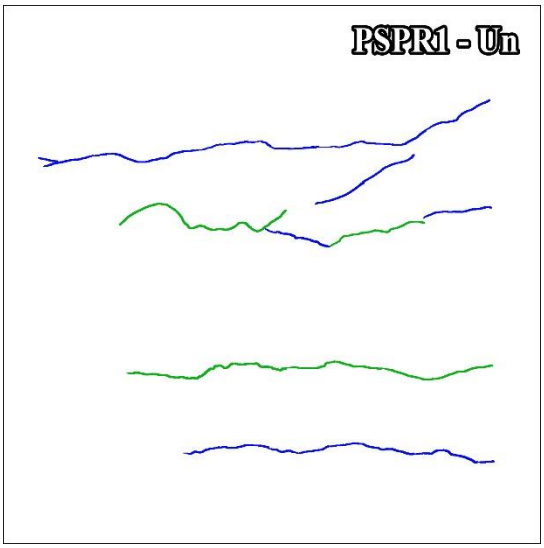

Computerized Mapping
Tension Face – Second Stage
Load: 53 kN
Crack Width: 0.47 mm

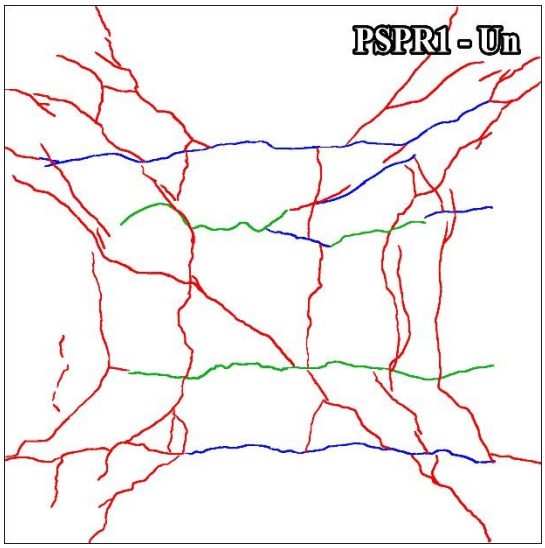

Computerized Mapping
Tension Face – Third Stage
Load: 150 kN
Crack Width: 2.34 mm

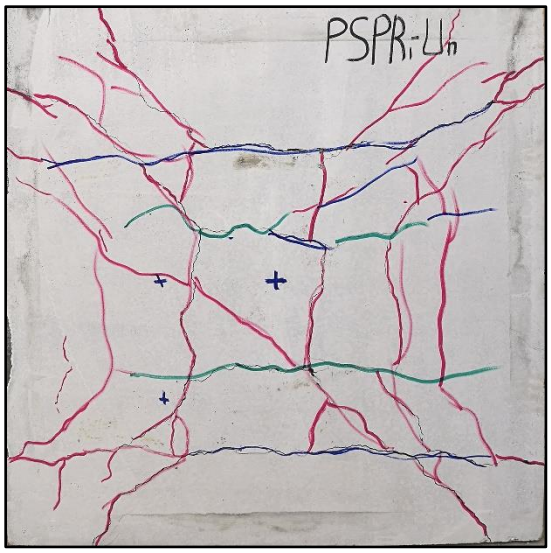

Actual Cracks
Tension Face – Third Stage
Load: 150 kN
Crack Width: 2.34 mm

Figure (4.58): Crack pattern for PSPR1-Un (Tension Face)

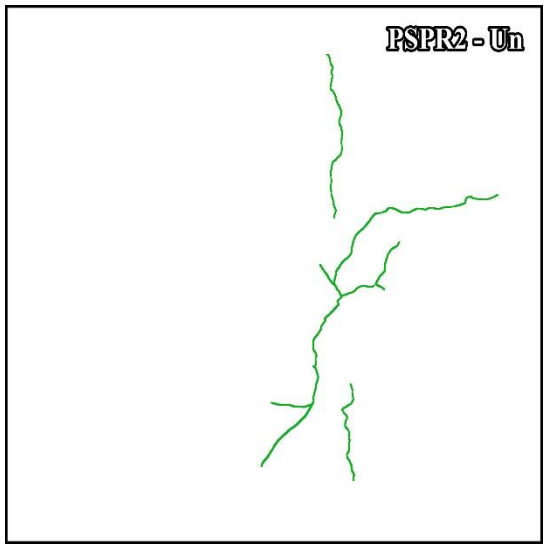

Computerized Mapping
Tension Face – First Stage
Load: 45 kN
Crack Width: 0.052 mm

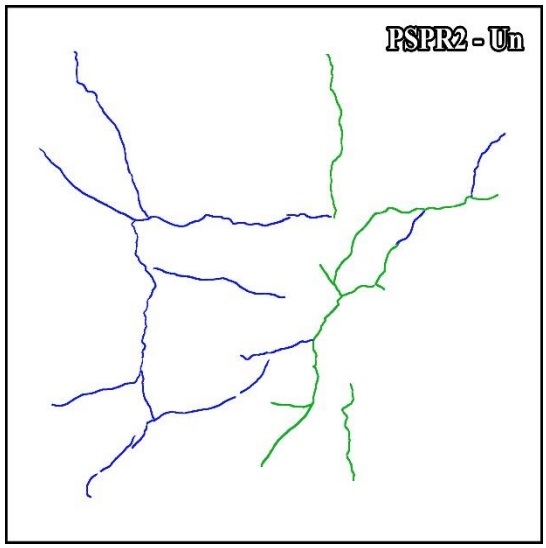

Computerized Mapping
Tension Face – Second Stage
Load: 80 kN
Crack Width: 0.340 mm

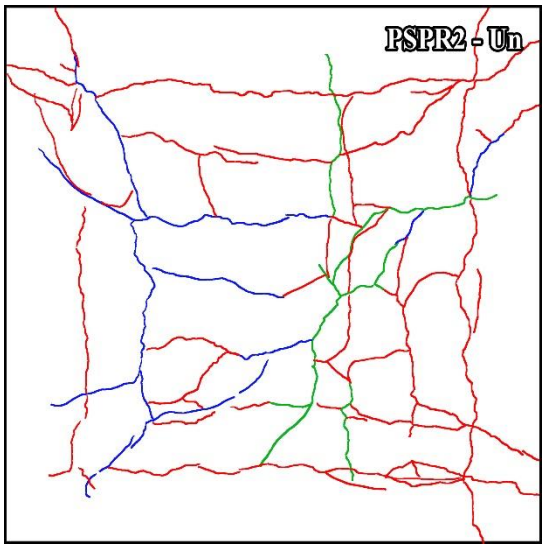

Computerized Mapping
Tension Face – Third Stage
Load: 205 kN
Crack Width: 2.02 mm

Actual Cracks
Tension Face – Third Stage
Load: 205 kN
Crack Width: 2.02 mm

Figure (4.59): Crack pattern for PSPR2-Un (Tension Face)

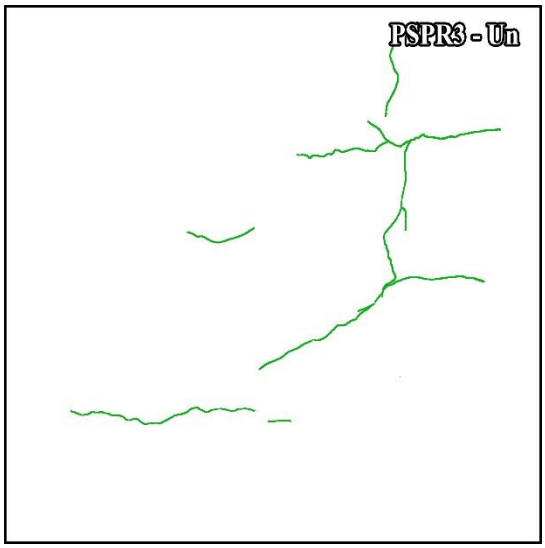

Computerized Mapping
Tension Face – First Stage
Load: 20 kN
Crack Width: 0.185 mm

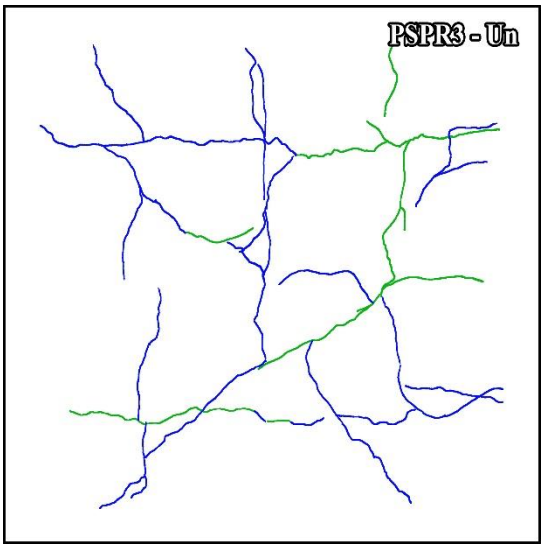

Computerized Mapping
Tension Face – Second Stage
Load: 50 kN
Crack Width: 0.65 mm

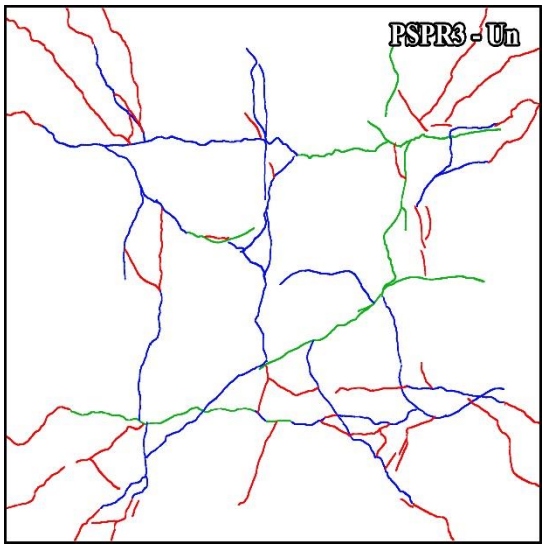

Computerized Mapping
Tension Face – Third Stage
Load: 161 kN
Crack Width: 2.47 mm

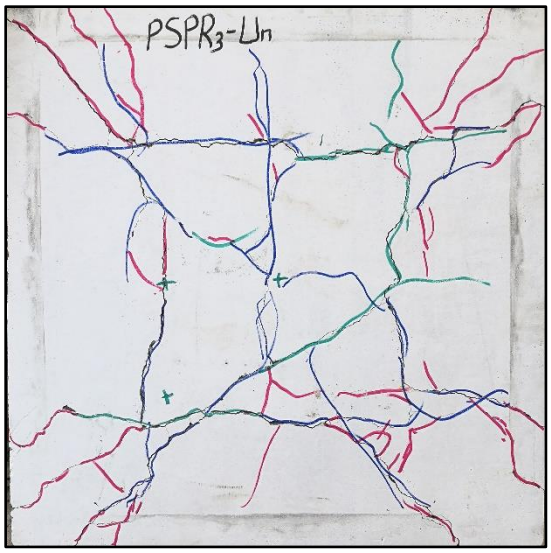

Actual Cracks
Tension Face – Third Stage
Load: 161 kN
Crack Width: 2.47 mm

Figure (4.60): Crack pattern for PSPR3-Un (Tension Face)

Cracks in compression face for all models are clarified in Figures (4.61) to (4.70):

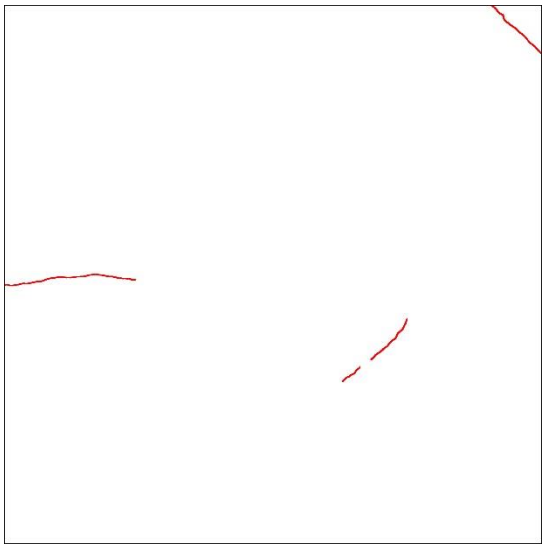

Computerized Mapping
Compression Face
Load: 148 kN

Actual Cracks
Compression Face
Load: 148 kN

Figure (4.61): Crack pattern for Re-Un (Compression Face)

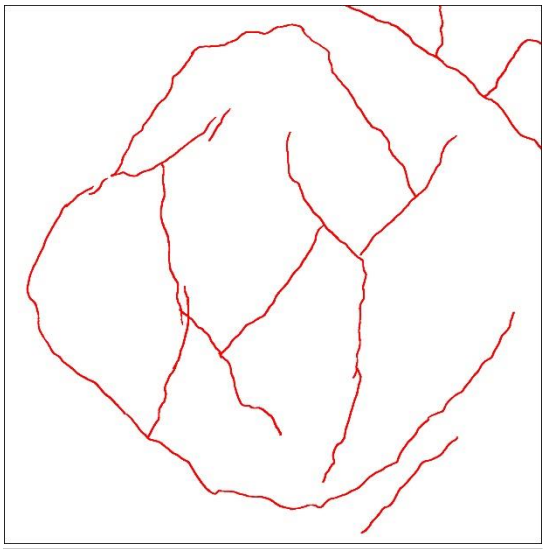

Computerized Mapping
Compression Face
Load: 145 kN

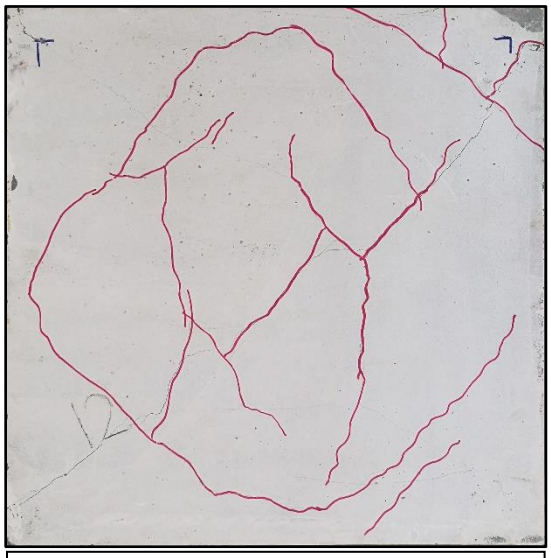

Actual Cracks
Compression Face
Load: 145 kN

Figure (4.62): Crack pattern for PSPC1-Un (Compression Face)

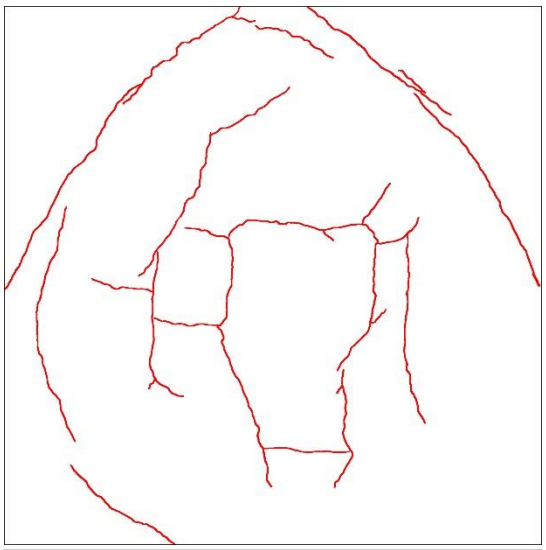

Computerized Mapping
Compression Face
Load: 183 kN

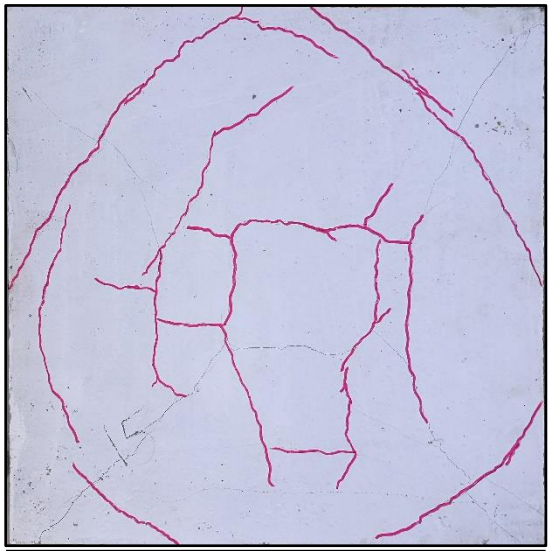

Actual Cracks
Compression Face
Load: 183 kN

Figure (4.63): Crack pattern for PSPC2-Un (Compression Face)

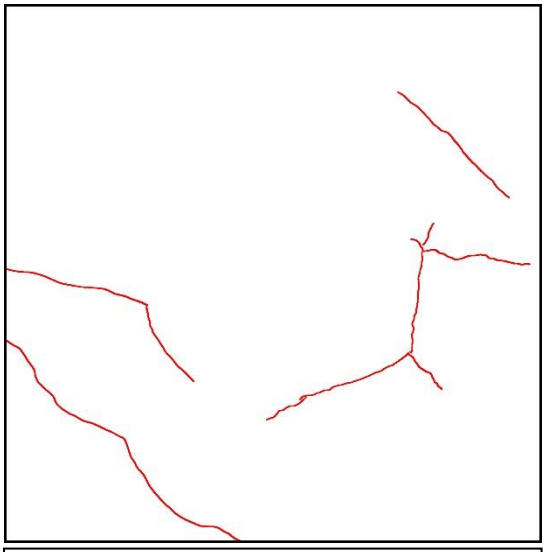

Computerized Mapping
Compression Face
Load: 150 kN

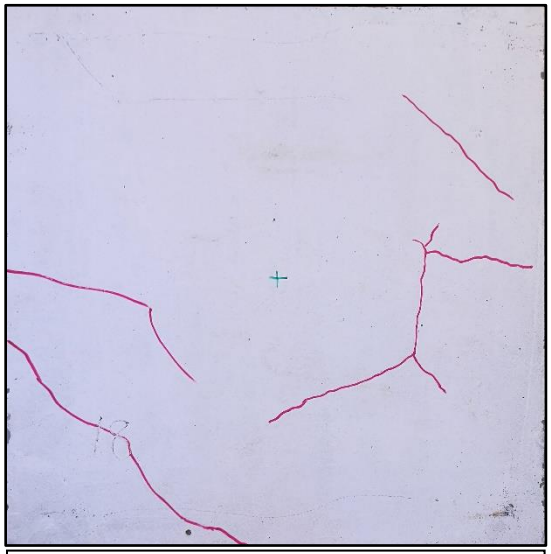

Actual Cracks
Compression Face
Load: 150 kN

Figure (4.64): Crack pattern for PSPC3-Un (Compression Face)

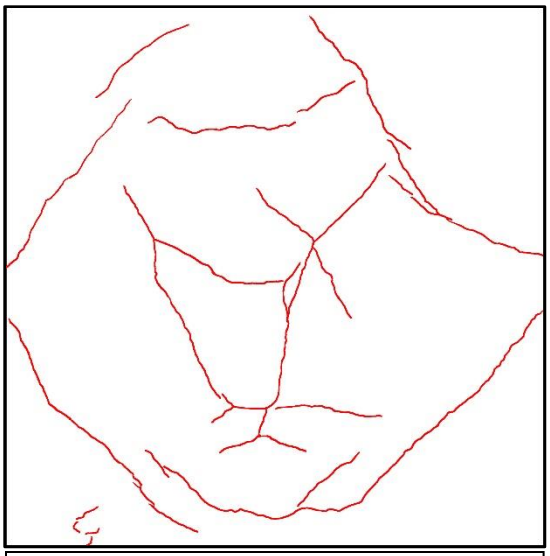

Computerized Mapping
Compression Face
Load: 158 kN

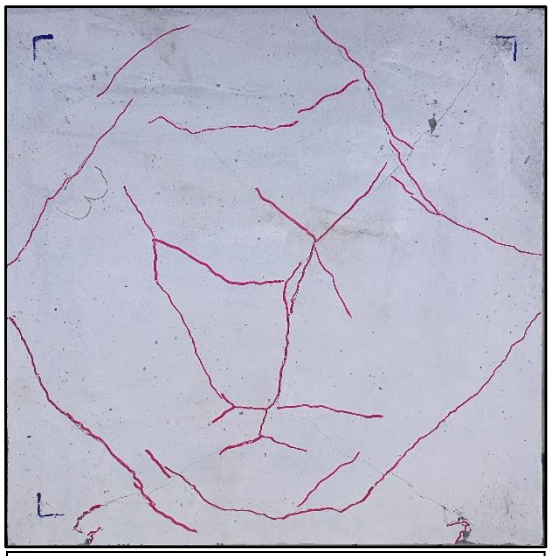

Actual Cracks
Compression Face
Load: 158 kN

Figure (4.65): Crack pattern for PSPO1-Un (Compression Face)

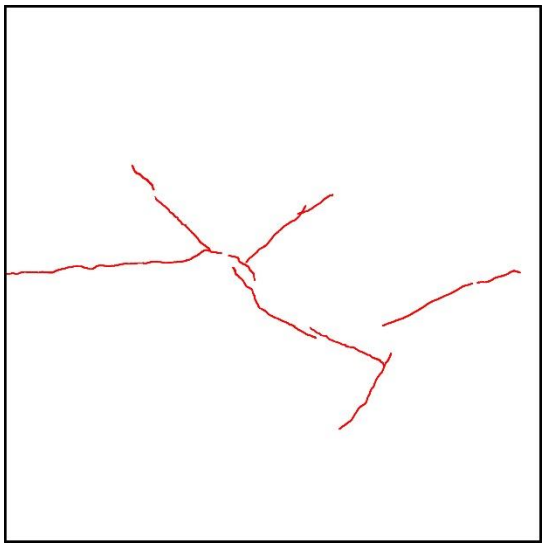

Computerized Mapping
Compression Face
Load: 178 kN

Actual Cracks
Compression Face
Load: 178 kN

Figure (4.66): Crack pattern for PSPO2-Un (Compression Face)

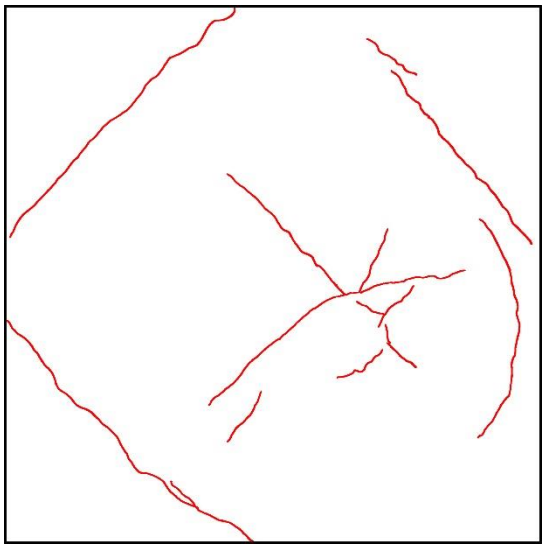

Computerized Mapping
Compression Face
Load: 155 kN

Actual Cracks
Compression Face
Load: 155 kN

Figure (4.67): Crack pattern for PSPO3-Un (Compression Face)

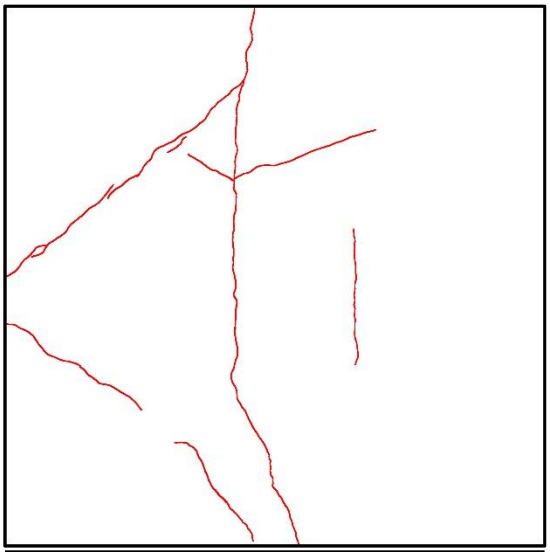

Computerized Mapping
Compression Face
Load: 150 kN

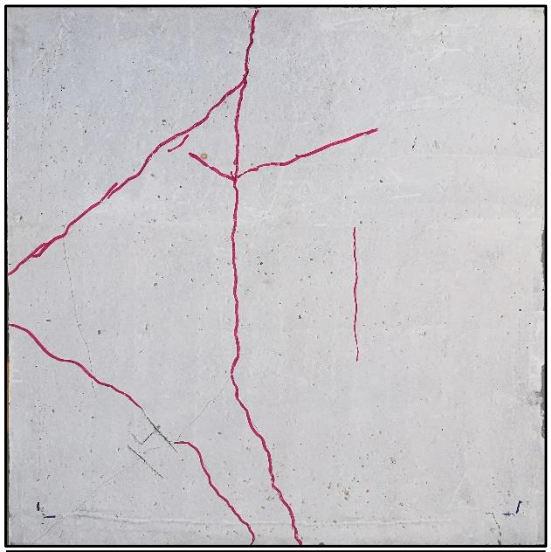

Actual Cracks
Compression Face
Load: 150 kN

Figure (4.68): Crack pattern for PSPR1-Un (Compression Face)

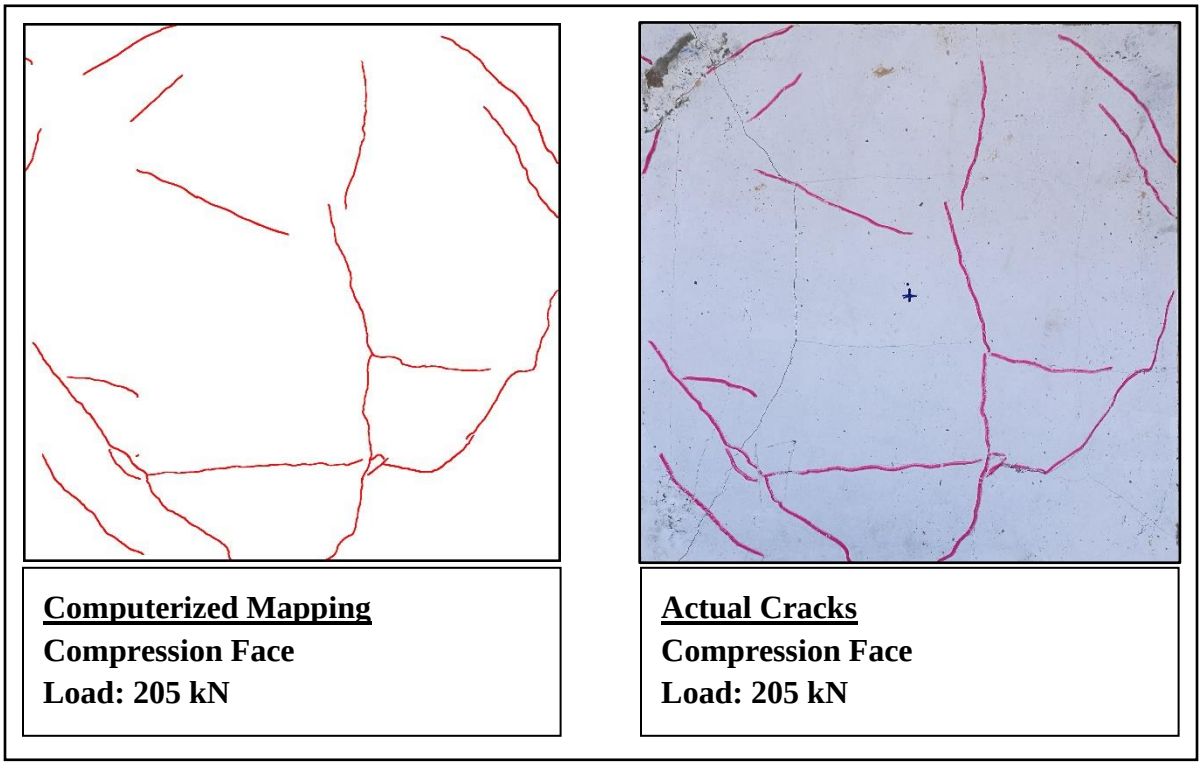

Computerized Mapping
Compression Face
Load: 205 kN

Actual Cracks
Compression Face
Load: 205 kN

Figure (4.69): Crack pattern for PSPR2-Un (Compression Face)

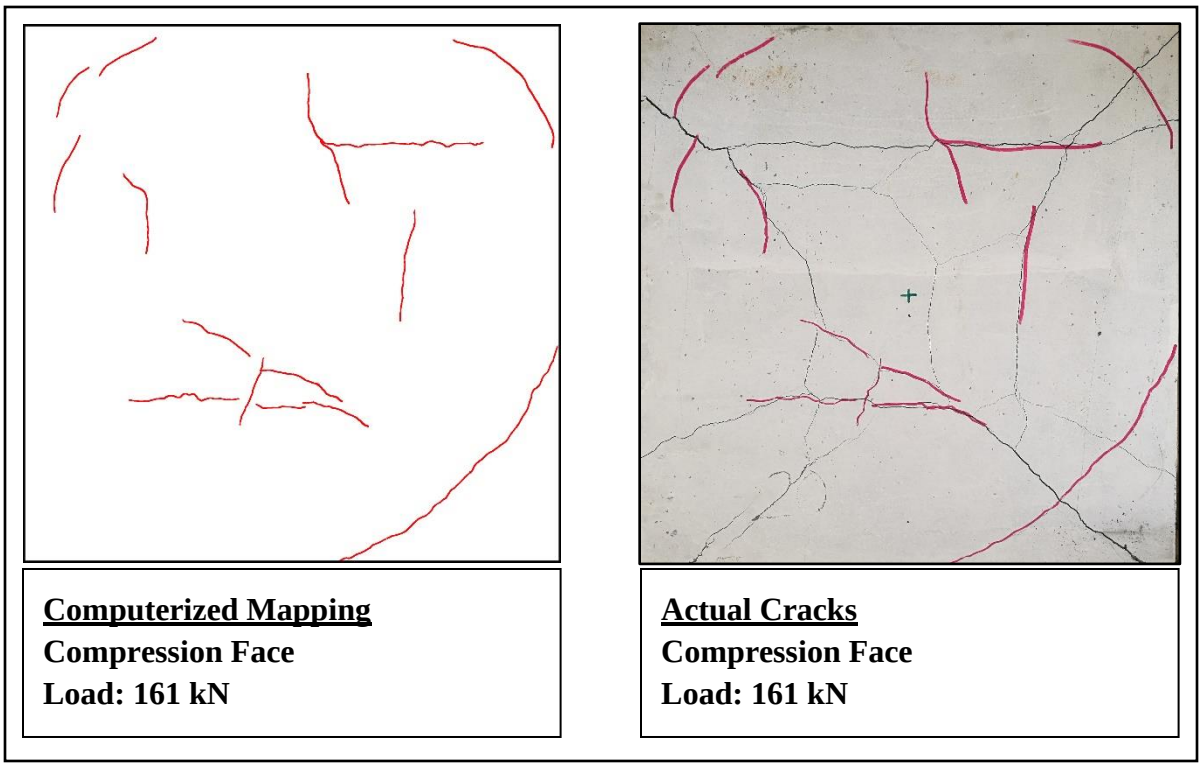

Computerized Mapping
Compression Face
Load: 161 kN

Actual Cracks
Compression Face
Load: 161 kN

Figure (4.70): Crack pattern for PSPR3-Un (Compression Face)

The cracks behavior for slabs reinforced by perforated steel plate were evaluated and discussed by comparison with a reference slab reinforced by normal reinforcement (deformed steel bar). Generally, all slabs reinforced by perforated steel plate: circular, octagonal and square shapes show very acceptable results.

The first noticeable cracks were specified, PSPC3-Un, PSPO3-Un and PSPR3-Un have less than the first cracking load than Re-Un because there is a wide area of concrete in tension face without steel strengthening due to the large area of opening.

The optimal models that have better resistance to first cracking are PSPC2-Un, PSPO2-Un and PSPR2-Un. These models have a first cracking load higher than Re-Un about 33.3%, 16.6% and 50% respectively.

The summary of previous results is illustrated in Table (4.6).

Table (4.6): Loads and corresponding crack's width – uniform load

No.	Model's name	Load kN	Crack's width mm	No.	Model's name	Load kN	Crack's width mm
1	Re - Un	30	0.11	6	PSPO2 – Un	35	0.176
		70	0.709			70	0.593
		148	2.54			178	2.01
2	PSPC1 - Un	31	0.53	7	PSPO3 – Un	15	0.104
		100	0.84			41.5	0.609
		145	2.29			155	5.13
3	PSPC2 – Un	40	0.334	8	PSPR1 – Un	20	0.073
		90	1.31			53	0.469
		183	4			150	2.34
4	PSPC3 - Un	20	0.17	9	PSPR2 – Un	45	0.052
		100	1.41			80	0.34
		150	3.24			205	2.02
5	PSPO1 – Un	50	0.28	10	PSPR3 – Un	20	0.185
		105	1.66			50	0.645
		158	4.48			161	2.47

CHAPTER FIVE

NONLINEAR FINITE ELEMENT MODELING

5.1 Introduction

This chapter of the dissertation attempts to create a numerical model using with Ansys program version 18.1 and to validate it by comparing numerical results with experimental results in both cases concentrated and uniform load. The optimal shape and number of openings will be adopted to verify the modeling.

After that, the model will be used to make a parametric study concerning the effect of changing the thickness of perforated steel plate with the same amount of steel.

5.2 Description of Modeling Steps in Ansys Program

In fact, the modeling of slabs reinforced by perforated steel plate has many challenges that should be solved. The perforated steel plate will make the concrete have three parts and should be worked as a one unit. The first part is located at the bottom and represents the cover of concrete. The second part represents the concrete that filled the openings of the plate. The third part is located at a level over the perforated steel plate. All these parts are clarified in Figure (5.1), where they simulate the modeling steps for the quarter slabs to reduce computational processing time.

The perforated steel plate should be embedded by making a suitable contact with the concrete from all sides.

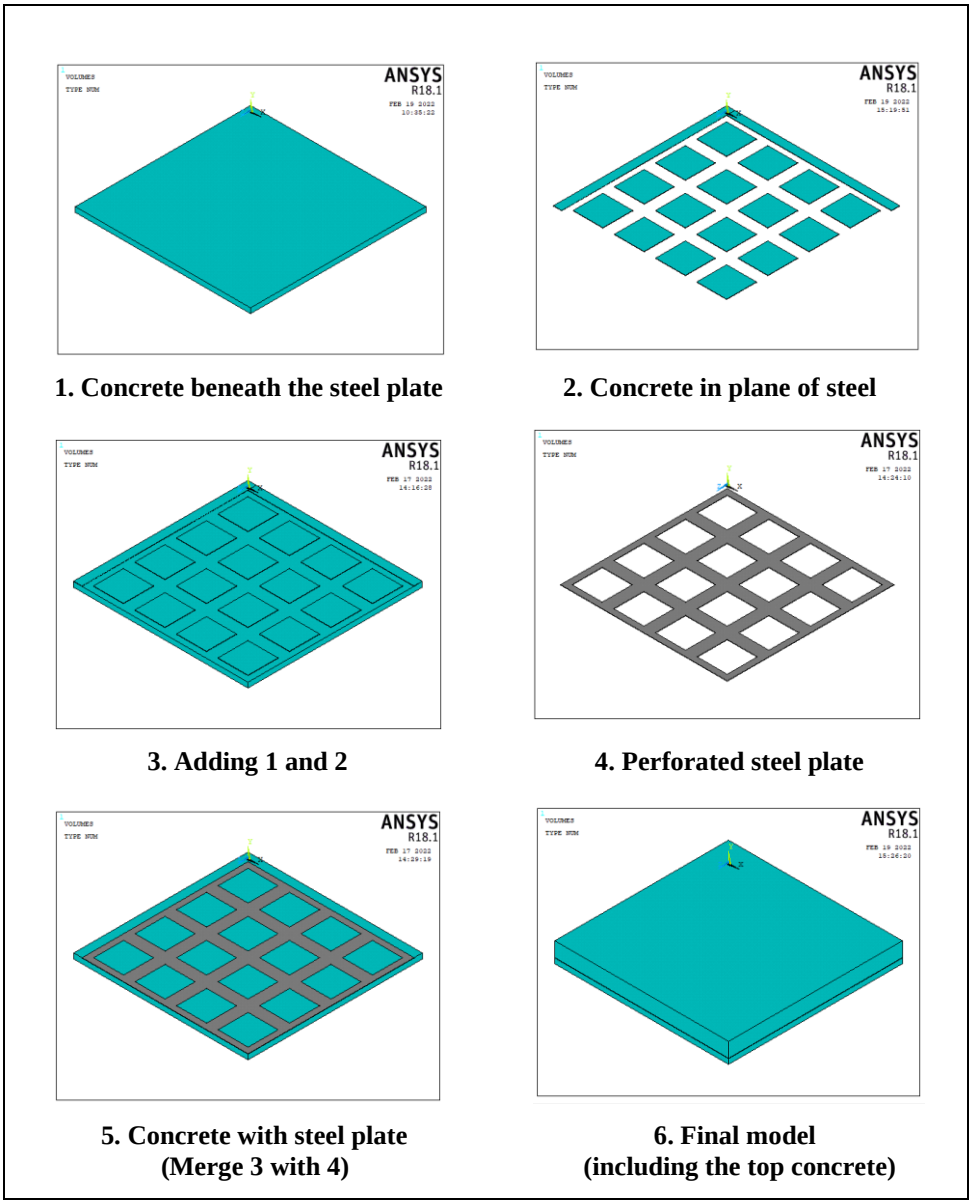

Figure (5.1): Steps of modeling a quarter slab

It should be stressed here that the perforated steel plate should have a suitable interface with the concrete.

5.2.1 Types of Elements

The types of elements for the concrete, steel and interface between them in modeling are clarified in Table (5.1), for more information see Appendix C:

Table (5.1): Elements types

Materials in real specimens	Elements used in Ansys model
Concrete	SOLID 65 *
Steel plate	SHELL 63
Interface between steel surface and concrete **	TARGE170
	CONTA174

* The effect of stress relaxing after cracking should be included in Solid65 because the default excludes this effect. If this option is not taken, the model will be stiffer than the real specimen. In any case, the finite elements model will remain stiffer than the real specimen because there are many conditions that the Ansys program is incapable of representing, like micro cracks that happen due to shrinkage or even those that happen due to transferring. These cracks are invisible, but they logically exist.

** A contact pair was created between steel plate as a target surface and concrete as a volume body with a coefficient of friction equal to 0.7 [41].

Concrete in program was defined in three stages:

First stage: linear isotropic where the modulus of elasticity is equal to 26265 MPa and Poisson's ratio is equal to 0.2.

Second stage: multilinear isotropic. The following equations were adopted to get points that were used in the program [42]:

$$f_c = \frac{\varepsilon E_c}{1+\left(\frac{\varepsilon}{\varepsilon_0}\right)^2} \quad \text{.....(5.1)}$$

$$\varepsilon_0 = \frac{2 f_c^{`}}{E_c} \quad \text{.....(5.2)}$$

$$f_c = \varepsilon E_c \quad \text{.....(5.3)}$$

f_c = stress at any specified strain
ε = strain at stress f_c
ε_0 = strain at ultimate compressive strength $f_c^{`}$

The values were obtained is clarified in Figure (5.2).

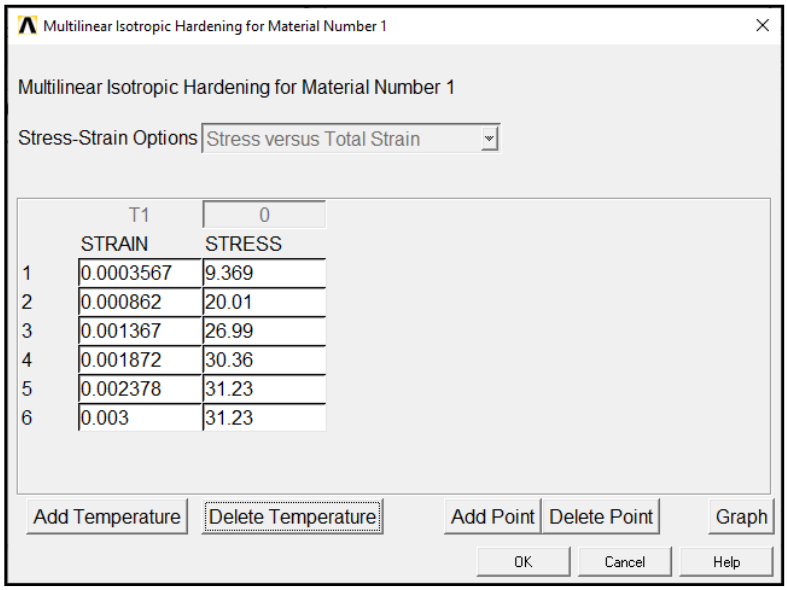

Figure (5.2): Multilinear isotopic hardening for concrete

Third stage: nonlinear inelastic which required the value of open shear transfer coefficient and closed shear transfer coefficient which they ranged between 0.0 to 1.0, the minimum value indicated that smooth cracks with complete loss of shear transfer while the maximum value refer to rough cracks with no loss of shear transfer. Figure (5.3) shows the adopted values in present study.

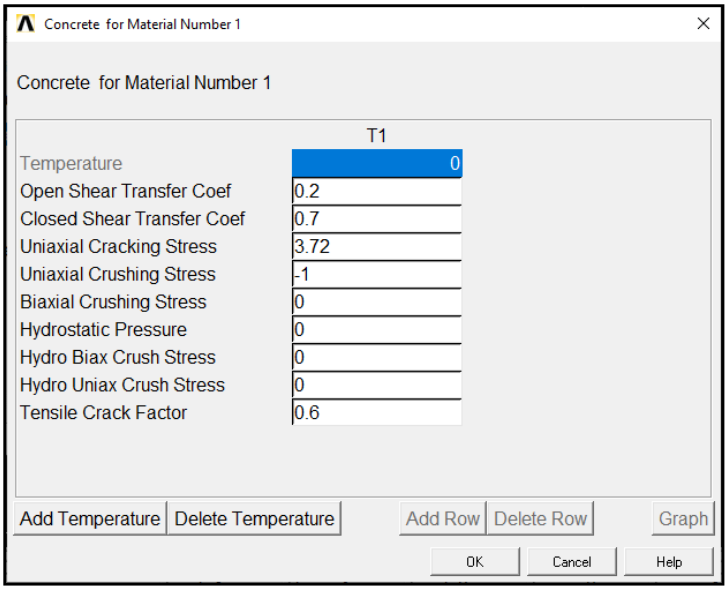

Figure (5.3): Concrete inelastic stage information

Steel in the program was defined in two stages:

First stage: linear isotropic with a modulus of elasticity of 200000 MPa and a Poisson's ratio of 0.3.

Second stage: bilinear isotropic, the yield stress and hardening modulus of the steel must be supplied for the bilinear model. According to experimental results, the yield stress was adjusted to 280 MPa, whereas the hardening modulus was set at 2000 MPa.

5.2.2 Meshing of the Model

The topology of the concrete volume requires the default meshing method, which was suggested by the Ansys program. The default mesh follows the tetrahedral shape elements with free style, which was specified as the best method for making a mesh in the Ansys software according to program recommendation, as shown in Figure (5.4).

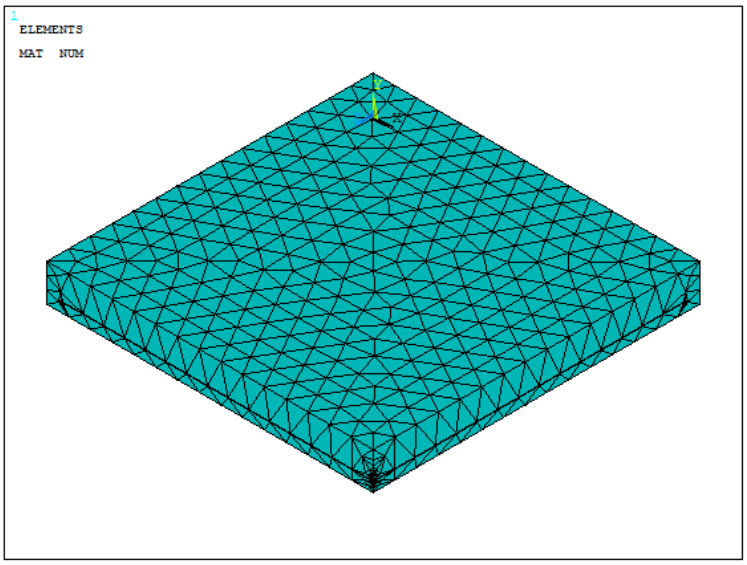

Figure (5.4): Meshing style

5.2.3 Boundary Conditions and Applied Load

To verify that the slab models behave as the experimental slabs, the displacement boundary conditions are necessary to simulate the slab models where the supports exist. The symmetry planes were required at the interior faces

due to modeling a quarter of the slab. As seen in Figure (5.5), the symmetry axis achieves zero displacement in the direction perpendicular to the symmetry planes.

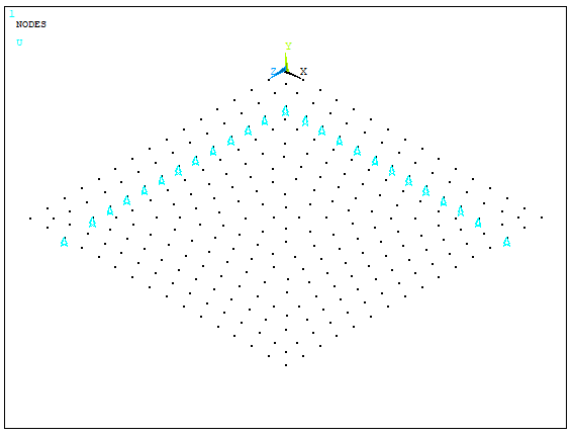

Nodes at bottom model

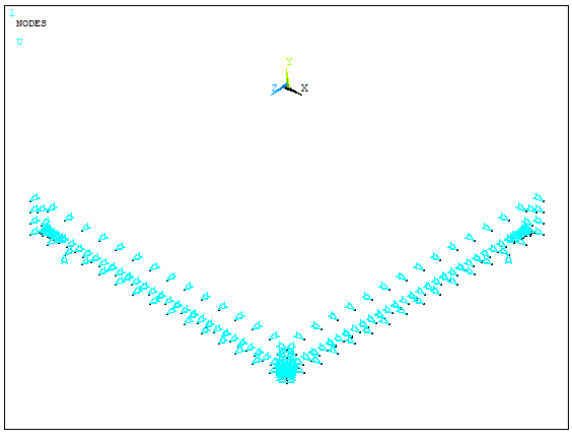

Nodes at edges of model

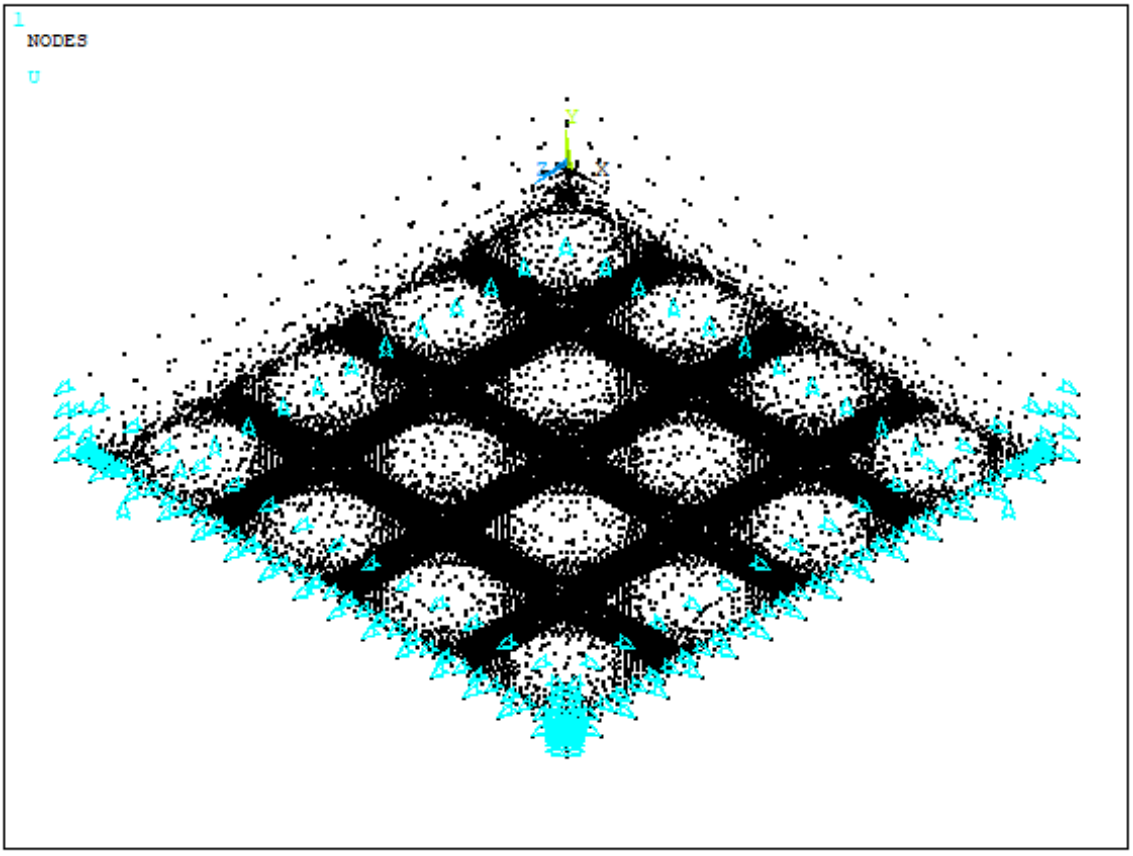

Nodes in overall model

Figure (5.5): Boundary and symmetry conditions

The load was defined in the program as a pressure subjected on nodes, which simulated the real position of tested specimens as shown in Figure (5.6).

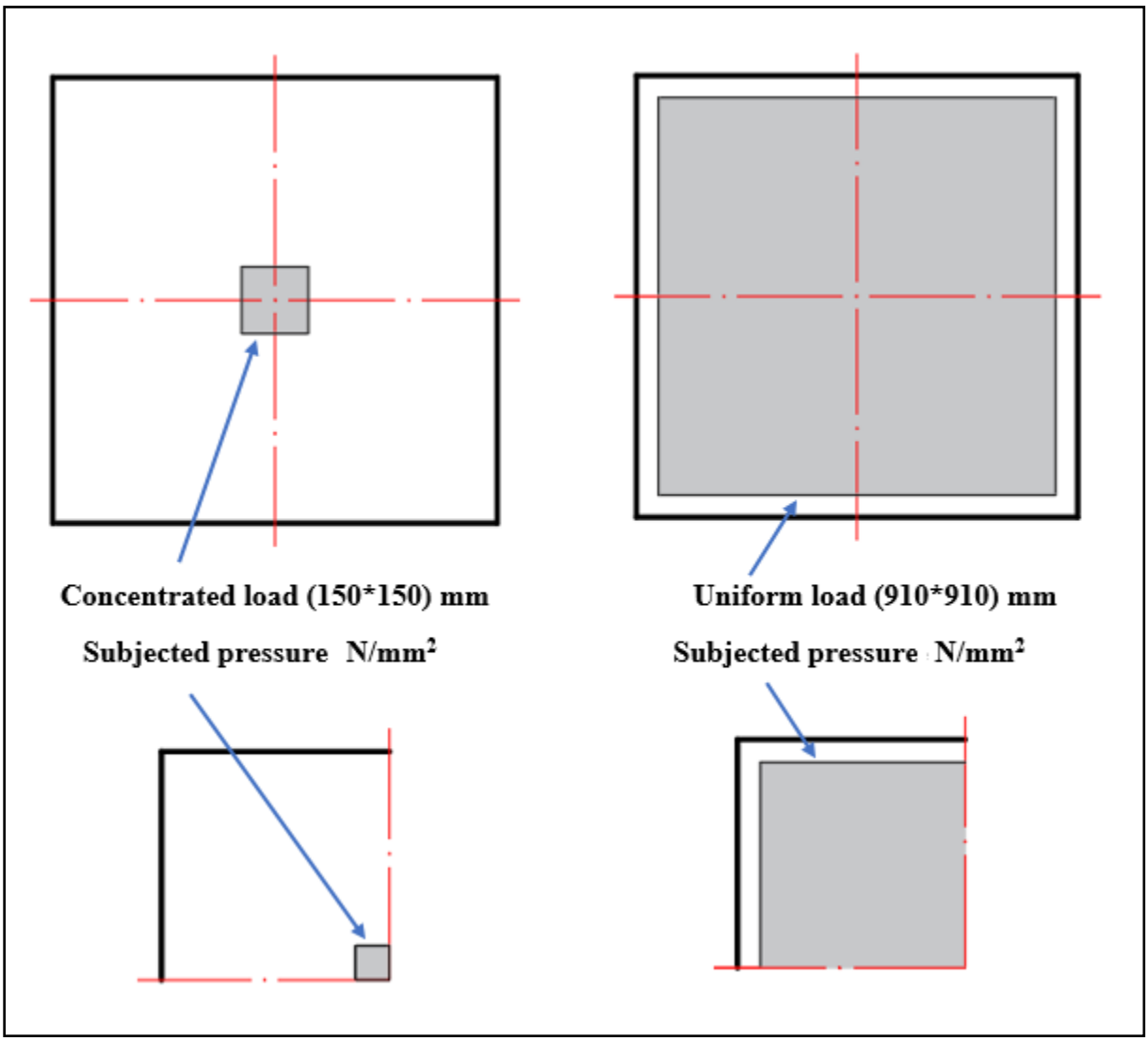

Figure (5.6): Details of concentrated and uniform load

5.3 Load-Deflection Curves

The comparison between the finite element model with experimental results is very important to check the accuracy of the results that obtained from the Ansys programs. In the next sections, the comparison for the optimal shape and the number of openings for the specimens PSPR2-Co and PSPR2-Un are carried out. PSPR2-Co and PSPR2-Un represent two-way concrete slabs

reinforced by perforated steel plate with 64 square openings, each openings have side length equal to 90.4 mm.

5.3.1 Load-Deflection Curve under Concentrated Load

The comparison of the experimental load deflection curve for PSPR2-Co and the finite element model is given in Figure (5.7).

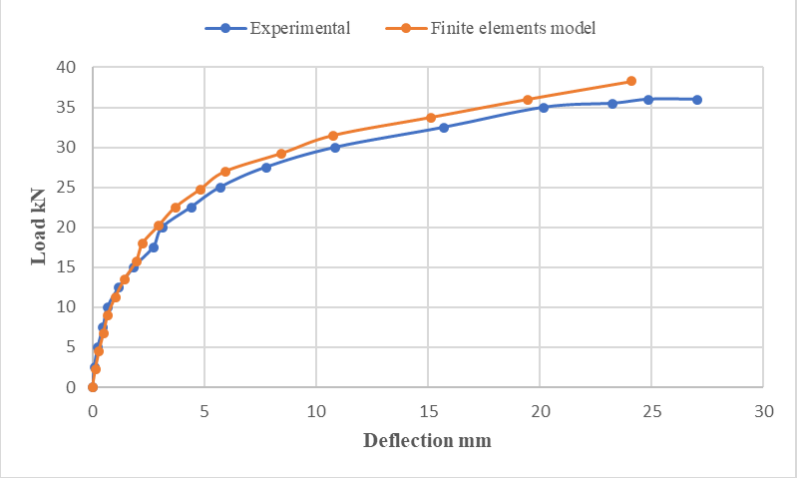

Figure (5.7): Comparison of load deflection curves by FEM with that by experimental work under concentrated load (for specimen PSPR2-Co)

It is obvious that the finite elements model is stiffer than experimental results. The ultimate load of the model was 38.25 kN, and it is larger than the laboratory results by about 6%. According to the degree of freedom for the quarter model, the y-component of the displacement is shown in Figure (5.8).

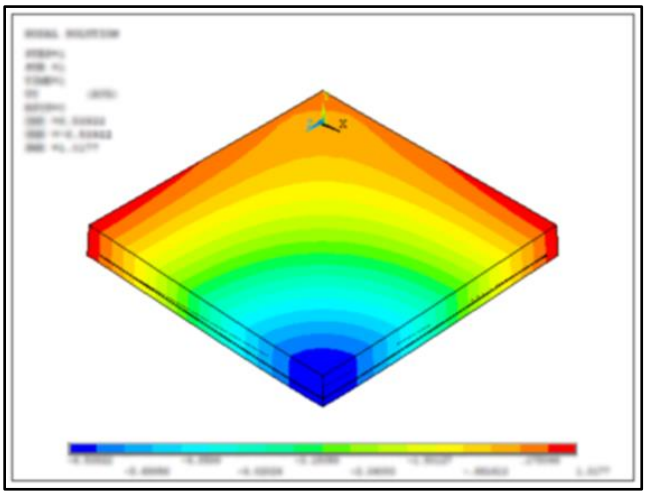

Figure (5.8): Nodal solution/ Y-component of displacement for PSPR2-Co

5.3.2 Load-Deflection Curve under Uniform Load

Figure (5.9) depicts a comparison of the experimental load deflection curve for PSPR2-Un and the finite element model.

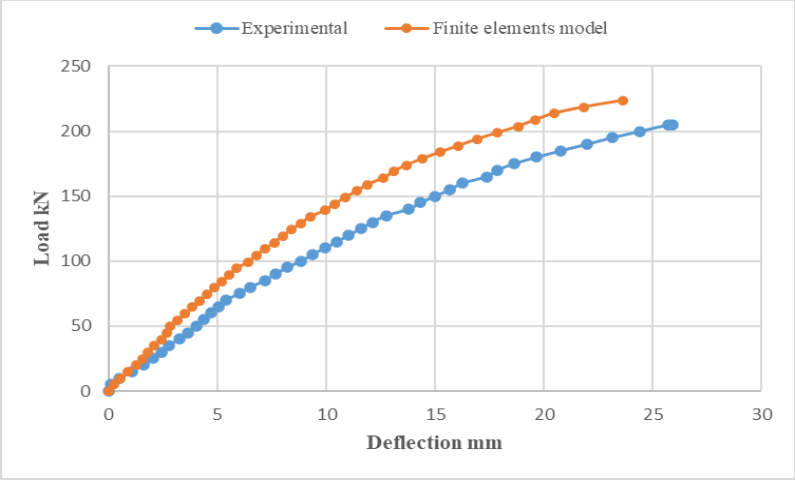

Figure (5.9): Comparison of load deflection curves by FEM with that by experimental work under uniform load (for specimen PSPR2-Un)

The finite elements model is also rather stiffer than the experimental data. The model's ultimate load was 223.5 kN, which was 9 % higher than the laboratory test specimen. Figure (5.10) presents the nodal solution for the Y-component of displacement in the quarter specimen PSPR2-Un.

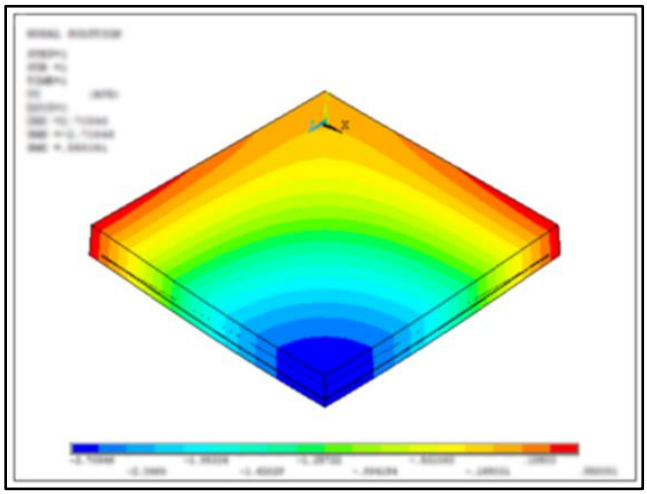

Figure (5.10): Nodal solution/ Y-component of displacement for PSPR2-Un

5.4 Parametric Study

The ultimate benefit of creating a model for experimental specimens is the ability to conduct a parametric investigation with additional parameters. The experimental part explores the shapes, sizes, and numbers of openings using the same amount of steel, with no regard to changing the plate thickness.

In this part, three different plate thicknesses will be studied for the optimal shape and number of openings. The square with 8×8 openings in both concentrated and uniform load was the best specimen that displayed the best behavior. The square openings of the reference plate have a 90.4 mm side length, with a distance between two successive edges openings was 34.6 mm. When the plate thickness is increased to 1.5 mm and 2 mm without changing the volume of steel, see Figure (5.9), the opening side lengths will be 103.3 mm and 109.1 mm, respectively, and the distance between two sequential edge openings is 21.7 mm and 15.9 mm.

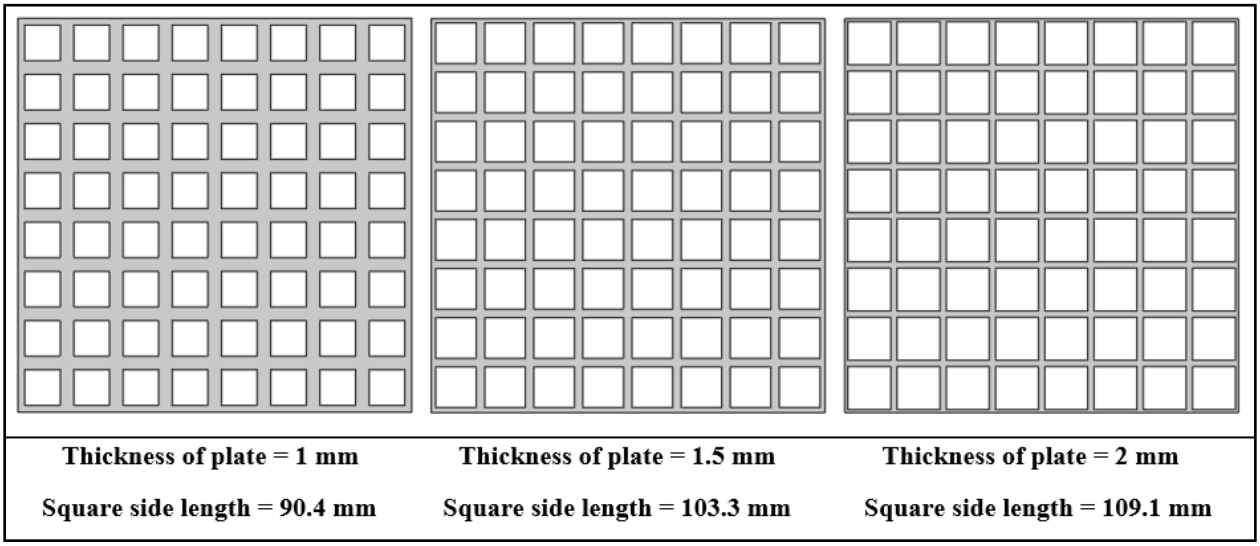

Figure (5.11): Different plate thickness

The load deflection curves for the three considered cases under concentrated load are drawn in Figure (5.10):

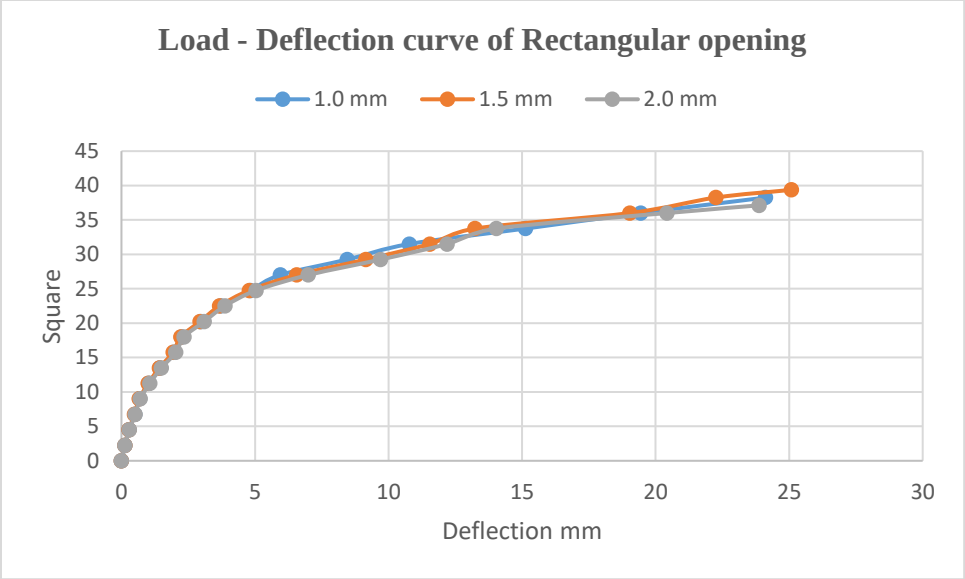

Figure (5.12): Theoretical comparison of load deflection curves under concentrated load

While the load deflection curves of the considered cases under uniform load are illustrated in Figure (5.11):

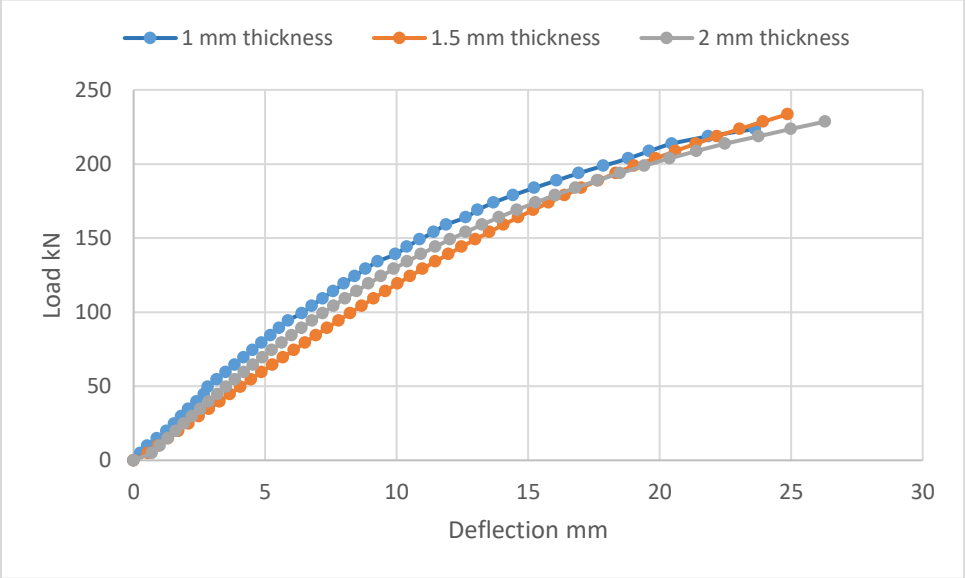

Figure (5.13): Theoretical comparison of load deflection curves under uniform load

The summary of ultimate load for the finite elements model are briefed in Table (5.2).

Table (5.2): Ultimate load of finite element models with experimental results for different thickness of plate

Thickness of plate	Ultimate load of finite element method and experimental results			
	Concentrated load kN		Uniform load kN	
	FEM	Experimental	FEM	Experimental
1 mm	38.3	36	223.6	205
1.5 mm	39.4	- - -	233.5	- - -
2 mm	37.1	- - -	228.6	- - -

It can be seen clearly that there is no significant effect due to changing the thickness of the plate. These results may provide good flexibility for this technique of reinforcing two-way slabs in the future.

CHAPTER SEVEN

CONCLUSIONS AND RECOMMENDATIONS

6.1 General

The main purpose of this research is to evaluate the structural behavior of a new type of reinforcing two-way concrete slab, which can be summarized by using perforated steel plate instead of traditional bar reinforcement. A total of twenty tests were conducted for the two-way concrete slabs, divided into two groups. The first group consisted of ten slabs tested under concentrated load, and the second group consisted of ten slabs tested under uniform load. Each group discussed the effect of changing the size and shape of the openings for the same amount of steel. In addition, nonlinear finite element numerical analysis using ANSYS 18.1 was introduced for the best specimens that provide the best behavior under concentrated and uninform load. A parametric study was carried out to show the effect of changing the thickness of the plate. This chapter will include the experimental and numerical conclusions that have been obtained, as well as recommendations for future work that will be reviewed afterward.

6.2 Conclusions

The key results and important outcomes that were obtained will be described in the following points:

1. The using of perforated steel plate as a reinforcing method in the two-way concrete slabs instead of traditional bar is a very effective technique modifying the overall behavior.
2. Self-compacting concrete is the best type of special concrete that provides good facilities during the casting and may be considered as one of the success keys of this reinforcing method.

3. According to the considered shapes of openings in perforated steel plates, the square openings show the best behavior as compared with the octagonal and circular shapes.

4. Based on the regarded sizes of openings, small, medium and large, the medium size (Opening Aspect Ratio, OAR, = 8.17×10^{-3}) displays a higher ultimate load in circular, octagonal and square shapes.

5. For the small size of openings (Opening Aspect Ratio, OAR, = 3.62×10^{-3}) in circular, octagonal and square shapes under concentrated load, the ultimate load was more than the reference slab, which was reinforced by traditional bar reinforcements by about 59%, 67%, and 80%, respectively.

6. The ultimate concentrated load was greater than the reference slab, which was reinforced by classical bar reinforcements by about 77%, 82%, and 85% for the medium size of openings (Opening Aspect Ratio, OAR, = 8.17×10^{-3}) in circular, octagonal and square shapes, in sequence.

7. Although the outcomes of large openings (Opening Aspect Ratio, OAR, = 32.68×10^{-3}) have the lowest increase ratio in the ultimate concentrated load, it is still regarded as a good ratio. It was more than the reference slab of about 44%, 54%, and 62% for the circular, octagonal, and square shapes respectively.

8. In case of small openings (Opening Aspect Ratio, OAR, = 3.26×10^{-3}) under uniform load, the suggested reinforcing technique carries an ultimate load greater than the reference slab by 3%, 7%, and 8%, respectively, with circular, octagonal and square openings.

9. The perforated steel plate as a reinforcing approach of two-way concrete slabs under uniform load reflects an ultimate load that is 23.65%, 20.27% and 38.51% larger than the reference slab for each medium (Opening Aspect Ratio, OAR, = 8.17×10^{-3}) circular, octagonal, and square opening size.

10. The ultimate uniform load in concrete slabs reinforced by perforated plate with large openings size (Opening Aspect Ratio, OAR, = 32.68×10^{-3}) is still greater than the reference slab by about 1.35%, 4.73%, and 8.78% for circular, octagonal and square openings, successively.

11. Experimental results proved that the shape of the opening has a slight effect on the stiffness of the specimens through the load deflection curve in the case of concentrated load, while this effect is not clear in the case of uniform load. However, the square shape can be considered the best because it reflects the largest ultimate load.

12. The Ansys 18.1 program is efficiently suitable to simulate the two-way concrete slabs reinforced by perforated steel plate.

13. The difference between the experimental ultimate load and the finite element model was about 6% in the case of concentrated load while it was 9% in the case of uniform load for the specimen reinforced by square openings with an Opening Aspect Ratio, OAR, of 8.17×10^{-3}.

14. According to the Ansys program results, the variation of the plate thickness from 1 mm to 2 mm (with the same volume of steel plate) does not affect the behavior of the slabs reinforced by the suggested method in both concentrated and uniform load.

6.3 Recommendations for Future Work

The proposed reinforcing technique can be considered as a new theme in reinforcing of two-way concrete slabs, so there are a huge number of recommendations that can be mentioned for future work, but the main points are:

1. Study the behavior of two-way concrete slabs reinforced by perforated steel plate under repeated load.

2. Investigate the impact resistance of the slabs reinforced by perforated steel plate.

3. Performance of this reinforcing technique Under fire conditions to show the ability of fire resistance.

4. Extending the present study to show the effect of using hybrid reinforcements, using bar reinforcements and perforated steel plates.

5. Using the fibrous self-compacting concrete with the perforated steel plate to show the effect of modifying the overall behavior of concrete slabs.

6. Study the behavior of one-way concrete slabs reinforced by perforated steel plate.

REFERENCES

[1] ACI Committee 318, "Building Code Requirements for Structural Concrete and Commentary," American Concrete Institute, Farmington Hills, MI, 2019.

[2] H. Okamura and M. Ouchi, “Self – Compacting Concrete,” Journal of Advanced Concrete Technology, Vol. 01, No. 01, 2003.

[3] A. C. Institute, “ACI 237R: Self Consolidating Concrete,” p. 29, 2007.

[4] S. P. Timoshenko and S. W. Krieger, “Theory of Plates and Shells”, McGRAW-HILL International editions, 1959.

[5] V. K. Paul, S. Khursheed and S. Jain, “Benefit Cost Analysis of Self Compacting Concrete,” International Journal of Research in Engineering and Technology, Vol. 06, 03, 2017.

[6] J. W. Zhang, J. G. Teng, Y. L. Wong and Z. T. Lu, “Behavior of Two – Way RC Slabs Externally Bonded with Steel Plate,” Journal of Structural Engineering, Vol. 127, pp. 390 – 397, 2001.

[7] U. Ebead and H. Marzouk, “Strengthening of Two-Way Slabs Using Steel Plates,” *ACI Struct. J.*, Vol. 99, No. 1, pp. 23–31, 2002, doi: 10.14359/11032.

[8] L. S. Rasheed and T. K. Al-Azawi, “Experimental Analysis of Reinforced Concrete Slabs Strengthened with Steel Plates,” *The Iraqi Journal for Mechanical and Material Engineering*, Vol. 13, No. 1, pp. 1-12, 2013.

[9] I. M. Metwally, “Three-dimensional finite element analysis of reinforced concrete slabs strengthened with epoxy-bonded steel plates,” *Adv. Concr. Constr.*, Vol. 2, No. 2, pp. 91–108, 2014, doi: 10.12989/acc.2014.2.2.091.

[10] H. M. F. Elbakry and S. M. Allam, “Punching strengthen ing of two-way slabs using external steel plates,” *Alexandria Eng. J.*, Vol. 54, No. 4, pp. 1207–1218, 2015, doi: 10.1016/j.aej.2015.09.005.

[11] M. Mohammed Rasheed and N. Nizar Abduhameed, “Behaviour of Self-

Consolidating Concrete Two Way Slabs Under Uniform Loading," Iraqi Journal of Civil Engineering, Vol. 8, No. 1, 2012.

[12] M. S. Kumar and B. S. Chandra, "Experimental Study on Self Compacting RC Slab With and With Out Opening," Vol. 3, No. 8, pp. 202–206, 2014.

[13] R. Patil and V. Harish, "Strength and deformation of square two way simply supported SFR-HSSCC slabs," *Int. Res. J. Eng. Technol.*, 2015, [Online]. Available: www.irjet.net.

[14] M. A. Ismael, "Flexural behavior of steel fiber-self compact concrete slabs," Diyala Journal of Engineering Sciences, 2nd Engineering Scientific Conference – College of Engineeing – University of Diyala, 2015.

[15] K. Heiza, F. Eid, and T. Masoud, "Behavior of Reinforced Concrete Slabs Cast with Light Weight Self Compacting Concrete," *J. Eng. Sci. Mil. Technol.*, Vol. 17, No. 17, pp. 1–12, 2017, doi: 10.21608/ejmtc.2017.21604.

[16] C. Higgins and H. Mitchell, "Behavior of Composite Bridge Decks with Alternative Shear Connectors," *Journal of Bridge Engineering*, Vol. 6, pp. 17–22, 2001.

[17] I. Yoshitake, A. Ogawa, Y. J. Kim, and Y. Mimura, "Development of a New Composite Slab System Using a Carbon Fiber–Blended Cementitious Adhesive," *J. Struct. Eng.*, Vol. 138, No. 11, pp. 1321–1330, 2012, doi: 10.1061/(asce)st.1943-541x.0000574.

[18] A. Shariati, N. Sulong, M. Suhatril and M. Shariati , "Various types of shear connectors in composite structures: A review," *Int. J. Phys. Sci.*, Vol. 7, No. 22, pp. 2876–2890, 2012, doi: 10.5897/ijpsx11.004.

[19] Z. Wang, Q. Li, and C. Zhao, "Ultimate shear resistance of perfobond rib shear connectors based on a modified push-out test," *Adv. Struct. Eng.*, Vol. 16, No. 4, pp. 667–680, 2013, doi: 10.1260/1369-4332.16.4.667.

[20] I. Yoshitake, Y. Kuroda, Y. Watada, and Y. J. Kim, “Fatigue performance of steel-concrete composite slabs with a cementitious adhesive subjected to water leakage,” *Constr. Build. Mater.*, Vol. 111, pp. 22–29, 2016, doi: 10.1016/j.conbuildmat.2016.02.048.

[21] S. Zheng, Y. Liu, T. Yoda, and W. Lin, “Parametric study on shear capacity of circular-hole and long-hole perfobond shear connector,” *J. Constr. Steel Res.*, Vol. 117, pp. 64–80, 2016, doi: 10.1016/j.jcsr.2015.09.012.

[22] E. Ellobody, “Finite element modelling and design of composite bridges with profiled steel sheeting,” *Adv. Struct. Eng.*, Vol. 20, No. 9, pp. 1406–1430, 2017, doi: 10.1177/1369433216678865.

[23] M. R. Veldanda and M. U. Hosain, “Behaviour of perfobond rib shear connectors: push-out tests,” *Can. J. Civ. Eng.*, Vol. 19, No. 1, pp. 1–10, 1992, doi: 10.1139/l92-001.

[24] E. C. Oguejiofor and M. U. Hosain, “Parametric study of perfobond rib shear connectors,” *Can. J. Civ. Eng.*, Vol. 21, No. 4, pp. 614–625, 1994, doi: 10.1139/l94-063.

[25] H. Y. Kim and Y. J. Jeong, “Experimental investigation on behaviour of steel-concrete composite bridge decks with perfobond ribs,” *J. Constr. Steel Res.*, Vol. 62, No. 5, pp. 463–471, 2006, doi: 10.1016/j.jcsr.2005.08.010.

[26] H. Y. Kim and Y. J. Jeong, “Steel-concrete composite bridge deck slab with profiled sheeting,” *J. Constr. Steel Res.*, Vol. 65, No. 8–9, pp. 1751–1762, 2009.

[27] H. Y. Kim and Y. J. Jeong, “Ultimate strength of a steel-concrete composite bridge deck slab with profiled sheeting,” *Eng. Struct.*, Vol. 32, No. 2, pp. 534–546, 2010.

[28] X. Xu, Y. Liu, and Y. Zuo, “Contribution of perforated steel ribs to load-carrying capacities of steel and concrete composite slabs under negative bending,” *Adv. Struct. Eng.*, Vol. 21, No. 12, pp. 1879–1894, 2018, doi:

10.1177/1369433218758774.

[29] R. Liu and Y. Yang, “Research on Fatigue Performance of Steel-Plate-Concrete Composite Slab,” Thin-Walled Structures, Vol. 160, pp. 1-14, 2021.

[30] A. M. Ibrahim, Z. S. M. Khaled and I. M. Abdul Ameer, “Effect of Using Internal Steel Plates for Shear Reinforcement on Flexural Behavior of Self-Compacting Concrete Beams,” J. Eng. Al-Nahrain Univ., Vol. 20, No. 5, pp. 1071–1082, 2017.

[31] M. M. Sarhan, M. N. S. Hadi and L. H. Teh, “Bond Behaviour of Steel Plate Reinforced Concrete Beams,” Constr. Build. Mater., Vol. 189, pp. 751–756, 2018.

[32] A. Ibrahim, M. J. Hamood and A. A. Mansor, “Study the Response of Bubbled Wide Reinforced Concrete Beams with Different Shear Steel Plate Spacing,” Diyala Journal of Engineering Sciences, Vol. 11, No. 2, pp. 1–13, 2018.

[33] A. M. Ibrahim, A. A. Mansor, W. D. Salman and M. J. Hamood, “Strength and Ductility of Bubbled Wide Reinforced Concrete Beams with Diverse Types of Shear Steel Plates,” International Journal of Engineering & Technology, Vol. 07, pp. 502-506, 2018.

[34] K. I. Qaddoory, A. A. Mansor, B. J. Noman, W. D. Salman and A. S. Mohammed, “Effect of Replacing the Main Reinforcement by Sheet Steel Plate in Reinforced Concrete Beams,” Diyala Journal of Engineering Sciences, Vol. 14, No. 3, pp. 141–151, 2021.

[35] K. I. Qaddoory, A. A. Mansor, A. S. Mohammed and B. J. Noman, “Effect of Using Different Aspect Ratio of Longitudinal Steel Plates in Reinforced Concrete Beams” E3S Web of Conferences 318, 03016, 2021.

[36] ASTM E8 / E8M – 16a, “ standard Test Methods for Tension Testing of Metallic Materials,” American Society for Testing and Materials, 2016.

[37] D. Feys, R. Verhoeven, and G. De Schutter, “Evaluation of time

independent rheological models applicable to fresh self-compacting concrete," *Appl. Rheol.*, Vol. 17, No. 5, 2007, doi: 10.1515/arh-2007-0018.

[38] G.De Schutter, "Measurement of Properties of Fresh Self-Compacting Concrete Testing-SCC," *Guidel. Test. Fresh Self-compacting Concr.*, No. September, pp. 187–207, 2008.

[39] P. and U. EFNARC The European Guidelines for Self-Compacting Concrete: Specification, "The European Guidelines for Self-Compacting Concrete: Specification, Production and Use," Eur. Guidel. Self Compact. Concr., No. May, p. 68, 2005.

[40] F. Naser and N. Alwash, "Shear behavior of light weight concrete slab panels reinforced with CFRP bars," The Iraqi journal for mechanical and material engineering, Conference issue (C), 367-385,2016.

[41] L. K. Al-Hadithy and M. Hassan, "Finite Element Modeling and Theoretical Analysis of SFRSCC Composite Beams Strengthened by Bottom Tensioned Steel Plates," *J. Eng. Al-Nahrain Univ.*, Vol. 19, No. 2, pp. 228–245, 2016.

[42] N. A. Alwash, G. M. Habeeb and F. H. Al-Mamoori, "Structural Behavior of Light Weight Concrete Slab Panels Reinforced with CFRP Bars," PhD Thesis, University of Babylon, Department of Civil Engineering, 2015.

[43] Iraqi Specification Standards IQS No. 5, 1984 "Portland Cement", Central Agency for Standardization and Quality Control, Planning Council, Baghdad, IRAQ,(in Arabic).

[44] Iraqi Specification Standards IQS No.45, 1984 "Aggregate from Natural Sources for Concrete and Construction", Central Agency for Standardization and Quality Control, Planning Council, Baghdad, IRAQ, (in Arabic).

Appendix A: Chemical and Physical Cement Properties

Chemical test		
Test	**Results**	**Iraqi specification (No.5/1984)**
SiO_2	18.38	-----
$A1_2O_3$	2.96	-----
Fe_2O_3	3.8	-----
Lime saturation factor	1.01	(1.02 – 0.66) % for Portland cement
MgO	2.53	< 5
Ratio of C3A	1.41	< 3.5
Content of SO_3 when C3A less than 5%	2.26	< 2.5 for Ordinary and Sulfates Resisting Cement
Content of SO_3 when C3A more than 5%	-----	-----
Loss on ignition	3.97	< 4
Insoluble residue	1.26	< 1.5
Al_2O_3	6.76	-----
Physical test		
Physical test	**Results**	**Iraqi specification (No.5/1984)**
Initial setting, min	90	> 45 min
Final setting, hr:min	2.6	< 10 hr
Fcu @3days (MPa)	31.2	> 15 MPa
Fcu @7days (MPa)	33.29	> 23 MPa

Appendix B: Fiber Laser Cutting Machine

XQL 鑫全利激光

PT. SIGN WORLD MEDIA
DISTRIBUTOR & TRADING COMPANY

XQL 1330/1530
鑫全利激光

ADVERTISING FIBER
LASER CUTTING MACHINE

MAIN MACHINE	ADVERTISING FIBER LASER
LASER POWER	300/500 WATT
MAX CUTTING AREA	1300 * 3000/1300 * 2500MM
LASER SOURCE	IPG 500W
LASER CUTTING HEAD	WSX
SERVO MOTOR	DELTA SERVO MOTOR
REDUCER	DELTA REDUCER
GEAR RACK	PRECISION LEVEL GEAR RACK
GUIDE RAIL	PRECISION LEVEL GUIDE RAIL(GERMANY ROUST)
LASER CUTTING CONTROL SYSTEM	CYPCUT 1000
EXHAUST FAN	PROFESSIONAL DUST EXHAUST FUN
TRANSMISSION SYSTEM	GEAR RACK + GUIDE RAIL (RACK & PINION)
CONSUMABLE PARTS	PROTECT LENS, NOZZLE
BEST RUNNING SPEED	0-15 M/MIN
THE FASTEST RUNNING SPEED	30 M/MIN
POSITIONING ACCURACY	< 0.1 MM/M
MACHINE POWER	≤ 3KW
POWER SUPPLY	220V ±5%/50Hz/20A
SUPPORT FORMAT	DXF,PLT,CNC,AI,CHF
COVERING AREA	4000*2000MM
MACHINE BED	A3 STEEL MATERIALS, 2 TONS
WEIGHT	3000 Kg

SAMPLE FOR METAL LASER 1330/1530

www.signworld.id

Appendix C: Types of Elements

1- SOLID65 Element: is used for 3-D modeling of solids with or without reinforcing bars (rebar). The solid is capable of cracking in tension and crushing in compression. In concrete applications, for example, the solid capability of the element may be used to model the concrete while the rebar capability is available for modeling reinforcement behavior. Other cases for which the element is also applicable would be reinforced composites (such as fiberglass), and geological materials (such as rock). The element is defined by eight nodes having three degrees of freedom at each node: translations in the nodal x, y, and z directions. Up to three different rebar specifications may be defined. See Figure 1.

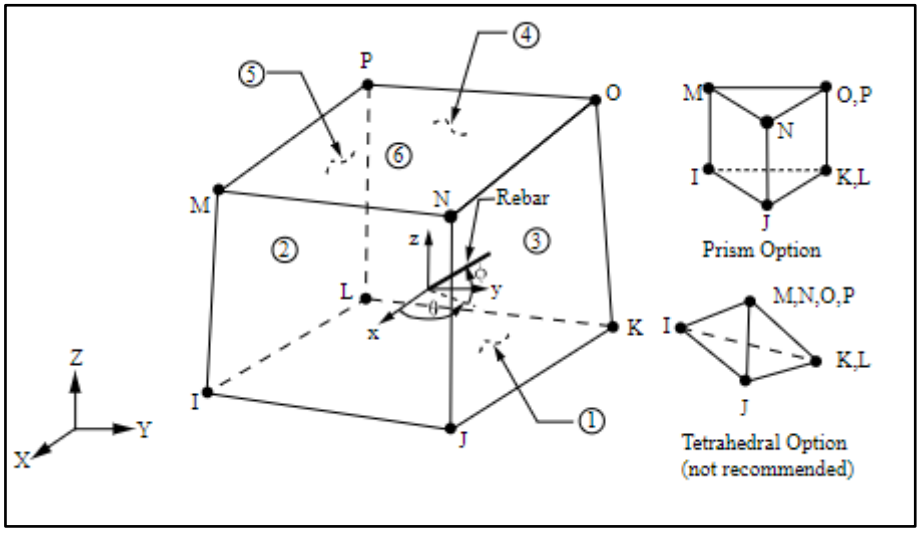

Figure 1: Solid65 Geometry

2- SHELL63: has both bending and membrane capabilities. Both in-plane and normal loads are permitted. The element has six degrees of freedom at each node: translations in the nodal x, y, and z directions and rotations about the nodal x, y, and z-axes. Stress stiffening and large deflection capabilities are included. See Figure 2.

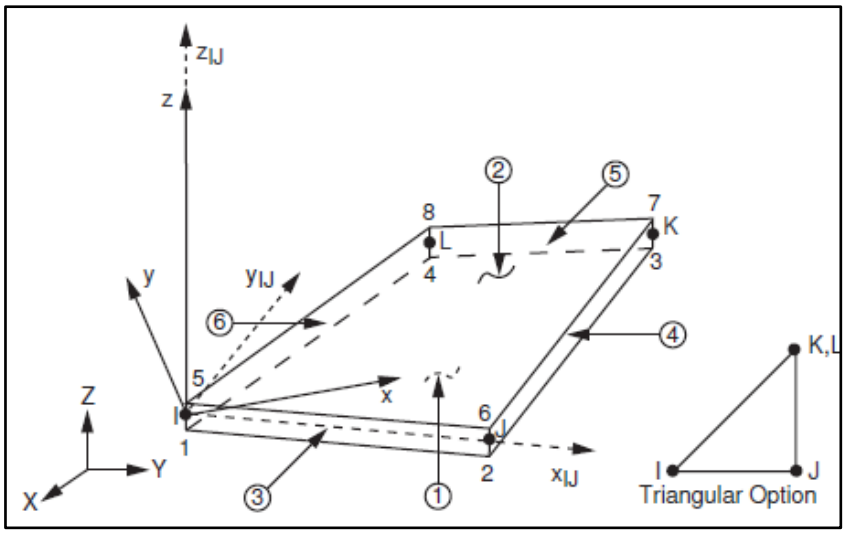

Figure 2: **SHELL63 Geometry**

3- TARGE170: is used to represent various 3-D "target" surfaces for the associated contact elements (CONTA173, CONTA174, CONTA175, CONTA176, and CONTA177). The contact elements themselves overlay the solid, shell, or line elements describing the boundary of a deformable body and are potentially in contact with the target surface, defined by TARGE170. See Figure 3.

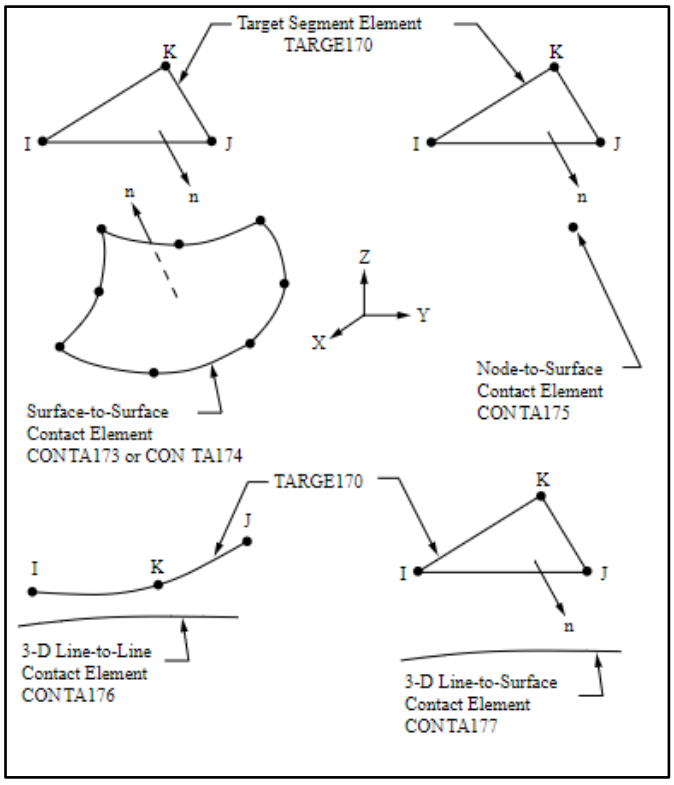

Figure 3: TARGE170 Geometry

4- CONTA174: is used to represent contact and sliding between 3-D target surfaces and a deformable surface defined by this element. The element is applicable to 3-D structural and coupled-field contact analyses. It can be used for both pair-based contact and general contact. See Figure 4.

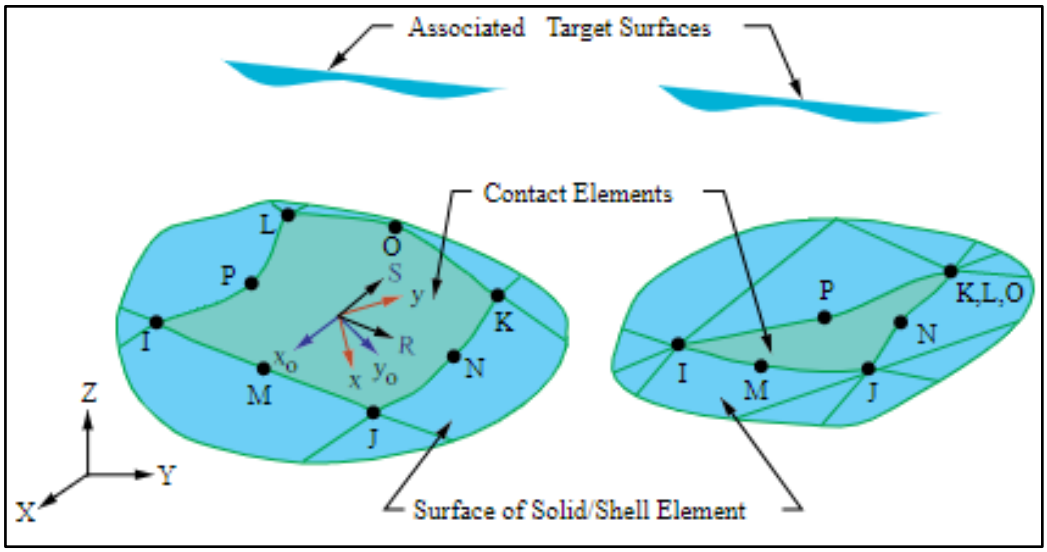

Figure 4: CONTA174 Geometry

الخلاصة

الجزء العملي والتحليلي يهدف إلى تأسييس تقنية جديدة تتعلق بتسليح السقوف الخرسانية ثنائية الأتجاه عن طريق استعمال الصفائح الفولاذية المثقبة كتسليح بدلا من قضبان حديد التسليح الأعتيادي باستخدام خرسانة ذاتية الرص.

البرناج العملي يتضمن صب عشرون نموذج سقف بابعاد (1050×1050×60) ملم بواقع مجموعتين، عشرة منها تم فحصها تحت تأثير حمل مركز في المنتصف والنماذج الباقية تم فحصها تحت تأثير الحمل المنتشر. في كل مجموعة هناك نموذج تم استخدام قضبان حديد التسليح الاعتيادي والتسعة الباقية تم استخدام الصفائح الفولاذية المثقبة مع الاخذ بنظر الاعتبار ان كمية الحديد في جميع النماذج متساوية.

المتغيرات التي تم اعتمادها في الدراسة هو تأثير تغير شكل الفتحة وكذلك تغير مساحتها وعدد الفتحات مع التأكيد على إبقاء جميع النماذج بكميات حديد متساوية. الاشكال التي اخذت بنظر الاعتبار هي (الدائرية والثمانية والمربعة) في حين تم دراسة ثلاثة احجام لكل شكل، حيث كانت الاحجام ثلاثة (فتحات صغيرة بواقع 144 فتحة (12×12)، فتحات متوسطة بواقع 64 فتحة (8×8) واخيرا فتحات كبيرة بواقع 16 فتحة (4×4). اما دراسة تأثير تغير سمك الصفيحة فقد تم دراسته عدديا باستخدام طريقة العناصر المحددة بواسطة برنامج Ansys 18.1.

النتائج بينت ان استخدام هذا الاسلوب في التسليح فعال جدا، وكانت نتائج الفحص بأن النماذج المسلحة بواسطة الصفائح الفولاذية أعطت حمل اقصى أعلى من النماذج المسلحة بقضبان حديد التسليح الاعتيادي بواسطة التحميل بنوعيه المركز والمنتشر، ففي حالة الحمل المركز كان معدل الحمل الاقصى للنماذج المسلحة بواسطة الصفائح الفولاذية اكثر بحوالي 67.5 % من النموذج المسلح بواسطة قضبان حديد التسليح الاعتيادي اما في حالة الحمل النتشر فقد كان معدل الحمل الاقصى للنماذج اكثر بحوالي 12.8%.

من بين جميع احجام الفتحات التي تم اعتمادها كانت الفتحات المتوسطة (Opening Aspect Ratio 8.17×10^{-3} =) هي الافضل من الفتحات الصغيرة والكبيرة حيث كان تحمل النماذج المسلحة بالصفائح ذات الفتحات المتوسطة تحت تاثيرالحمل المركز اكثر بمقدار 7.6% و 18.4% من معدل تحمل النماذج المسلحة بالصفائح ذات الفتحات الصغيرة والكبيرة على التوالي. اما في حالة الحمل المنتشر فكان معدل تحمل النماذج المسلحة بالصفائح المثقبة ذات الفتحات المتوسطة اكثر بمقدار 20.3% و 21.5 من النماذج المسلحة بالفتحات الصغيرة والكبيرة.

اما اذا اخذنا تاثير شكل الفتحات فأن الفتحات المربعة هي الأفضل من الفتحات الدائرية والثمانية وعليه يكون النموذج المسلح بالفتحات المتوسطة وبشكلها المربع هو افضل نموذج تم اجراء الاختبار عليه.
نتائج التحليل العددي اثبتت ان تأثير تغير سمك الصفيحة الفولاذية من 1 ملم الى 1.5 ملم ومن ثم الى 2 ملم غير مؤثر بشكل كبير على نتائج التحليل مما يوفر حرية ومرونة اكثر في اختيار سمك الصفائح الفولاذية المستخدمة بالتسليح مستقبلا.

جمهورية العراق
وزارة التعليم العالي والبحث العلمي
جامعة بابل
كلية الهندسة
قسم الهندسة المدنية

تصرف السقف الخرساني ثنائي الأتجاه المسلح بواسطة صفيحة فولاذية مثقبة باستخدام الخرسانة ذاتية الرص

أطروحة

مقدمة إلى كلية الهندسة في جامعة بابل

كجزء من متطلبات نيل درجة الدكتوراه فلسفة في الهندسة / الهندسة المدنية/ انشاءات

من قبل

علي عدنان عبد جواد

إشراف

أ.د. نمير عبد الامير علوش

1444 هـ